

# **Nanoemulsion formulations for Brain Tumour Therapy**

**by**

**Alisha N. Kadam**

**A thesis submitted in partial fulfilment for the requirements for  
the degree of MSc**

**(by Research) at the University of Central Lancashire**

**January 2013**

## **Declaration**

I declare that whilst registered as a candidate for the research degree, for which this submission is made, I have not been a registered candidate or enrolled student for another award of the university or any other professional institution. No material contained in this thesis has been used in any other submission for an academic award.

Signed

## **Acknowledgements**

There are many people who have supported me throughout this research. I would like to start by thanking my supervisor Dr. Abdelbary Elhissi for his guidance, kindness and patience throughout my research. I would also like to show gratitude to my second supervisors Dr. Ka-Wai Wan and Prof. Waqar Ahmed for their valuable assistance and generous advice. My special thanks to Dr. Kai-Wai Wan, Dr. Phillip Welsby, Dr. Gail Welsby and Tony Dickson for their support with the cell culture studies. I thank Dave McCarthy (UCL School of Pharmacy) for the wonderful TEM pictures. Also, I thank Professor Jaipaul Singh for his motivation and advice.

I express my gratitude to all my friends who have always supported me. I would specially like to thank Mohit, Bettina, Jane, Preet, Ritesh, Nimisha, Chinmay, Prasanna and Niraj as they helped me unwind at the end of a stressful week. I express my gratitude towards my labmates Sneha, Oshadie, Huner, Nozed, Ifti, Seema, Samriddhi, Basel and Urwashi for always being helpful in my research.

I am forever indebted to my parents, who have supported me as I chase my dreams, even when that meant me spending a few years apart from them. I especially thank them for their endless love, trust, understanding and support; and the wonderful care-packages that they send regularly. I would also like to thank my relatives for their kind wishes and faith in me.

I am thankful for the excellent Formula One season this year, especially Kimi Raikkonen, for helping me take my mind off the imminent workload for a few hours.

Lastly, I would like to thank Pigwidgeon for being my constant source of happiness.

## **Abstract**

Patients with malignant glioma have poor prognosis in spite of the advances in cancer therapy. Only 15% of the glioma patients survive more than five years after diagnosis. This is because the drug cannot reach the tumour site in sufficient amounts.

The aim of this project is to investigate the hypothesis that nanoemulsion formulations play an effective role as drug-delivery vehicles for the treatment of glioma. Two commercially available nanoemulsion formulations (Clinoleic TPN 20% and Intralipid TPN 20%) were used in this experiment. They were first characterised based on their size, zeta potential, pH and storage stability. Paclitaxel was used as the anti-cancer agent and the methods of loading efficiency determination (via spectrophotometry analysis) and Tissue culture were utilised to measure the effect of the formulation on glioma cell lines (U87-MG- grade IV and SVGP12 - normal glial cells).

Droplet size of the Clinoleic emulsion was increased from 254.1 nm to 264.7 nm when paclitaxel (6 mg/ml) was loaded into the formulation compared to drug-free formulation. Similarly with the Intralipid, the measured size was 283.3 nm and upon inclusion of 6mg/ml paclitaxel the size increased to 294.6 nm. The Polydispersity Index (PDI) of all the nanoemulsion formulations (Clinoleic and Intralipid) were lower than 0.2 irrespective of paclitaxel concentration indicating that all nanoemulsion formulations used were homogenous. The pH values for the Clinoleic formulations (7.1-7.5) were slightly higher (i.e. formulation's basicity was higher) than those of the Intralipid formulations (6.5-6.9). The Zeta Potential of Clinoleic has a greater negative value than that of Intralipid. The values for Intralipid are closer to neutral. When stored at 4° C and room

temperature for two weeks major changes were observed in the characteristics of Intralipid formulations, but the Clinoleic formulations remained stable at both temperatures.

In the Clinoleic formulations 70.4 - 80.2% loading efficiencies were observed for paclitaxel. Conversely, lower loading efficiencies were obtained for the Intralipid formulations, being 44.2 - 57.38 %. Clinoleic loaded with paclitaxel successfully decreased the U87-MG cell viability to  $6.4 \pm 2.3$  %, while Intralipid loaded with paclitaxel lowered the cell viability to  $21.29 \pm 3.82$ %. On the other hand, both nanoemulsions are less toxic to the normal glial cells (SVG-P12), decreasing the cell viability to 25-35%. This study suggests that nanoemulsions are useful and potentially applicable vehicles of paclitaxel for treatment of glioma.

## List of Abbreviations

ANOVA	Analysis of variance
DMSO	Dimethyl Sulfoxide
HPLC	High Performance Liquid chromatography
MEM	Minimum Essential Media
MTT	3-(4,5-Dimethylthiazol-2-yl)-2-5-diphenyltetrazolium bromide
O/W	Oil in Water
PBS	Phosphate Buffer Saline
PCS	Photon Correlation Spectroscopy
PDI	Polydispersity Index
PLL	Poly-L-Lysine
SD	Standard Deviation
SVG-P12	Normal glial cell line
TEM	Transmission Electron Microscopy
TPN	Total Parenteral Nutrition
U87-MG	Grade IV glioma cell line
UV	Ultraviolet
ZP	Zeta Potential

## Table of Contents

Chapter	Page
<b>Declaration</b> .....	ii
<b>Acknowledgement</b> .....	iii
<b>Abstract</b> .....	iv
<b>List of Abbreviations</b> .....	vi
<b>Table of Contents</b> .....	vii
<b>List of Figures</b> .....	x
<b>List of Tables</b> .....	xiv
<b>Chapter 1: Introduction</b> .....	1
1.1 Cancer Pathophysiology.....	2
1.2 Glioma.....	6
1.3 Therapeutic options for glioma.....	11
1.4 Nanoemulsion formulations.....	14
1.5 Nanoemulsions for the treatment of glioma.....	20
1.6 Working hypothesis.....	23
1.7 Aims of the study.....	23
<b>Chaptr 2: Materials and methods</b> .....	24

2.1 Materials.....	25
2.1.1 Chemicals.....	25
2.1.2 Equipments.....	26
2.2 Methods.....	26
2.2.1 Solubilisation of Paclitaxel in nanoemulsion formulations.....	26
2.2.2 Characterization of the Nanoemulsion formulations.....	27
2.2.3 Stability studies.....	27
2.2.4 Calibration curve of Paclitaxel.....	27
2.2.5 Loading efficiency using UV Spectrophotometer.....	29
2.2.6 Tissue culture.....	29
2.2.6.1 Preparation of Tissue culture media.....	30
2.2.6.2 Subculture and Re-suspension of Cells.....	30
2.2.6.3 Cell Counting.....	31
2.2.6.4 Seeding and Growth curves.....	32
2.2.6.5 Cytotoxicity assay (MTT).....	34
2.3 Statistical analysis.....	35
<b>Chapter 3: Characterization of Nanoemulsion formulations.....</b>	<b>36</b>
3.1 Size of the nanoemulsion formulations.....	39
3.2 Polydispersity Index (PDI) of nanoemulsion formulations.....	40
3.3 pH of Nanoemulsion formulations.....	46
3.4 Zeta Potential (ZP) of Nanoemulsion formulations.....	48
3.5 Stability of Nanoemulsion formulations.....	50
3.5.1 Formulations stored at 4° C.....	50

3.5.2 Formulations stored at room temperature.....	52
3.6 Loading Efficiency of nanoemulsion formulations.....	57
<b>Chapter 4: Tissue culture.....</b>	<b>60</b>
4.1 Growth Curves.....	63
4.2 MTT Assays for assessing the cytotoxicity of formulations.....	68
<b>Chapter 5: Conclusions and Future prospects.....</b>	<b>80</b>
5.1 General conclusions.....	81
5.2 Future work.....	87
<b>References</b>	<b>89</b>

## List of figures

<b>Number</b>	<b>Title</b>	<b>Page</b>
1.1	Normal mitosis (shown in the centre) as compared to abnormal mitosis that occurs due to absence of Mitotic Checkpoints (MC) leading to aneuploidy	3
1.2	Relationship between age and the incidence of cancer	4
1.3	The six hallmarks of Cancer	5
1.4	The major parts of the brain; primarily differentiated into the cerebrum, cerebellum and the brainstem	6
1.5	The Supratentorial and Infratentorial regions as divided by the tentorium cerebelli.	9
1.6	The tight junctions at the BBB that do not allow water-soluble molecules to pass.	12
1.7	Nanoemulsion [A] and a macroemulsion [B]. The translucent appearance of the nanoemulsions is attributed to the nano size of the dispersed droplets	14
1.8	The technique of High-pressure homogenization for preparation of Nanoemulsions	16
1.9	A presentation showing the instability manifestations of emulsions	17
1.10	Surfactant molecules coating the surface of the oil droplet in an emulsion	18
1.11	Structure of paclitaxel ( $2\alpha,4\alpha,5\beta,7\beta,10\beta,13\alpha$ )-4,10-bis(acetyloxy)-13- {[(2R,3S)- 3-(benzoylamino)-2-hydroxy-3-phenylpropanoyl]oxy}- 1,7- dihydroxy-9-oxo-5,20-epoxytax-11-en-2-yl benzoate	20

2.1	Neubauer Haemocytometer, each large square gives an area of 1 mm <sup>2</sup> (1 mm x 1 mm) with a depth of 0.1 mm.	31
2.2	A 96 well plate template. A 96 well plate is made up of twelve columns (numbered 1-12) and eight rows (A-H)	33
3.1	Size between formulations of Clinoleic and Intralipid using a range of paclitaxel concentrations (n=3, ± SD)	39
3.2	PDI values for the Clinoleic and Intralipid nanoemulsions (n=3, ± SD).	41
3.3	TEM photograph of the Clinoleic formulation with a paclitaxel concentration of 3 mg/ml	42
3.4	TEM image of the Intralipid nanoemulsion with a paclitaxel concentration of 3mg/ml.	43
3.5	pH of Clinoleic and Intralipid nanoemulsions using a range of paclitaxel concentrations (n=3, ± SD).	45
3.6	ZP values of Clinoleic and Intralipid nanoemulsions using a range of paclitaxel concentrations (n=3, ± SD).	47
3.7	Size analysis of Clinoleic and Intralipid formulations stored at 4°C using a range of paclitaxel concentrations (n=3, ± SD)	49
3.8	pH analysis of Clinoleic and Intralipid nanoemulsions containing a range of paclitaxel concentrations when stored at 4°C for two weeks (n=3, ± SD)	50
3.9	Zeta potential analysis of Clinoleic and Intralipid nanoemulsions upon storage for two weeks at 4° C (n=3, ± SD).	51
3.10	Size analysis of Clinoleic and Intralipid formulations stored at	53

	room temperature for a 14 days (n=3, ± SD).	
3.11	Changes in pH for the Clinoleic and Intralipid formulations when stored for two weeks at RT (n=3, ± SD).	54
3.12	Changes in ZP values for the Clinoleic and Intralipid formulations when stored for two weeks at RT (n=3, ± SD).	55
3.13	Calibration curve showing the absorbance plotted against the concentration of paclitaxel per 100 ml of ethanol.	57
3.14	Loading efficiency of paclitaxel in nanoemulsion droplets using the Clinoleic and Intralipid nanoemulsions (n=3 ± SD).	58
4.1	Percentage growth of the 10 <sup>3</sup> , 10 <sup>4</sup> and 10 <sup>5</sup> seeding densities of the SVG-P12 cell line.	63
4.2	Microscopic photographs showing the SVG-P12 cells using three different seeding densities [10 <sup>5</sup> (A), 10 <sup>4</sup> (B) and 10 <sup>3</sup> (C)].	64
4.3	Percentage growth using 10 <sup>3</sup> , 10 <sup>4</sup> and 10 <sup>5</sup> seeding densities of the U87-MG cell line.	66
4.4	Microscopic photographs showing the U87-MG cells using three different seeding densities [10 <sup>5</sup> (A), 10 <sup>4</sup> (B) and 10 <sup>3</sup> (C)].	67
4.5	Cytotoxic effects of the formulations on the SVG-P12 cells: Dextran, Blank Clinoleic, Blank Intralipid, Clinoleic loaded with paclitaxel, Intralipid loaded with paclitaxel, PLL and Paclitaxel.	69
4.6	Inverted light microscopic photographs of SVG-P12 cells treated with Clinoleic containing paclitaxel. These images show the declining number of cells as more paclitaxel is added per ml of	72

	media. [0.0 mg (A), 0.5 mg (B), 1.5 mg (C) and 3 mg (D) per ml]	
4.7	Inverted light microscopic images of SVG-P12 cells treated with Intralipid containing paclitaxel. These images show the decreasing number of cells as higher concentrations of paclitaxel were added [0.0 mg (A), 0.5 mg (B), 1.5 mg (C) and 3 mg (D) per ml].	73
4.8	U87-MG showing the cytotoxic effects of the formulations in percent cytotoxicity: Dextran, Blank Clinoleic, Blank Intralipid, Clinoleic loaded with paclitaxel, Intralipid loaded with paclitaxel, PLL and Paclitaxel	74
4.9	Inverted light microscopic images of U87-MG cells treated with Clinoleic containing paclitaxel. These images show the dwindling number of cells as more paclitaxel was added. [0.0 mg (A), 0.5 mg (B), 1.5 mg (C) and 3 mg (D) per ml].	77
4.10	Inverted light microscopic images of U87-MG cells treated with Intralipid containing paclitaxel. These images show the dwindling number of cells as more paclitaxel was added. [0.0 mg (A), 0.5 mg (B), 1.5 mg (C) and 3 mg (D) per ml].	78

## **List of tables**

2.1	List of chemicals and their suppliers	25
2.2	A table showing the amount of stock solution and ethanol to be used to make serial dilutions.	28
2.3	Concentrations at which the controls/formulations were added to the 96-well plates	35
3.1	Compositions of Clinoleic and Intralipid TPN.	38
4.1	IC <sub>50</sub> Values of the formulations in mg for SVG-P12 cells	71
4.2	IC <sub>50</sub> Values of the formulations in mg for U87-MG cells	76

# **Chapter 1: Introduction**

## **1.1 Cancer pathophysiology**

Cancer can be defined as a large group of diseases in which some abnormal cells do not follow the standard rules of cell division and growth. Normal individual cells are not autonomous as they depend on signals from their external environment that instruct the cells whether to multiply, differentiate or die. By contrast the abnormal cancerous cells are resistant to these signals and hence they divide and proliferate uncontrollably. Almost 90% of deaths due to cancer are because of metastasis which is the process of the tumour spreading to other locations of the body. A cancerous tumour originates from a single mutated abnormal cell.

Except reproductive cells, all cells divide and multiply by the process of mitosis. Mitosis is the nuclear and cellular division that produces two identical daughter cells; it involves Interphase, Prophase, Prometaphase, Metaphase, Anaphase and Telophase. Cancer is fundamentally a disease of mitosis as the normal rules of mitosis are ignored by the cancer cells. Cancer cells show aneuploidy, i.e., they have an abnormal number of chromosomes.

The p53 gene controls the proper functioning of the mitotic cycle. However, in over 50% of incidences of cancer, the p53 gene is mutated.

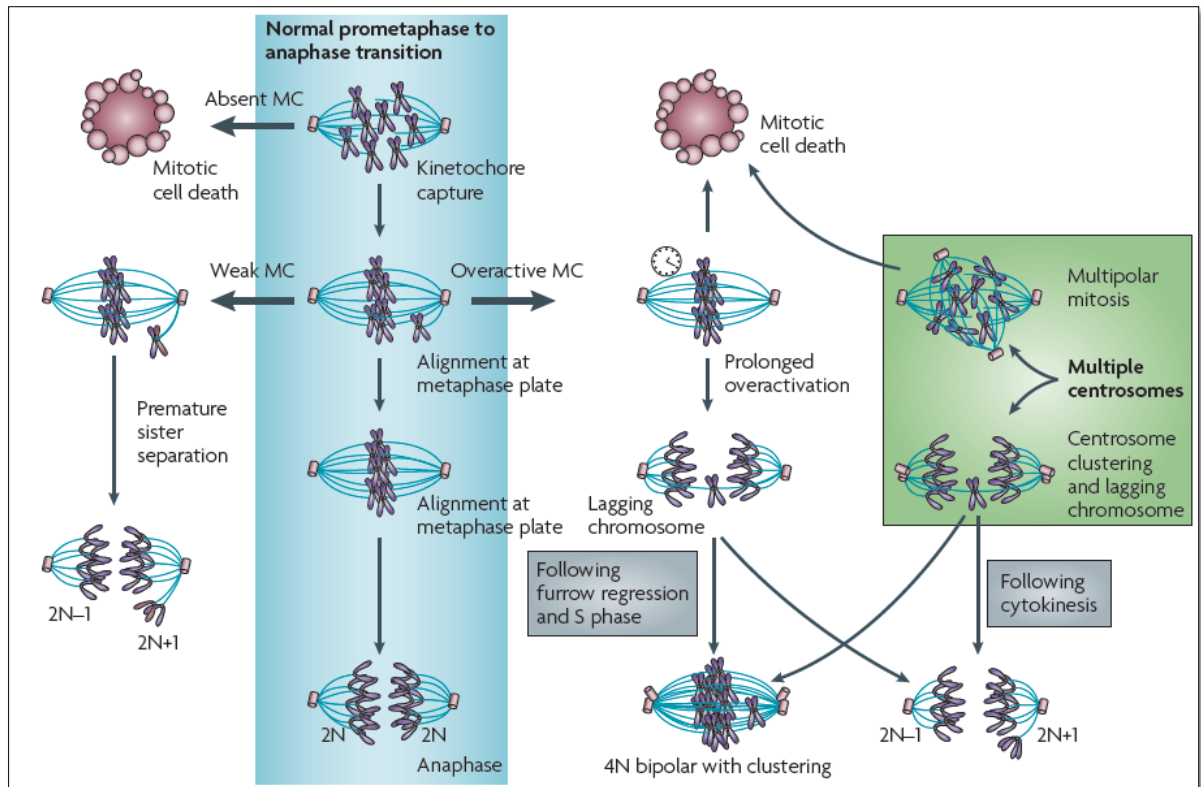


**Figure 1.1: Normal mitosis (shown in the centre) as compared to abnormal mitosis that occurs due to absence of Mitotic Checkpoints (MC) leading to aneuploidy (Source: Schwartzman *et al*, 2010).**

The formation and development of a tumour depends on external and internal factors. External factors include all of the environmental factors that may cause cancer such as tobacco, alcohol, radiation, chemicals and viral infections. Internal factors may involve the genetic background such as hormones, inherited mutations and immune system abnormalities. One in every three individuals is susceptible to and shows signs of cancer. However, the rate of incidence varies significantly among countries suggesting that either some of these populations carry cancer-susceptibility genes or the external environmental factors contribute to their high cancer incidence rates.

Cancer can arise in people from any age group (Figure 1.2), but it is more common amongst the elderly individuals (over 65 years of age).

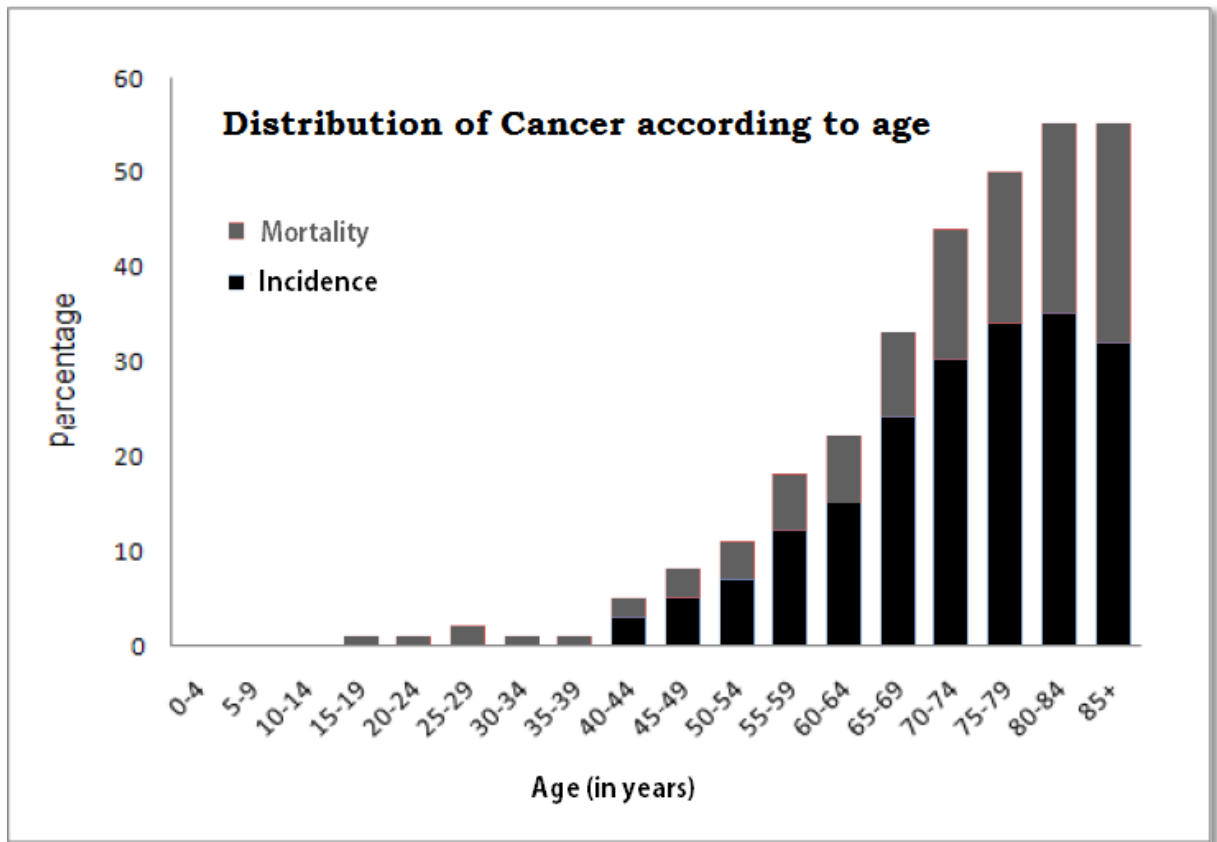


**Figure 1.2: Relationship between age and the incidence of cancer.**

(Source: Howlander et al, 2011).

Hanahan and Weinberg (2000) proposed a model of the six hallmarks of cancer describing how the cancerous cells boost their growth and proliferation (Figure 1.3). These hallmarks are:

- Cancer cells are **immortal**; they possess the quality of constant replication.
- Cancer cells produce **growth factors** from oncogenes.
- Cancer cells **ignore anti-growth signals** from the Tumour suppressor genes.

- Cancer cells are **resistant to apoptosis**.
- Cancer cells may cause the formation of new blood vessels (**angiogenesis**).
- Cancer cells exhibit **Metastasis** (spread to other locations in the body).

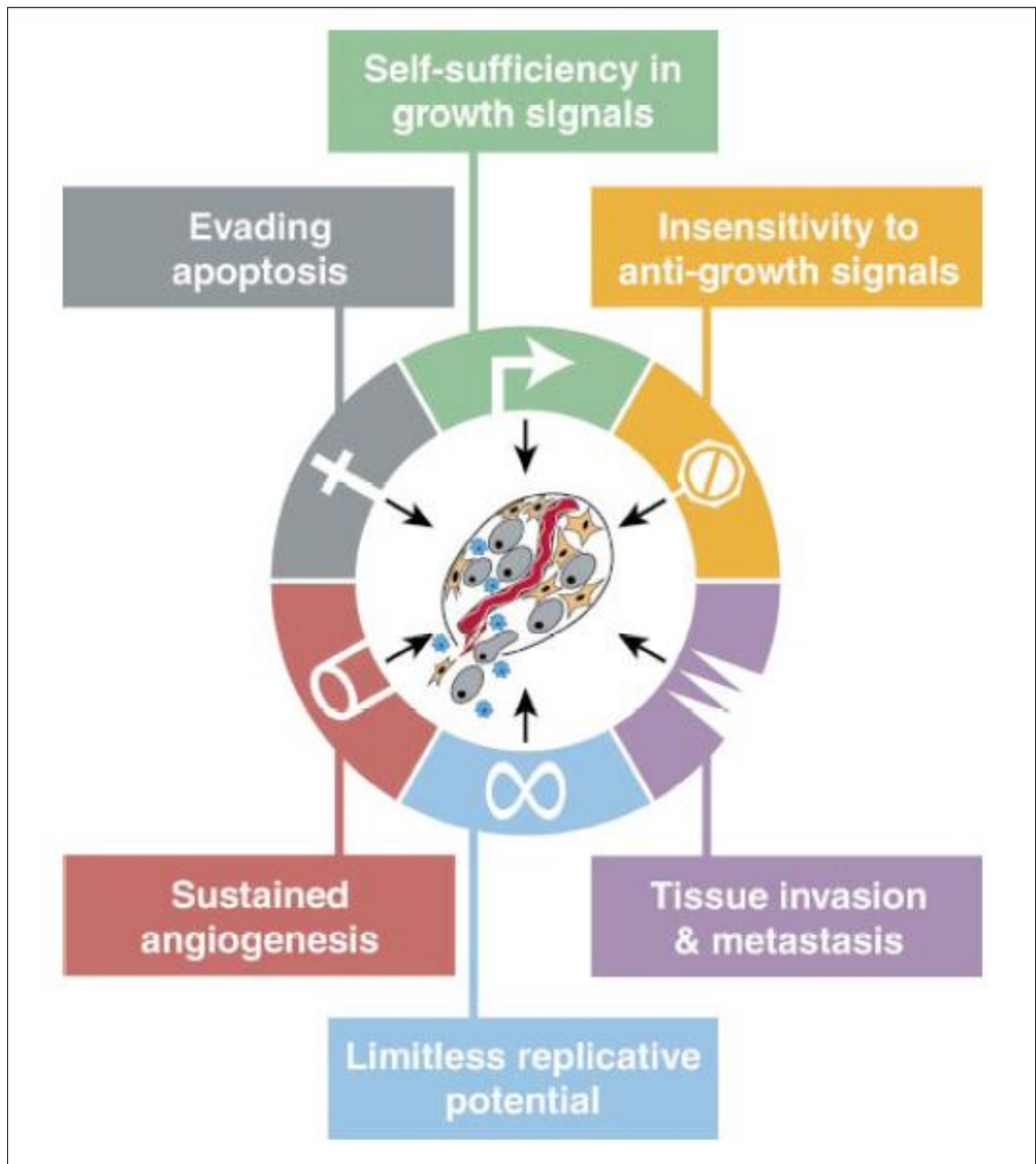


**Figure 1.3: The six hallmarks of Cancer. (Source: Hanahan *et al*, 2000).**

## 1.2 Glioma

The brain is the most complex organ of the body and it is also one of the most essential organs. It is the centre of the Nervous system and is made up of billions of cells called neurons. All body functions (voluntary or involuntary) are controlled by the brain. The brain and the spinal cord form the Central Nervous System (CNS). The brain is divided into three major parts: Cerebral cortex (cerebrum – split into right and left hemispheres), cerebellum and brainstem (Figure 1.4).

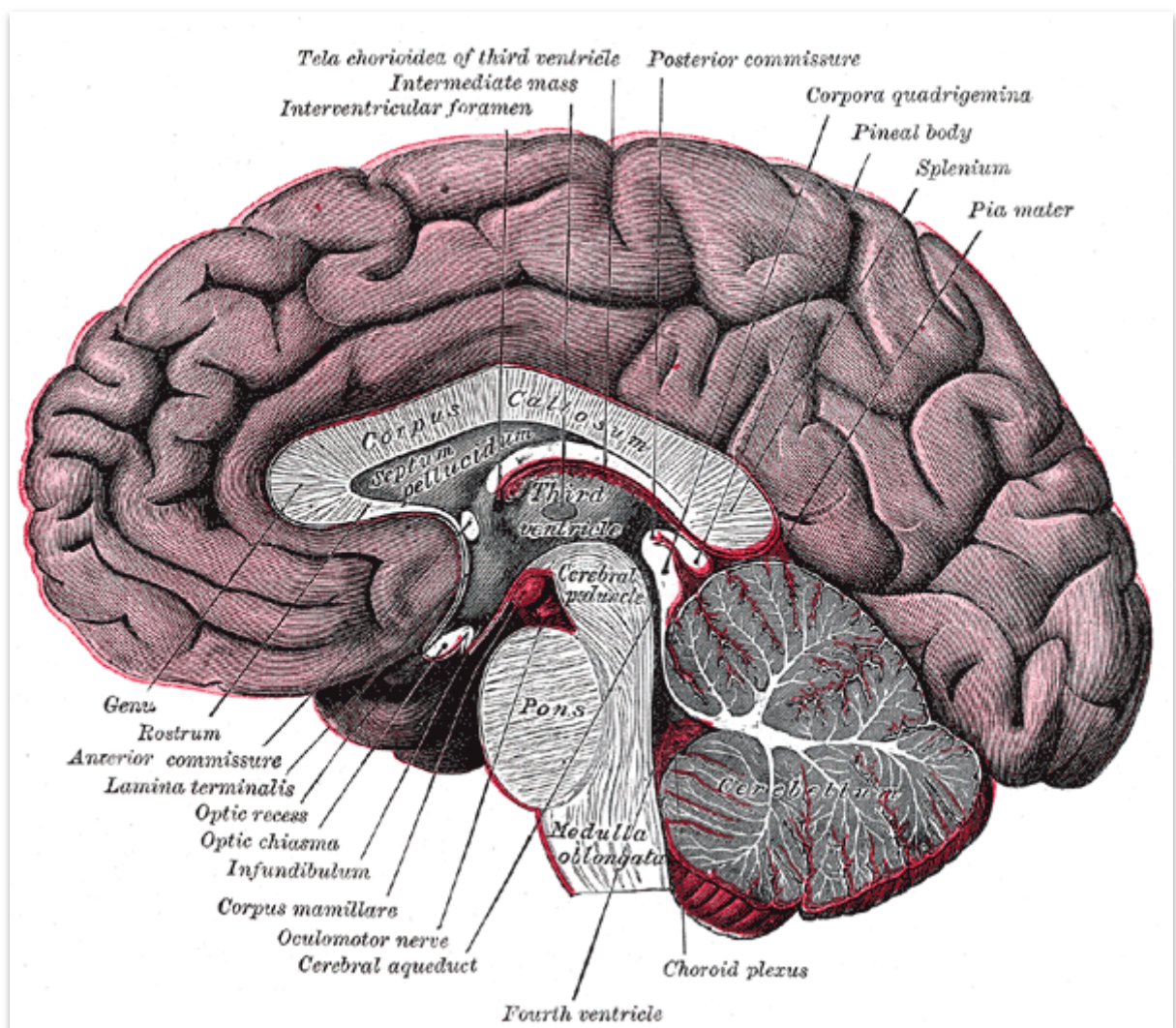


**Figure 1.4: The major parts of the brain; primarily differentiated into the cerebrum, cerebellum and the brainstem. (Source: Nieuwenhuys *et al*, 2008).**

The cerebral cortex is sub-divided into the frontal lobe, parietal lobe, occipital lobe and temporal lobe. There is also a ventricular system in the brain. Ventricles are cerebrospinal fluid-filled spaces between the cerebrum and the brainstem. There are four such ventricles: the right and left ventricles (one in each cerebral hemisphere), third ventricle and fourth ventricle.

A glioma is a neoplasm (or tumour) that originates in the brain or the spine. In spite of advances in cancer therapy, most of the patients with malignant glioma have poor prognosis. Most brain tumours develop from cancerous ‘glial cells’ and are hence called gliomas. Gliomas are classified by cell type, grade or location. Every year in Western Europe, North America and Australia, there are about 6–11 new cases of primary (originating in the brain) glioma tumours per 100,000 populations in men and 4–11 new cases in women (Ohgaki H. et al, 2005). In 2011, in the United States alone there were 22,340 new cases of Glioma and 13,110 deaths due to this disease. Only 15% of the people diagnosed with Glioma survive more than five years after diagnosis in the UK (Cancer Research UK). Gliomas are less common in other parts of the world.

The grade of glioma is verified by performing a pathological evaluation of the tumour. According to the World Health Organisation (WHO) gliomas are classified into four grades, from grade I (least advanced) to grade IV (most advanced).

- **Low-grade gliomas [WHO grades I and II]** are not anaplastic, i.e., the cells are well-distinguished. These are slow-growing malignant tumours which are less aggressive and hence the patients have better prognosis when compared to grades III and IV. Low

grade gliomas are quite common in children (about 50-70% of the cases). In the UK, there are around 4500 new cases of Glioma every year; 20% out of these tumours are low-grade gliomas.

- **High-grade [WHO grades III and IV]** gliomas are anaplastic (lack of differentiation in cancerous cells). These are malignant tumours that have a very poor prognosis (Siew-Ju, *et al* 2007).

Gliomas are also categorized according to the histological cell features:

- **Astrocytomas** are neoplasms that originate from star-shaped brain cells called astrocytes. They can be located anywhere in the brain but are mostly found in the frontal lobe of the cerebrum. Astrocytomas are characterized by their slow growth, cyst formation and invasion of the surrounding tissue. Glioblastoma multiforme is the most common astrocytoma and it is also the most aggressive type of all gliomas (Grade IV).
- **Ependymomas** is a type of tumour that originates from the ependymal tissue of the central nervous system. It is usually seen in the fourth ventricle (Figure 1.4) but can sometimes spread to the spinal cord. Rarely, ependymomas originate in the spinal cord. Ependymomas account for nearly 6% of all primary brain tumours.

- **Oligodendrogliomas** are neoplasms that arise from the oligodendrocytes of the brain. They most commonly originate in the four lobes on the cerebral cortex. Although it can occur in children, it is mostly seen in adults.

Some tumours are of a ‘mixed’ category and contain a mixture of glial cells, e.g. oligoastrocytomas.

The cerebrum is separated from the cerebellum by a membrane called the tentorium cerebelli (Figure 1.5). Thus, gliomas can also be classified according to whether they are located above or below the tentorium (Larjavaara *et al*, 2007).

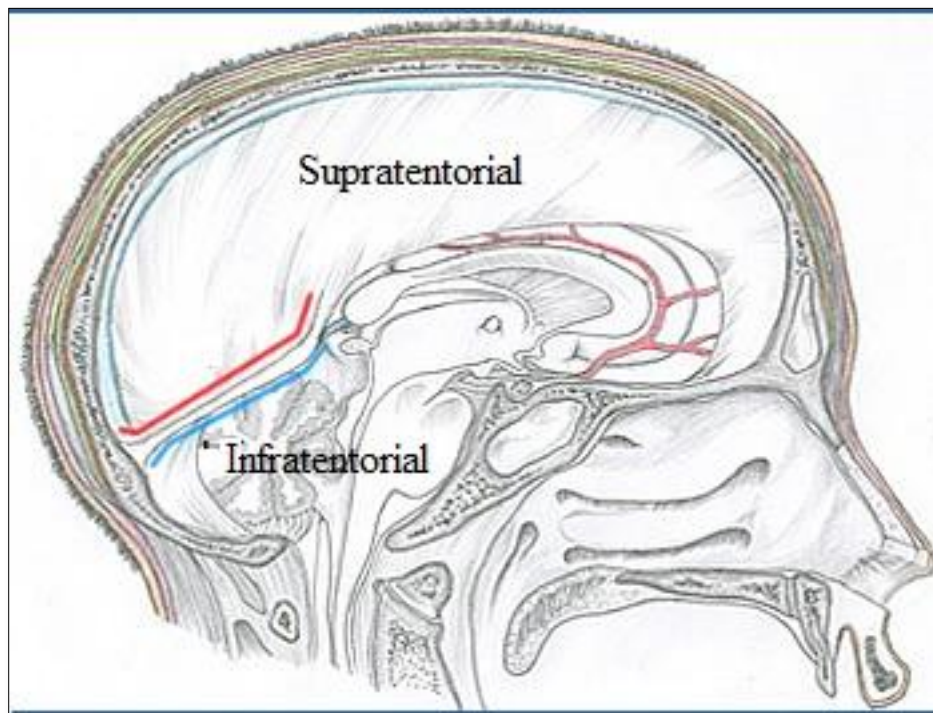


**Figure 1.5: The Supratentorial and Infratentorial regions as divided by the tentorium cerebelli. (Source: Carter *et al.*, 2009).**

- **Supratentorial** gliomas are where the tumour originates in the cerebrum, above the tentorium. These tumours are commonly seen in adults. Supratentorial tumours account for about 80% of all intra-cranial tumours that are newly diagnosed. These are mostly seen in adults although they are highly common in infants who are less than a year old.
  
- **Infratentorial** gliomas are where the tumour originates below the tentorium, in the cerebellum and these are commonly seen in children. In fact, infratentorial gliomas account for 50-55% of all gliomas seen in children. Infratentorial tumours are seen most frequently in the cerebral hemispheres, followed by the brainstem and the fourth ventricle (Gusnard, 1990).
  
- **Pontine** gliomas (or brainstem gliomas) are where the tumour is found in the pons of the brainstem. These are very aggressive and hard to treat as the pons controls important functional centres in the brain such as the breathing centre. These gliomas occur mostly in children (Angelini *et al*, 2011).

### **1.3 Therapeutic options for Gliomas**

The therapeutic options for glioma depend on the grade, location, size and cell type of glioma. Usually, surgery, chemotherapy and radiation therapy are all used in conjunction. Chemotherapy ends the growth of cancer cells by utilizing drugs, either by killing the cells or by stopping them from division. Common drugs used for glioma are temozolomide, vincristine and carmustine (Dall'oglio *et al*, 2008). They are administered either orally or intravenously.

However despite the best possible treatment with these drugs, most patients still show poor prognosis.

Malignant gliomas are vascular tumours and the main reason for their progression in the brain is angiogenesis (i.e. formation of new blood vessels) which involves endothelial cell proliferation, migration, reorganisation of extracellular matrix and tube formation (Rahman *et al*, 2010). Bevacizumab, Cediranib, Sorafenib and Thalidomide are potent anti-angiogenic drugs.

Another problem that most drugs encounter is the blood brain barrier (BBB). The BBB is characterized by relatively impermeable endothelial cells with tight junctions, preventing the passage of water-soluble molecules from the blood circulation into the CNS. Thus, most drugs fail to cross the BBB effectively and hence do not reach the target area in the brain in sufficient concentrations.

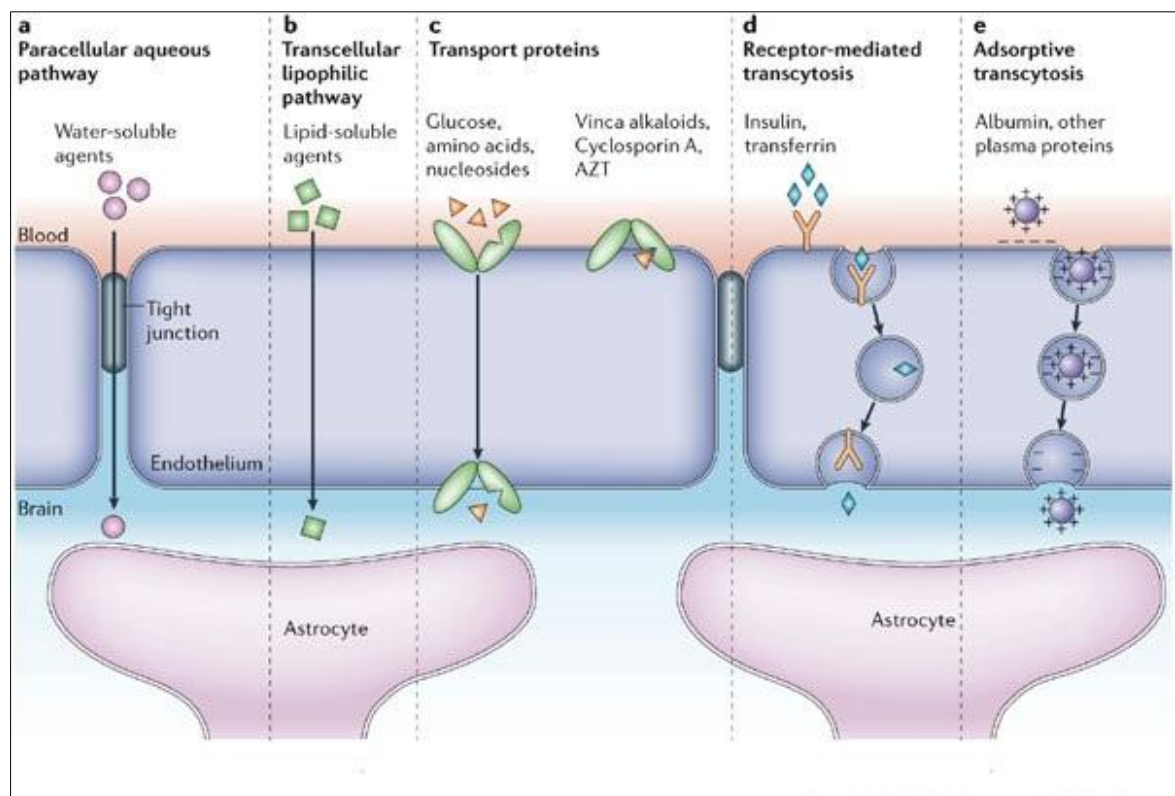


**Figure 1.6: The tight junctions at the BBB that do not allow water-soluble molecules to pass. (Source: Abbott *et al*, 2006).**

Another major problem is the reticuloendothelial system (RES), also known as the Mononuclear phagocyte system. When a large foreign particle (drug) is injected into the body on its own, the RES views the drug as a toxic substance, causing the phagocytic cells of the RES to engulf the drug rendering them ineffective. Most of the drug is lost due to

this and hence it fails to reach the tumour site in the brain. This can be avoided if the droplet size of the particles is in nm.

Nanotechnology may help the drug to escape the RES as nanoparticles like nanoemulsion formulations, liposomes, niosomes are made of phospholipids (the same materials that the body cells are made from) or similar materials so the RES cells might not view them as toxic substances, providing that the formulation is robustly optimized (Eccleston, 2006). Hence, the drug might be able to reach the tumour site in larger concentrations. Nanoemulsion formulations may also help in enhancing the permeability of these drugs across the BBB as due to their extremely small size they might be able to pass through the BBB in advanced cases of glioma (Garcia-Garcia, 2005).

#### 1.4 Nanoemulsion formulations

An emulsion is a heterogeneous preparation of two or more immiscible liquids, one of which is dispersed uniformly as fine droplets throughout the other. The phase present as droplets is known as the dispersed (internal) phase, while the surrounding liquid is known as the continuous (external) phase. An emulsion may be described as a macroemulsion, microemulsion or a nanoemulsion based on the droplet size of the dispersed phase. Nanoemulsions can be defined as oil-in-water (o/w) or water-in-oil (w/o) emulsions with mean droplet diameters ranging from 50 to 1000 nm. Usually, the average droplet size of nanoemulsions is between 100 and 500 nm. Droplet size less than 100 nm is not recommended as it is difficult to accommodate the drug in sufficient concentrations (Jong *et al*, 2008)

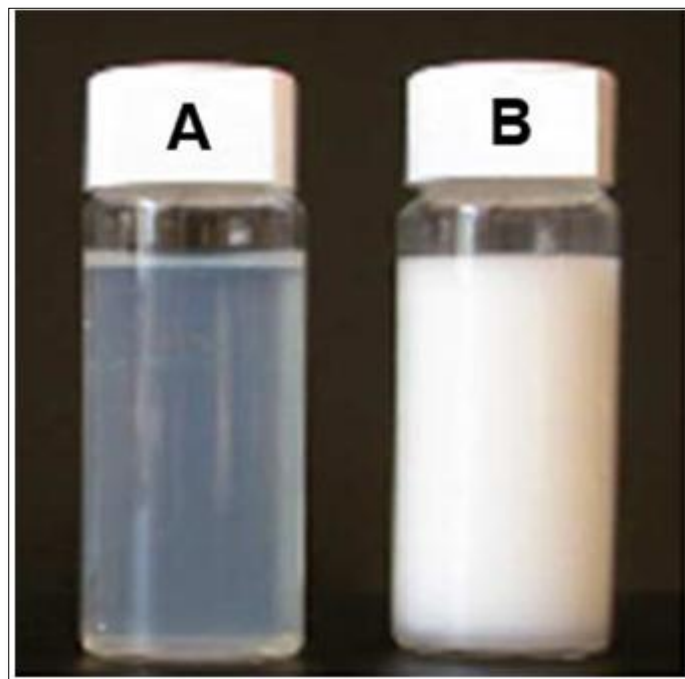


**Figure 1.7: Nanoemulsion [A] and a macroemulsion [B]. The translucent appearance of the nanoemulsions is attributed to the nano size of the dispersed droplets.**

(Source: Shah *et al*, 2010).

Nanoemulsions were first developed over 20 years ago and as shown in Figure 1.7, they appear transparent (or translucent) because of their inability to scatter light (McClements, 2002). To be able to scatter light a particle must be more than one-fourth the size of the wavelength of visible light and hence nanoemulsions are transparent due to their small size. The terms sub-micron emulsion and mini-emulsion are also used as synonyms for nanoemulsions.

Nanoemulsions are commonly prepared using two methods: high-energy methods and low-energy methods. The high-energy methods of High-pressure homogenization and Microfluidization are used at both laboratory and industrial scale, as they are very effective in reducing the droplet size of the dispersed phase. Low-energy methods like the Phase-inversion temperature technique and spontaneous emulsification method are used when macromolecules like proteins and nucleic acids are involved so that heat generated that might cause macromolecule degradation is avoided. In High-pressure homogenization, the crude mixture of the aqueous and oil phase is passed through a small orifice at an operating pressure of 500-5000 psi, where the mixture is exposed to extreme turbulence. This produces a finely-dispersed emulsion with a very small droplet size (Panayiotis *et al*, 2008).

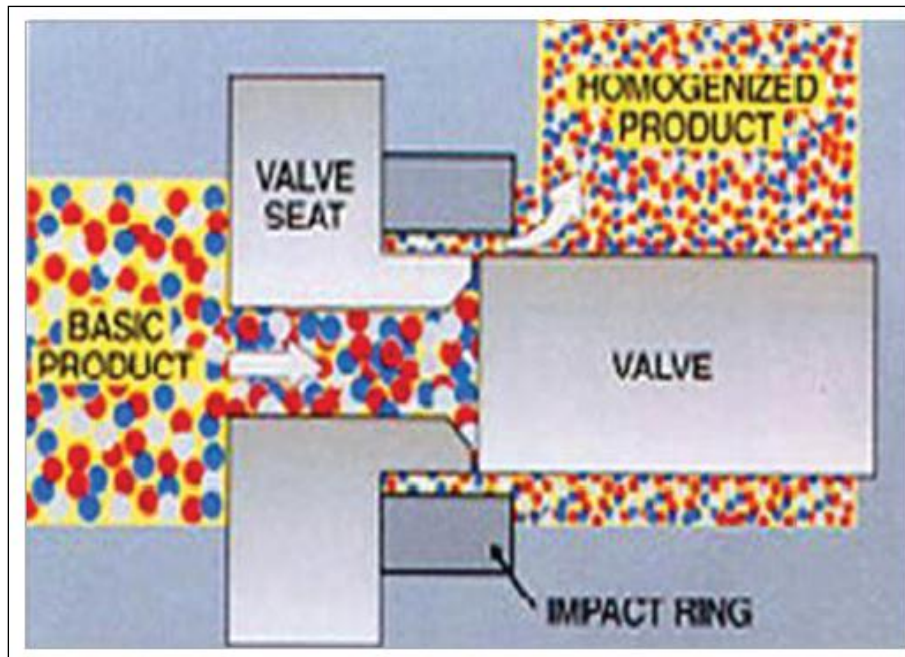


**Figure 1.8: The technique of High-pressure homogenization for preparation of Nanoemulsions. (Source Shah *et al*, 2010).**

Similarly, in the process of Microfluidization a solution of oil and water is pumped into the Microfluidization processor under an immense pressure ranging from 1500 to 40000 psi. The mixture is then passed through an extremely small orifice (smaller than the diameter of a human hair follicle) at a very high speed (e.g. hundreds of meters per second). This creates a considerably high shear rate, causing highly efficient droplet size reduction (Jafari, 2007). But these formulations are not stable for long durations.

In the low energy method of Phase-inversion temperature technique, an oil-in-water emulsion transforms to a water-in-oil emulsion as the temperature rises and vice versa. When the preparation is made above the phase inversion temperature and followed by rapid cooling it produces emulsions that have very fine droplet size and long-term stability

(Forster *et al*, 1990). In 1878, Johannes Gad discovered the spontaneous emulsification method (also known as the Ouzo effect). In this method a hydrophobic essential oil is mixed with a water-miscible solvent (e.g. ethanol) and it spontaneously forms an oil-in-water emulsion with minimal stirring (Theissen, 1999).

An emulsion is said to be stable when the dispersed droplets retain their nature and remain evenly distributed throughout the continuous phase for a long duration. Emulsions are susceptible to a number of instability problems like coalescence, flocculation, creaming and breaking (Figure 1.9). Coalescence is a process in which two or more droplets combine to form a larger droplet upon contact, while flocculation is when multiple droplets adhere to each other to form clusters of droplets without merging to form a single large droplet. Creaming occurs when the dispersed phase either migrates upwards or sinks downwards (sediments) in the mixture. Emulsions are also prone to breaking due to surface tension.

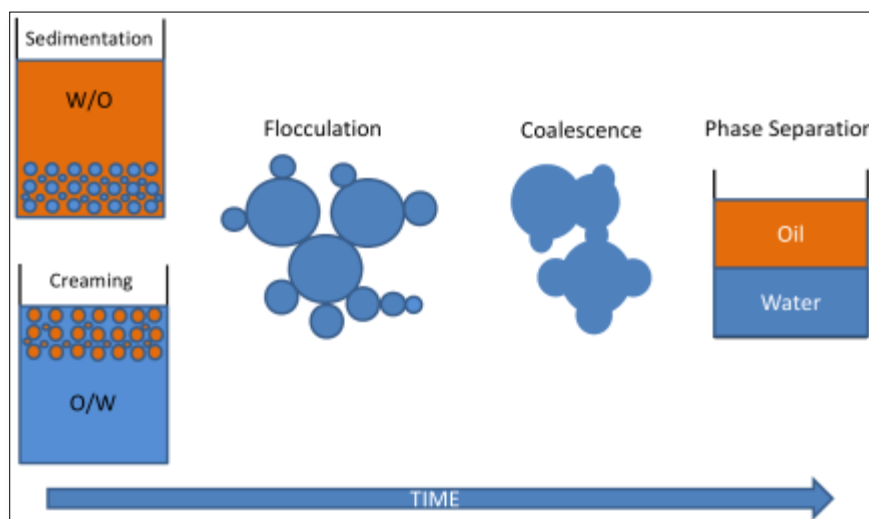


**Figure 1.9: A presentation showing the instability manifestations of emulsions.**

(Source: Alvarado *et al*, 2011).

These instability problems can be overcome by using emulsifiers (i.e. emulsifying agents). The most common type of emulsifiers is the surface active agents (surfactants). Surfactants are organic amphiphilic compounds that lower the surface tension between the two immiscible liquids of the emulsion by coating the dispersed phase droplets (Figure 1.10) and hence increasing the emulsions kinetic stability. Polysorbate 20 (Polyethylene glycol sorbitan monolaurate) and cetareth 20 (C16~18 fatty alcohol polyoxyethylene ether) are two examples of emulsifying agents.

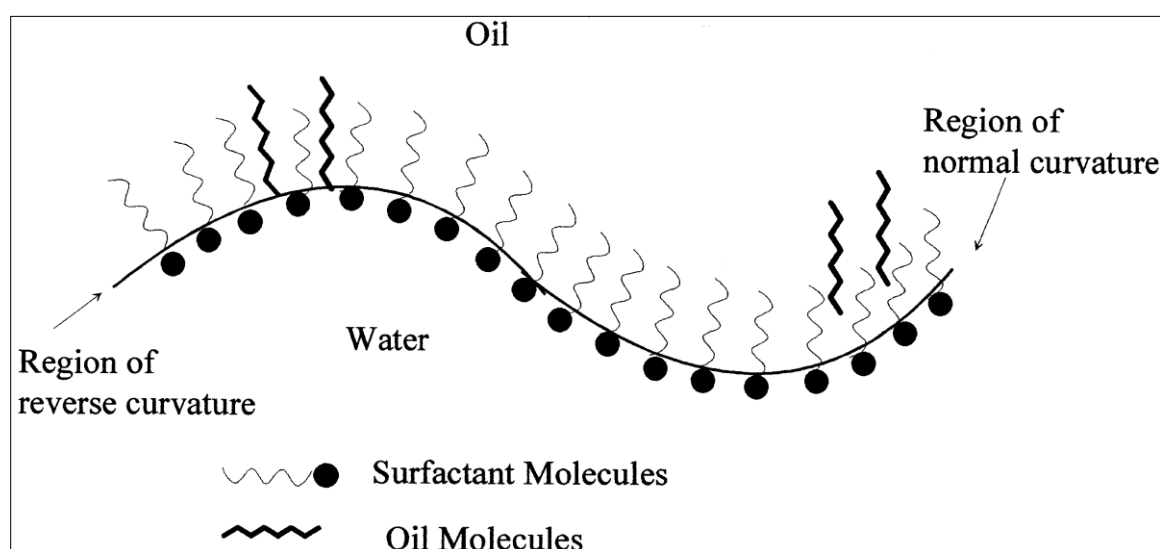


**Figure 1.10: Surfactant molecules coating the surface of the oil droplet in an emulsion. (Source: Lawrence *et al*, 2000).**

Unlike microemulsions (which are thermodynamically stable), nanoemulsions are only kinetically stable. A chemical substance is said to be thermodynamically stable (or in thermodynamic equilibrium) when it is in its lowest energy state, i.e. it is in complete

equilibrium with its surroundings. A thermodynamically stable substance will not change unless energy in some form is provided. Kinetic stability on the other hand, is when a chemical substance reacts (changes) extremely slowly and remains constant over a long period of time. However the long-term physical stability of nanoemulsions, due to their small droplet size and non-coalescent properties, makes them unique and they are sometimes referred to as “approaching thermodynamic stability” (Bouchemal *et al*, 2004).

Nanoemulsions can be formulated as liquids, sprays, foams, creams, ointments and gels and are used extensively in manufacturing cosmetics, pastes, pharmaceuticals etc. They are used especially as controlled drug-delivery vehicles for poorly water soluble drugs. They are non-toxic and non-irritant in nature making them ideal vehicles for therapeutic agents (Aboofazeli, 2010).

Although the term ‘nanoemulsion’ was not coined then, phospholipid-stabilized soybean oil emulsions were first approved safe for intravenous administration for nutritional purposes over 40 years ago (Driscoll, 2006). The size range for these emulsions was in the ‘nano’ scale (around 300 nm), making them the first nanoemulsion formulations used. Nowadays, nanoemulsions are routinely administered as ‘Total Parenteral Nutrition’.

## 1.5 Nanoemulsions for the treatment of Glioma

Paclitaxel is a naturally occurring diterpene alkaloid occurring in the bark of the Pacific Yew tree, *Taxus brevifolia*. It was discovered in 1967 by Monroe E. Wall and Mansukh C. Wani as the outcome of the investigation of over 12,000 natural compounds for anti-cancer activity by the U.S. National Cancer Institute. Paclitaxel inhibits mitosis by disrupting microtubule integrity, thereby causing cell death (Sheng *et al*, 1999). The chemical structure of Paclitaxel is shown in Figure 1.11.

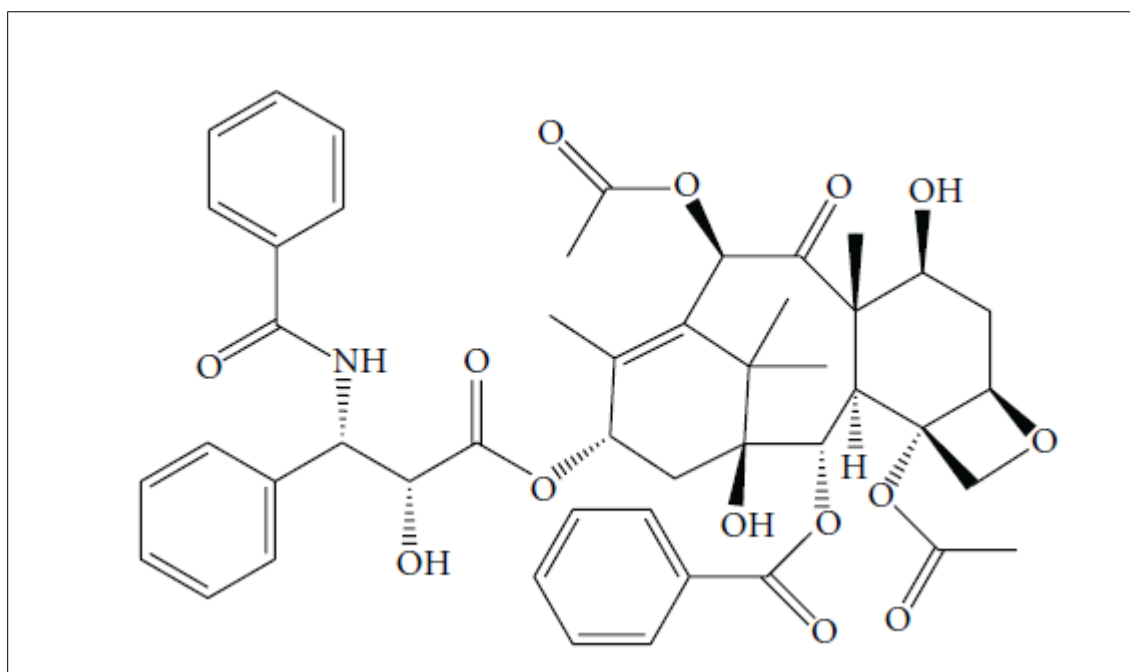


**Figure 1.11: Structure of paclitaxel (2 $\alpha$ ,4 $\alpha$ ,5 $\beta$ ,7 $\beta$ ,10 $\beta$ ,13 $\alpha$ )-4,10-bis(acetyloxy)-13-[[[(2R,3S)- 3-(benzoylamino)-2-hydroxy-3-phenylpropanoyl]oxy]- 1,7-dihydroxy-9-oxo-5,20-epoxytax-11-en-2-yl benzoate. (Source: Surapaneni *et al*, 2012).**

In the last 15-20 years Paclitaxel has been widely used in anti-cancer therapy, especially against ovarian and breast cancer. Terzis *et al* (1997) tested Paclitaxel for its anti-migrational, anti-invasive and anti-proliferative effect on human glioma cell lines and found that cells showed nuclear fragmentation, indicating an induction of apoptosis. The only drawback of Paclitaxel is that it is poorly soluble in water and needs an appropriate delivery vehicle for intravenous administration. In a range of studies Cremophor EL was used as the non-aqueous delivery vehicle but it caused some serious side-effects such as hypersensitivity reactions, nephrotoxicity and neurotoxicity (Singla *et al*, 2002). Thus, provision of safe alternative vehicles for this drug is crucial.

Recently, nanoemulsions formulations have been used as delivery vehicles for Paclitaxel. Paclitaxel readily dissolves in the dispersed lipid phase and can be easily administered intravenously due to the external aqueous phase. Zhao *et al* (2010), tested magnetic nanoparticles loaded with Paclitaxel *in vitro* and in glioma-bearing rats and found that the nanoparticles successfully delivered the Paclitaxel to the glioma and boosted its anti-tumour activity.

In this project, two commercially available nanoemulsions that are routinely used in total parenteral nutrition (TPN) were used to solubilise Paclitaxel for applications on glioma cell lines. The nanoemulsions are the Intralipid TPN (Fresenius Kabi, Germany) and the ClinOleic TPN (Baxter, USA), which are lipid nanoemulsions having different types of excipients. Dr Elhissi's research group have shown that both of these

nanoemulsions are suitable for solubilising the highly hydrophobic antifungal drug amphotericin B and formulations have been shown to generate inhalable aerosols by air-jet nebulisation (results have been submitted for publication).

Intralipid is composed of egg phospholipids, soybean oil and glycerine, while Clinoleic is made up of refined Olive oil (80%) and soybean oil (20%). Thus, the effects of different excipients in formulations were investigated in terms of formulation stability when Paclitaxel was included and with regard to the activity against the glioma cell lines. The findings were compared with paclitaxel by itself (without a delivery vehicle) in terms of anti-cancer effect and their toxicity against normal glial cells.

## **1.6 Working Hypothesis**

The main aim of this project is to test the hypothesis that Nanoemulsion formulations play an effective role as drug-delivery vehicles for hydrophobic drugs for the treatment of glioma.

## **1.7 Aims of the study**

- To solubilize the hydrophobic anti-cancer agent paclitaxel into two different nanoemulsions formulations using various concentrations.
- To characterize the nanoemulsion formulations on the basis of size, PDI, zeta potential and pH.
- To carry out a stability study on both nanoemulsion formulations to investigate how the size, PDI, zeta potential and pH are affected by storing the formulations at different temperatures (room temperature and 4° C) over a period of two weeks.
- To measure the loading efficiency of the nanoemulsion formulations to find the amount of drug loaded onto the nanoemulsion droplets.
- To analyse the effect of these formulations on two glioma cell lines: U87-MG (normal glial cells) and SVG-P12 (grade IV glioma cells)

# **Chapter 2 :**

## **Materials and Methods**

## **2.1 Materials**

### **2.1.1 Chemicals**

<b>Supplier</b>	<b>Products</b>
European Collection of Cell cultures (ECACC)	U87-MG – Grade IV glioma cells  SVG-P12 – normal glial cells
Baxter Healthcare, USA	ClinOleic TPN 20%
Fresenius Kabi, Germany	Intralipid TPN 20%
Lonza, Switzerland	Eagle’s Minimum Essential media (EMEM) (Lonza, Switzerland), Non-essential amino acid solution (100x), 2 mM L-glutamine
Sigma Aldrich, UK	Sodium Pyruvate, Phosphate Buffer Saline (PBS), Trypan Blue, Dextran (mol wt. 5000), Poly-L-Lysine (PLL – mol wt 70,000), Phosphate buffered saline, Paclitaxel, Dimethyl sulfoxide (DMSO).
Fisher Scientific, UK	Trypsin-EDTA solution, Absolute Ethanol, 70% Ethanol, HPLC grade water

**Table 2.1: List of chemicals and their suppliers.**

### **2.1.2 Equipment**

Zetasizer Nano zs (Malvern Instruments, UK), UV Spectrophotometer (Biowave, UK), Inverted microscope (Leica DMIL microsystems, Germany), Eclipse e200 Compound Microscope (Kodak, Japan), Corning 220 pH meter (Cole-Palmer, UK), pipette controller (Bio-gene, UK), Plate reader (Tecan, Switzerland), grant sub28 water bath (Grant instruments, UK), Galaxy 170s CO<sub>2</sub> incubator (New Brunswick, Scotland), Laminar flow safety cabinet (Gelaire flow laboratories, Italy), Sigma 3-16 pk centrifuge (DJB Labcare, Germany), Whirlimixer (FESONS, UK),

## **2.2 Methods**

### **2.2.1 Solubilisation of Paclitaxel in nanoemulsion formulations**

Paclitaxel was weighed in increasing amounts of 10, 20, 30, 40, 50 and 60 mg in separate glass vials using a weighing balance. 10 ml of Clinoleic or Intralipid was added to each glass vial. Glass vials were vortexed for 5 min and then kept in a bath sonicator at 40° C for 2 h.

### **2.2.2 Characterization of the Nanoemulsion formulations**

The Zetasizer Nanoseries zs (Malvern Instruments Ltd, UK) was used to measure the size and zeta potential of the nanoemulsions. The Zetasizer employs the principle of Photon correlation Spectroscopy (PCS) and accurately measures size in the range of 0.3 nm to 10  $\mu\text{m}$ . 40  $\mu\text{l}$  of nanoemulsion sample was mixed with 1 ml of HPLC grade water in a cuvette and the average of three readings was calculated. Specialized cuvettes were used to measure the zeta potential. The pH was measured using a pH meter. The pH meter was first calibrated using the provided pH 4 and pH 7 solutions and then the measurement of each nanoemulsion sample was conducted with washing the electrode by distilled water after each measurement.

### **2.2.3 Stability studies**

Two sets of Formulations containing 0, 10, 30 and 60 mg of Paclitaxel each per 10 ml of nanoemulsion were prepared for both ClinOleic and Intralipid. One set of each was stored in the refrigerator (at 4°C) and the second set of each was stored at room temperature (approximately 23°C) for a period of 2 weeks. Their size, zeta potential and pH were regularly measured using the Zetasizer and the pH meter. Also, changes in their physical appearances were noted at the end of the 2 weeks.

### **2.2.4 Calibration curve of Paclitaxel**

10 mg of paclitaxel was weighed in a 100 ml volumetric flask which was then filled with absolute ethanol to make the volume up to 100 ml (Stock solution). The solution was

stirred till the paclitaxel had completely dissolved in the ethanol. A serial dilution was then carried out by mixing the stock solution with ethanol as demonstrated in Table 2.2 –

<u>Concentration required</u> <u>(mg/100 ml)</u>	<u>Amount of stock solution</u> <u>added (ml)</u>	<u>Amount of ethanol added</u> <u>(ml)</u>
1	1	9
2	2	8
3	3	7
4	4	6
5	5	5
6	6	4
7	7	3
8	8	2
9	9	1
10	10	0

**Table 2.2: A table showing the amount of stock solution and ethanol to be used to make serial dilutions.**

The absorbance of each sample was measured at 270 nm and a calibration curve was plotted using the absorbance values obtained. The  $R^2$  value and calibration curve equation were obtained.

### **2.2.5 Loading efficiency using UV Spectrophotometer**

The nanoemulsion formulations containing paclitaxel in the amounts of 10, 30 and 60 mg per 10 ml were filtered through a 400 nm syringe filter. The residual (un-entrapped) crystals of paclitaxel left behind on the filter were dissolved in 10 ml of ethanol and their absorbance was measured at 270 nm. These absorbance values were then substituted in the equation obtained from the calibration curve to find out the amount of the un-entrapped drug in mg. The amount of un-entrapped drug was then subtracted from the total amount of drug added in the formulation to find out the quantity of the entrapped drug.

### **2.2.6 Tissue culture**

All tissue culture procedures were carried out aseptically in a Laminar flow safety cabinet and all materials were sterilised by autoclaving before use. Materials and media were warmed to 37° C before adding to the cells to avoid shock. Additionally, all the working surfaces were always cleaned with 70% ethanol before beginning the procedures. Experiments were carried out with passage numbers 13-31 and 7-18 for U87MG and SVGP12 respectively.

### **2.2.6.1 Preparation of tissue culture media**

A fresh bottle of media was prepared every week; separate bottles were used for U87MG and SVGP12 cell lines to avoid cross contamination.

The ingredients for the complete media were as follows –

EMEM (500 ml) + 10% foetal bovine serum (50 ml) + 2 mM L-glutamine (1 ml) + 1 mM sodium pyruvate (1 ml) + 0.1 mM (or 1%) non-essential amino acids (1 ml)

All materials were warmed to 37° C and mixed together under sterile conditions.

### **2.2.6.2 Subculture and Re-suspension of Cells.**

Cells were allowed to grow until they were 80-90% confluent (observed using an inverted light microscope). The U87MG cells were passaged every four days and the SVG-P12 cells were passaged every six days. The medium was first removed without disturbing the cells and then the cells were washed three times with PBS (10 ml). To detach the cells from the surface of the flask, a 0.25% trypsin-EDTA (Ethylenediaminetetraacetic acid) solution (1.5 ml) was added to the cells followed by incubation for 2-3 min at 37° C. Gentle agitation (tapping) to the culture flask was carried out to aid in the detachment of cells (verified by observing under the inverted microscope). Fresh media (2.5 ml) was added immediately to the detached cells to neutralize the effect of the trypsin-EDTA. The cell suspension was then centrifuged at 1000 x g for 5 min. The supernatant (trypsin-EDTA + media) was discarded and required amount of fresh media (5-10 ml) was added to the cell pellet. A syringe and needle (23 G; 0.6 mm x 25 mm) were used to re-suspend the cell pellet three times into the media, to

ensure the segregation of the cells. The cells were then added to new culture flasks at the appropriate seeding density.

### 2.2.6.3 Cell Counting

Viable cell count was obtained by mixing 100  $\mu\text{l}$  of the cell suspension (obtained after re-suspending the cells in fresh media, as described earlier) with 100  $\mu\text{l}$  of trypan blue solution and 10  $\mu\text{l}$  of the mixture was placed on the Neubauer Haemocytometer slide with a cover slip properly placed on top of the chamber. The non-viable cells had taken up the dye and were stained blue, while the viable cells appeared pale yellow.

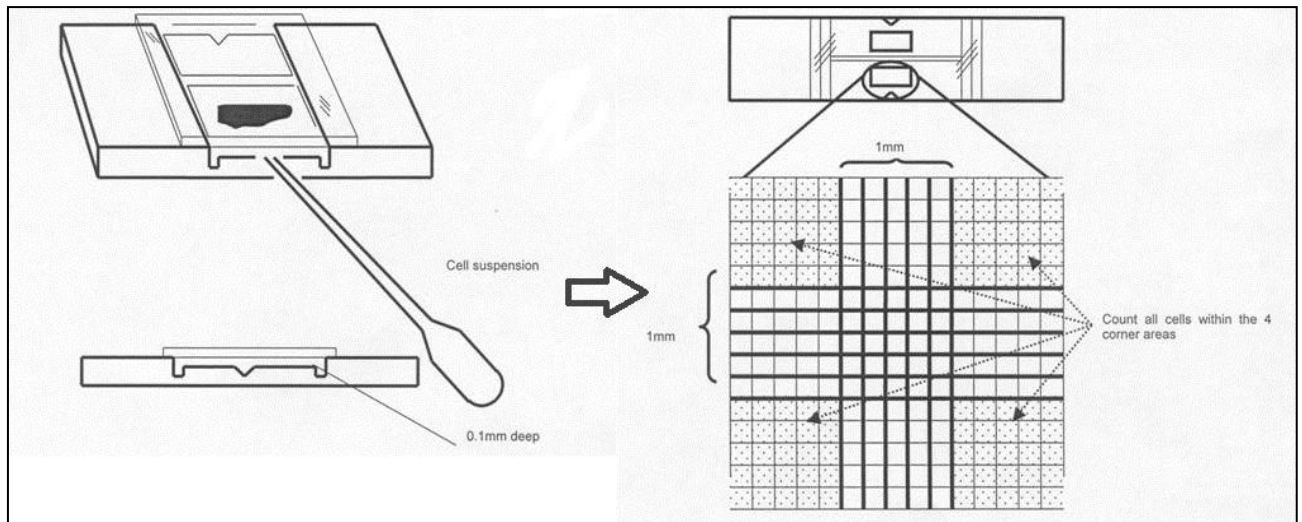


**Figure 2.1: Neubauer Haemocytometer, each large square gives an area of  $1 \text{ mm}^2$  (1 mm x 1 mm) with a depth of 0.1 mm.**

Since, a large square is  $1 \text{ mm}^2$  in area; each large square provides  $0.1 \text{ mm}^3$  ( $1 \text{ mm} \times 1 \text{ mm} \times 0.1 \text{ mm} = 10^{-4} \text{ cm}^3$  or  $10^{-4} \text{ ml}$ ) of cells. The average number of viable cells per ml was obtained by measuring the number of viable cells in five large squares (then divided

by five to achieve average) and then multiplied by the dilution factor (x2, as the cell suspension was diluted 1:1 with trypan blue solution) and x 10<sup>4</sup>.

#### **2.2.6.4 Seeding and Growth curves**

The cells were seeded into 96 well plates for the MTT (3-(4,5-Dimethylthiazol-2-yl)-2,5-diphenyltetrazolium bromide) assay. To determine the most appropriate seeding density, growth curves were constructed. For the growth curves, cell suspensions were diluted to attain the densities of 10<sup>3</sup>, 10<sup>4</sup> and 10<sup>5</sup> cells per well. This was done using the following equation –

$$C_1 \times V_1 = C_2 \times V_2$$

Where, C<sub>1</sub> is the cell viability count (obtained via using the haemocytometer)

V<sub>1</sub> is the total amount of cell suspension to be added to fresh media (unknown factor)

C<sub>2</sub> is the required cell density (10<sup>3</sup>, 10<sup>4</sup> or 10<sup>5</sup>) and

V<sub>2</sub> is the total volume of cells + media required to fill the 96 wells.

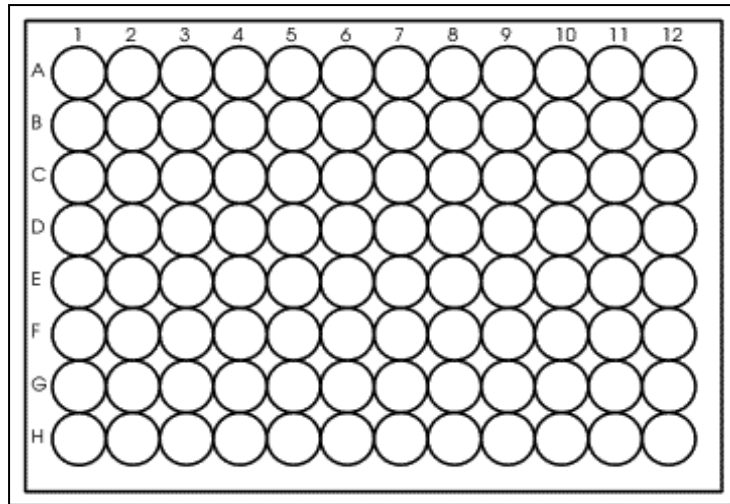


**Figure 2.2: A 96 well plate template. A 96 well plate is made up of twelve columns (numbered 1-12) and eight rows (A-H)**

The outer rows and columns (columns 1 and 12 and rows A and H) of the well plate were filled with Phosphate buffered saline (PBS) to avoid evaporation of the cell suspension. Columns 2-4 were filled with 200  $\mu$ l each with the  $10^3$  cells/well dilution and columns 5-8 were filled with the  $10^4$  cells/well dilution and columns 9-11 were filled with the  $10^5$  cells/well dilution.

Five plates were prepared for both of the cell lines to check their growth over a seven-day period (Tue-Fri, Mon). They were incubated at 37° C for 24 h, 48 h, 72 h, 96 h and 144 h respectively. Each morning, 5 h before the end of the incubation times, 20  $\mu$ l of MTT solution (5mg MTT dissolved per ml of PBS) was added to each well and kept back in the incubator. Viable cells reduce the MTT to a water-insoluble blue-coloured salt called formazan. Then, at the end of the incubation time, all the MTT-containing media (220  $\mu$ l) was pipetted out from the wells carefully, to avoid disturbing the blue formazan crystals at

the bottom of the plate. This was followed by addition of 100 µl of cell-culture grade DMSO (Dimethyl sulfoxide) to each well in order to solubilise the formazan crystals. The plates were then further incubated for 30 min at 37° C before spectrophotometric analysis at 612 nm using the Tecan microtitre plate reader. The absorbance readings were then plotted on a graph and the most appropriate seeding density was chosen for the cytotoxicity assays.

#### **2.2.6.5 Cytotoxicity assay (MTT)**

The cytotoxicity of the nanoemulsion formulations (with and without paclitaxel) and paclitaxel alone were tested on both the cell lines using the MTT assay. Their results were compared against the positive control Poly-L-lysine (PLL) and the negative control Dextran.

A paclitaxel solution was made by adding 30 mg of the drug to 100 µl of ethanol. The formulation was kept in the water bath at 50° C until the paclitaxel was completely dissolved. Then 4.9 ml of media were added to the formulation to make up a final volume of 5 ml (and to achieve a drug concentration of 6mg/ml). Dextran and PLL solutions were made by adding the compounds directly to the media (as they are water soluble) to achieve a formulation with a concentration of 5 mg/ml.

Cells at the chosen seeding density were seeded into the inner rows of the 96 well plates. A different well plate was used for each formulation. The cells were then allowed to grow for 24 h. At the end of the 24 h, the formulations were added to all the inner wells of the plate in ascending concentrations. All the formulations were filtered using 0.4 µm

and 0.22  $\mu\text{m}$  sterile syringe filters before addition to the plates to avoid contamination.

The concentrations for the formulations are as follows –

Column number	2	3	4	5	6	7	8	9	10	11
Concentration (mg/ml)	0	0.001	0.005	0.01	0.05	0.1	0.5	1	3	6

(Note: columns 1 and 12 contain PBS, hence no formulations were added to them)

**Table 2.3: Concentrations at which the controls/formulations were added to the 96-well plates**

The cells were then incubated for 72 h. MTT (20 $\mu\text{l}$ ) was added to each well 5 h before the end of incubation. At the end of incubation time, the wells were emptied and 100  $\mu\text{l}$  of DMSO was added to each well before their absorbance was read at 612 nm. The absorbance readings were then plotted on a graph to compare the toxicity of the compounds.

### 2.3 Statistical analysis

All the experiments were performed three times and the results were expressed as mean  $\pm$  SD. The student's *t*-test and one-way ANOVA tests were performed using SPSS 14.0 software to calculate the significance between groups. A difference was considered to be significant if the P-value was less than 0.05.

**Chapter 3:**

**Characterization of Nanoemulsion**

**Formulations**

Paclitaxel is a widely-used anti-cancer agent. In the past 20-25 years paclitaxel has been proven to be effective against ovarian, lung, breast, head and neck cancers. Paclitaxel inhibits mitosis by disrupting microtubule integrity, thereby causing cell death (Sheng *et al*, 1999). But paclitaxel has a major drawback: it exhibits low aqueous solubility of less than 0.01 mg/ml (Surapaneni *et al*, 2012). Hence to be administered intravenously, paclitaxel requires a lipid-based delivery vehicle.

Nanoemulsion formulations are essentially oil droplets dispersed in an aqueous phase. Lipophilic drugs like paclitaxel readily dissolve in the lipid phase of nanoemulsions and can be easily administered intravenously due to the external aqueous phase. Nanoemulsions may help the drug to escape the RES as are made of phospholipids (the same materials that the body cells are made from) or similar materials as the RES cells might not view them as toxic substances, providing that the formulation is robustly optimized (Eccleston, 2006). Hence, the drug might be able to reach the tumour site in larger concentrations. Nanoemulsion formulations may also help in enhancing the permeability of these drugs across the BBB as due to their extremely small size they might be able to pass through the BBB in advanced cases of glioma (Garcia-Garcia, 2005).

The characteristics of nanoemulsions were studied before and after the inclusion of the anti-cancer drug Paclitaxel in order to evaluate the effect of the drug on the formulations. Intralipid TPN and Clinoleic TPN were the two commercially available nanoemulsion formulations used in these experiments and compared against each other. These two formulations differ in their compositions (Table 3.1)

<b>Clinoleic TPN</b>	<b>Intralipid TPN</b>
<ul style="list-style-type: none"> <li>- Mixture of refined olive oil (approx. 80%) and refined soybean oil (approx. 20%) 20 g</li> <li>- Essential fatty acids 4 g</li> <li>- Glycerol 2.25 g</li> <li>- Purified egg phosphatides 1.2 g</li> <li>- Sodium oleate 0.03 g</li> </ul>	<ul style="list-style-type: none"> <li>- Refined soybean oil 20 g</li> <li>- Purified egg phospholipids 1.2 g</li> <li>- Glycerol anhydrous 2.2 g</li> </ul>

Table 3.1: Compositions of Clinoleic and Intralipid TPN.

Another important aspect that was investigated was the stability of these formulations. Any mixture of oil and water is susceptible to instabilities but these can be avoided (or delayed) by storing the formulations at the right temperature. Two sets of formulations of Clinoleic and Intralipid were stored at room temperature and at 4° C and their characteristics were investigated over a period of 14 days.

Paclitaxel was added to the formulations in increasing concentrations of 1 mg – 6 mg per ml of nanoemulsion. The loading efficiency experiments of paclitaxel in nanoemulsions were carried out to find the amount of drug the nanoemulsions can accommodate and retain.

In this chapter, nanoemulsion formulations were characterised in terms of their size, zeta potential, polydispersity index, and pH using a range of paclitaxel concentrations. Also, the loading efficiency of the drug in nanoemulsions was investigated.

### 3.1 Size of the nanoemulsion formulations.

According to Figure 3.1, the droplet size of both Clinoleic and Intralipid increased when more paclitaxel was loaded into the formulations. This indicates the inclusion of the drug into the droplets. Droplet size of the Clinoleic emulsion increased from 254.1 nm to 264.7 nm when paclitaxel (6 mg/ml) was loaded into the formulation, which is a 4.17% increase in size. Similarly with the Intralipid emulsion, the measured size was 283.3 nm and upon inclusion of 6mg/ml paclitaxel the size increased to 294.6 nm, which is a 3.99% increase in size.

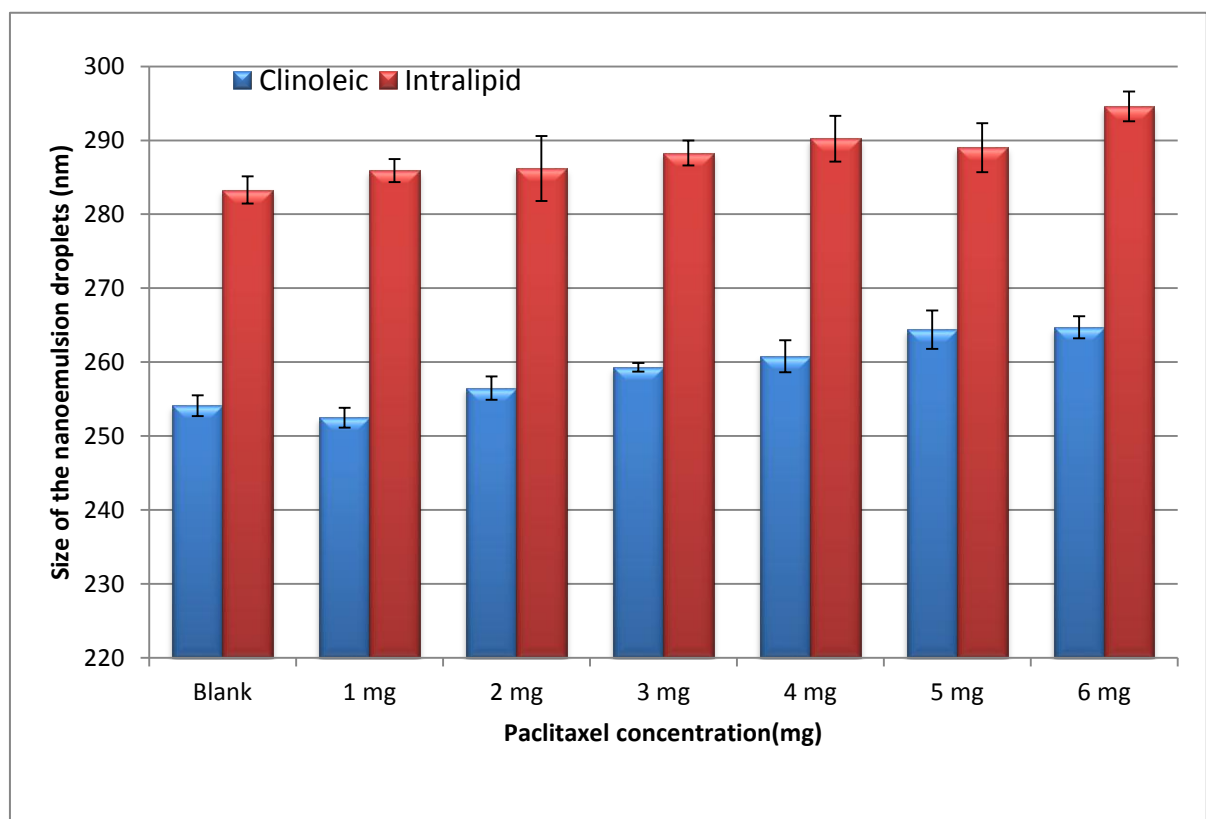


**Figure 3.1: Size between formulations of Clinoleic and Intralipid using a range of paclitaxel concentrations (n=3,  $\pm$  SD)**

Statistical analysis showed that the sizes increased significantly for Clinoleic when 3 mg/ml or more paclitaxel was loaded ( $P < 0.05$ ). However for the Intralipid nanoemulsions, the increase in size was significant ( $P < 0.05$ ) only when 6 mg/ml paclitaxel was added. The increase of droplet size as a result of drug loading indicates that paclitaxel has possibly influenced the interfacial properties of the o/w emulsions, suggesting that drug molecules might partially localise at the o/w interface (Nasr *et al*, 2012). Mastropaolo *et al*, 1995 studied the structure of paclitaxel encapsulated into lipid-carriers and found that the size of the particles differed from 2 nm to 800 nm and displayed a wide variety in shape. This may be another reason why there is an increase in droplet size on addition of drug.

### **3.2 Polydispersity Index (PDI) of nanoemulsion formulations**

According to Figure 3.2, the PDI of all nanoemulsion formulations were lower than 0.2 regardless of emulsion type and paclitaxel concentration. Previous studies using extruded liposomes (0.4  $\mu\text{m}$ ) showed PI values around 0.5 (Elhissi *et al*, 2007). This indicates that all nanoemulsions were highly homogenous when compared to liposomes.

For nanoemulsions, the droplets are considered monodispersed if the PDI value is under 0.2 (Bernardi, 2011). A monodispersed suspension possibly means that the drug paclitaxel is accommodated in the bulk of the oil droplets and is not leaking out of the nanoemulsion droplets. It is hence expected that if paclitaxel was leaking out (i.e. located at the aqueous

phase or the interfacial region of the emulsion), the PDI might become higher as paclitaxel crystals have different shape and size compared to nanoemulsion droplets.

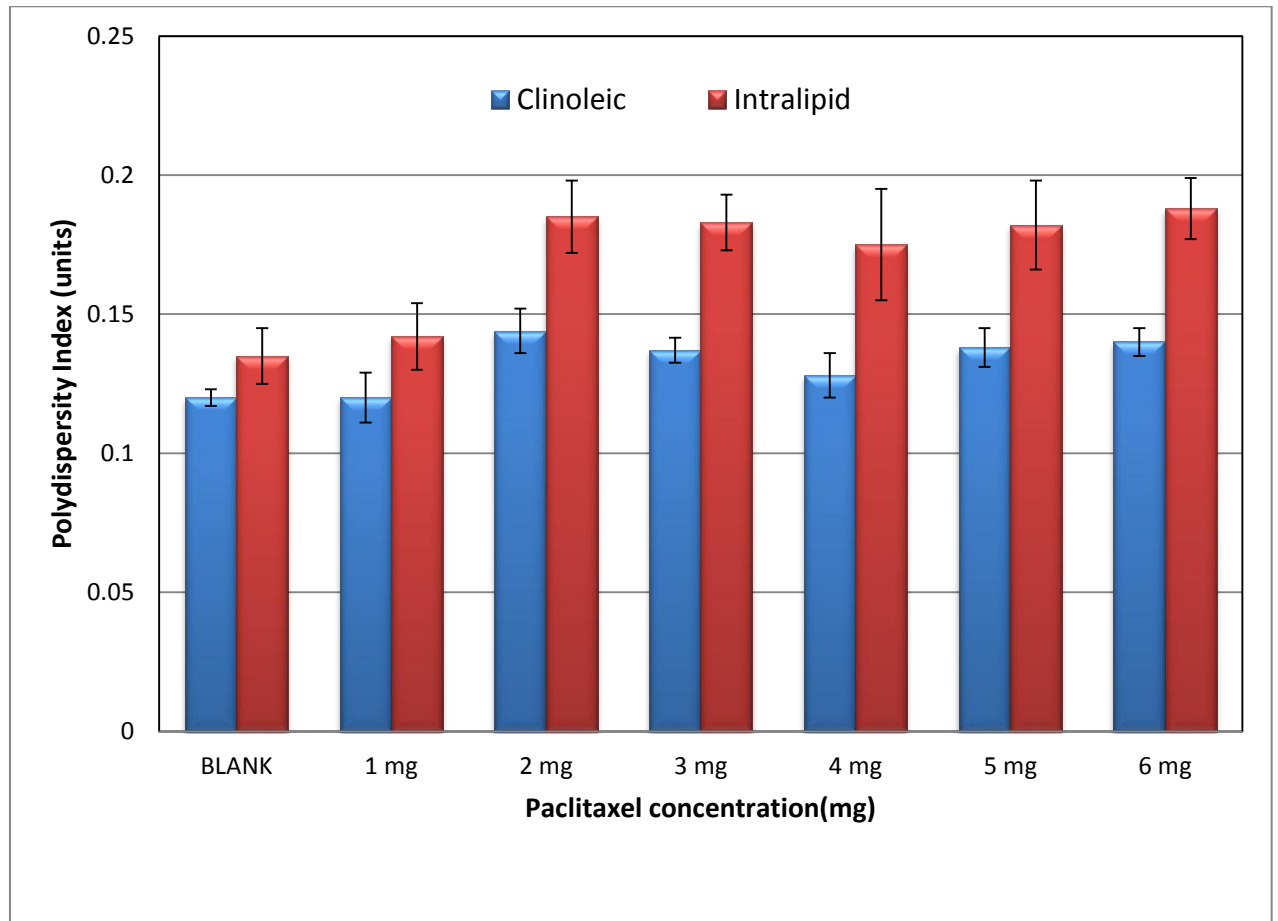
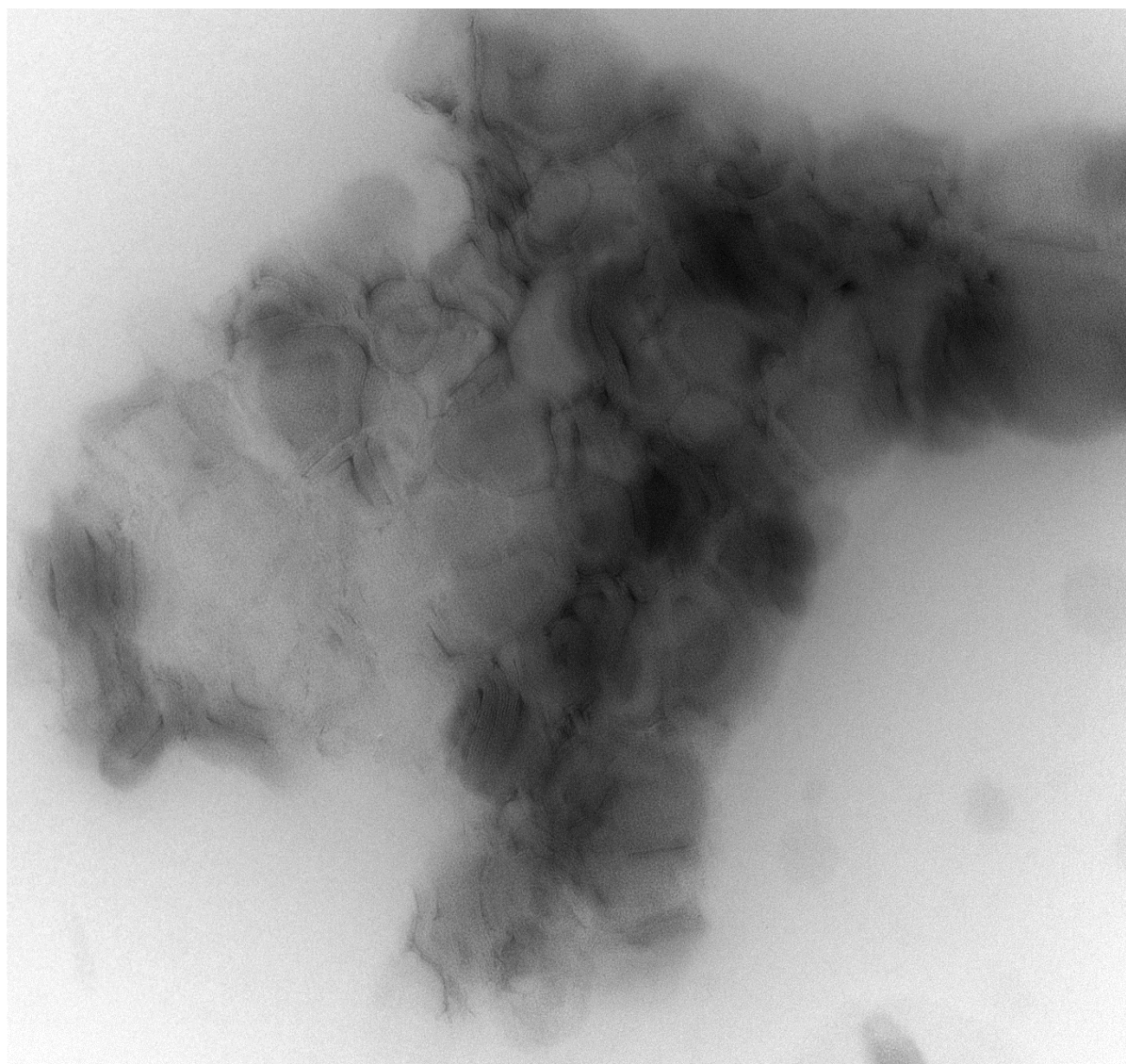


**Figure 3.2: PDI values for the Clinoleic and Intralipid nanoemulsions (n=3,  $\pm$  SD).**

There was a 16.6 % rise in the PDI of Clinoleic when 6mg/ml paclitaxel was added. By contrast there was an increase by 39.25% in the PDI of Intralipid when 6mg/ml of paclitaxel was added. This indicates that Clinoleic retains its homogeneity more successfully compared to the Intralipid emulsions on addition of paclitaxel.

The greater size and higher PDI of the Intralipid droplets for both drug-free and loaded nanoemulsions suggests that the different ingredients had an influence on the size and size distribution of the nanoemulsion droplets.



Ald.tif

2185.A1 1%UA

Alish Clinoleic

10:05:40 14/06/2012

100 nm

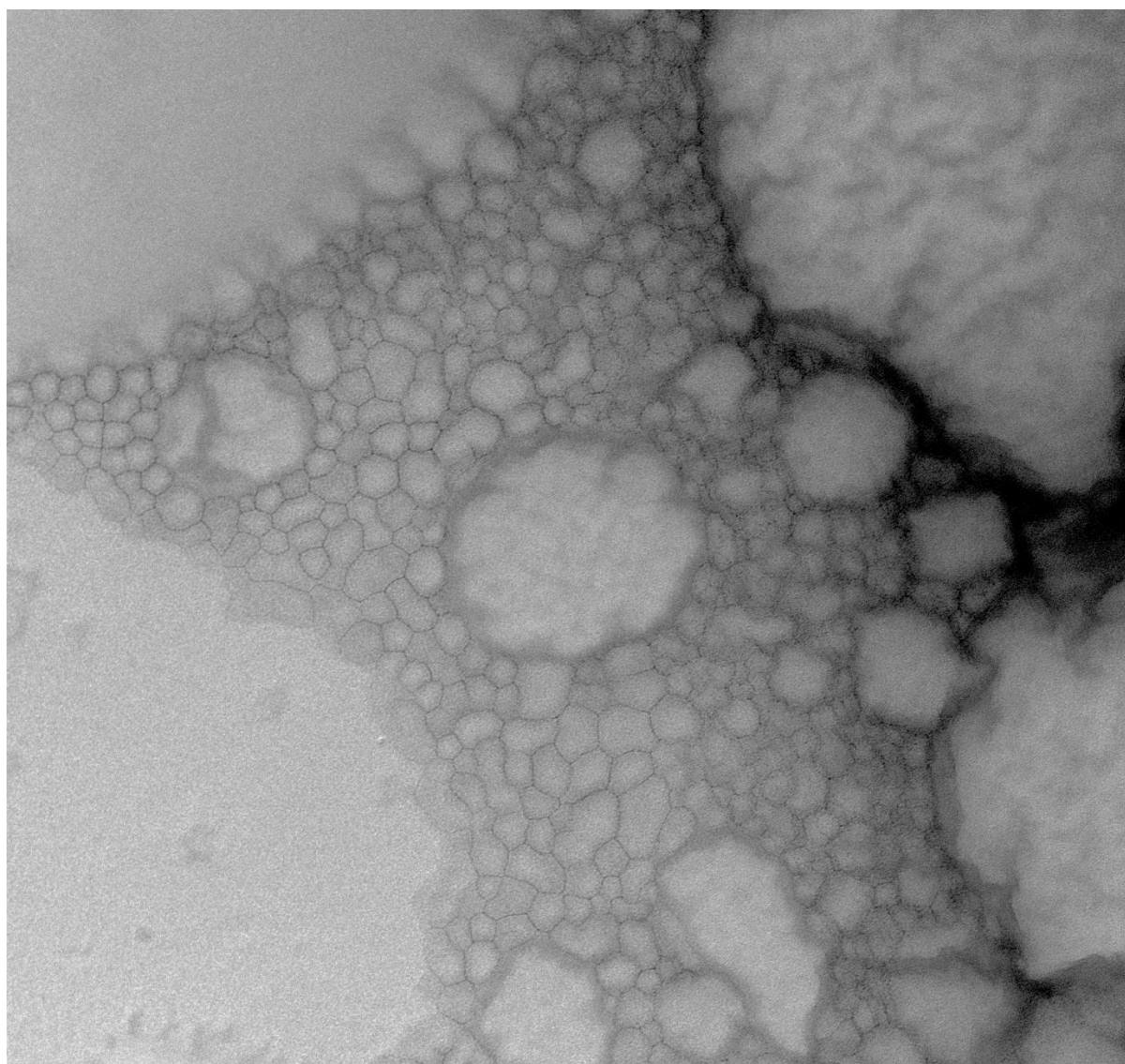
HV=120.0kV

Direct Mag: 65000x

UCL School of Pharmacy

**Figure 3.3: TEM photograph of the Clinoleic formulation with a paclitaxel concentration of 3 mg/ml.**

Figure 3.3 shows a TEM image of the Clinoleic nanoemulsion (with a paclitaxel concentration of 3mg/ml). The size according to the scale provided matches with the size obtained from the characterization study shown in Figure 3.1 (approximately 250 nm). It is apparent that the size of the droplets are evenly arranged, this is confirmed by the PDI values shown in Figure 3.2. Some aggregates are also observed in the image, these occur as the sample tends to dry whilst capturing the image. Also, phospholipid bilayers are observed within the droplets, which are formed due to the presence of egg phosphatides in the Clinoleic TPN.



A2c.tif

2185.A2 1%UA

Alisha Intralipid

10:11:22 14/06/2012

500 nm

HV=120.0kV

Direct Mag: 65000x

UCL School of Pharmacy

**Figure 3.4: TEM image of the Intralipid nanoemulsion with a paclitaxel concentration of 3mg/ml.**

According to Figure 3.4, the size of the Intralipid formulation (with a paclitaxel concentration of 3mg/ml) is in the range of 250-300 nm according to the scale provided, hence confirming the results obtained in Figure 3.1. But the droplets are not evenly

arranged, hence leading to a higher PDI value (as confirmed in Figure 3.2). The larger droplets observed in the picture are air bubbles.

### 3.3 pH of Nanoemulsion formulations

The pH values for the Clinoleic formulations were slightly more basic than those of the Intralipid nanoemulsions (Figure 3.5). For both nanoemulsions, the influence of paclitaxel concentration on the measured pH was minimal with no specific trend of increase or decrease of pH as a result of drug inclusion. However, although influence of paclitaxel on pH seemed minimal for both nanoemulsions, the statistical analysis indicate that difference in pH was not significant ( $P>0.05$ ) only for the Intralipid formulations. But, it was significant for the 3mg/ml sample from the Clinoleic formulations ( $P>0.05$ ).

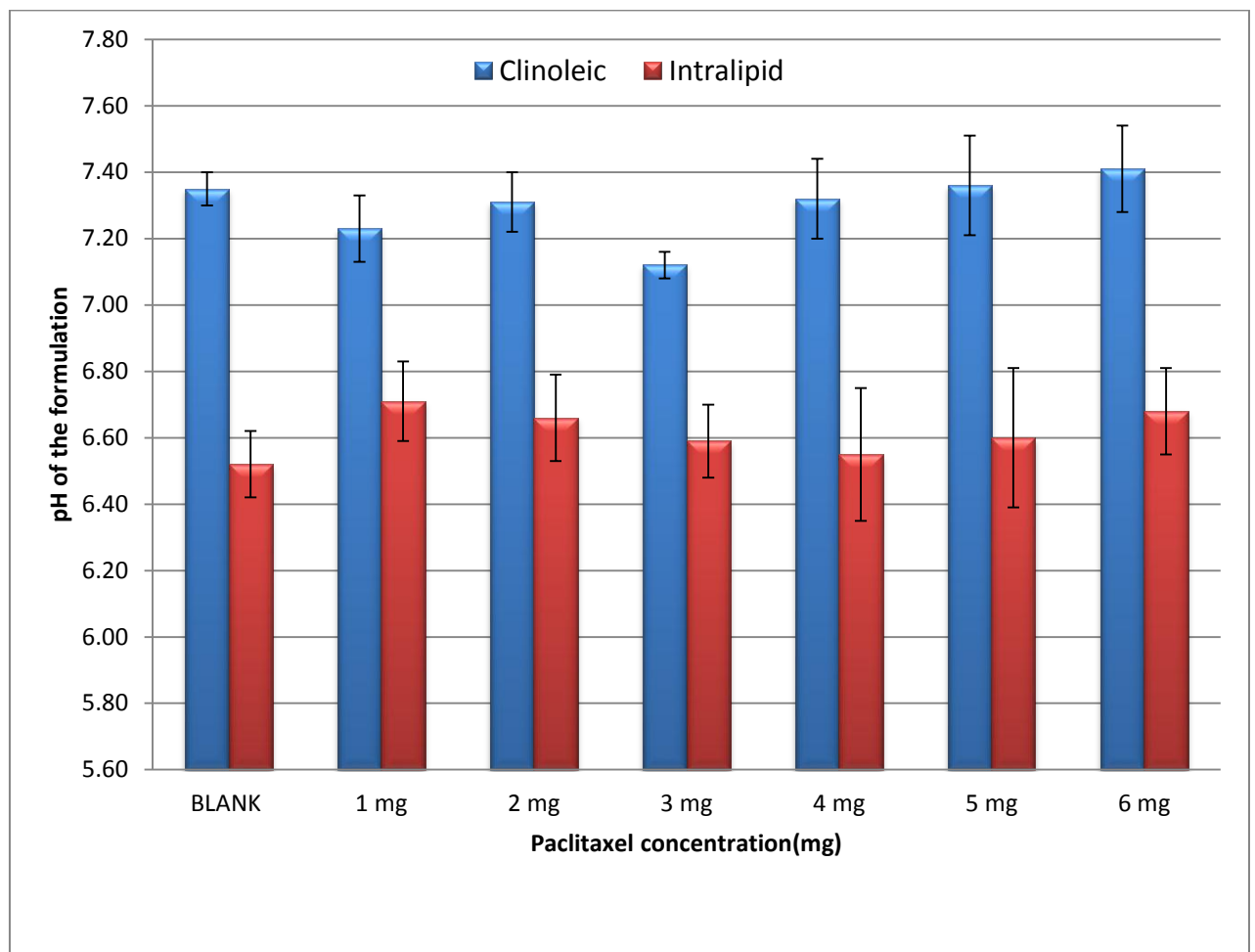


**Figure 3.5: pH of Clinoleic and Intralipid nanoemulsions using a range of paclitaxel concentrations (n=3,  $\pm$  SD).**

The pH of blood in humans is approximately 7.365. Hence if these formulations are to be injected intravenously, their pH also needs to be similar to the biological pH. A pH value in the range of 6.0-8.0 is considered ideal for intravenous administration. This clearly suggests that these nanoemulsions would be suitable for intravenous administration with accordance to pH values.

### 3.4 Zeta Potential (ZP) of Nanoemulsion formulations.

The zeta potential of Clinoleic has a higher negative intensity than that of Intralipid (Figure 3.6). The values for Intralipid are closer to neutral. This reason for this might be that Olive oil carries a ZP value closer to 0, which Soybean oil always carries a positive ZP. The values for Intralipid using paclitaxel (2 mg/ml and 4 mg/ml) are significantly higher ( $P < 0.05$ ) than that of the drug-free Intralipid emulsion. The ZP values for Clinoleic as well show a trend of decrease in the negative intensity. This indicates that paclitaxel had an influence on the surface charge of the nanoemulsion droplets.

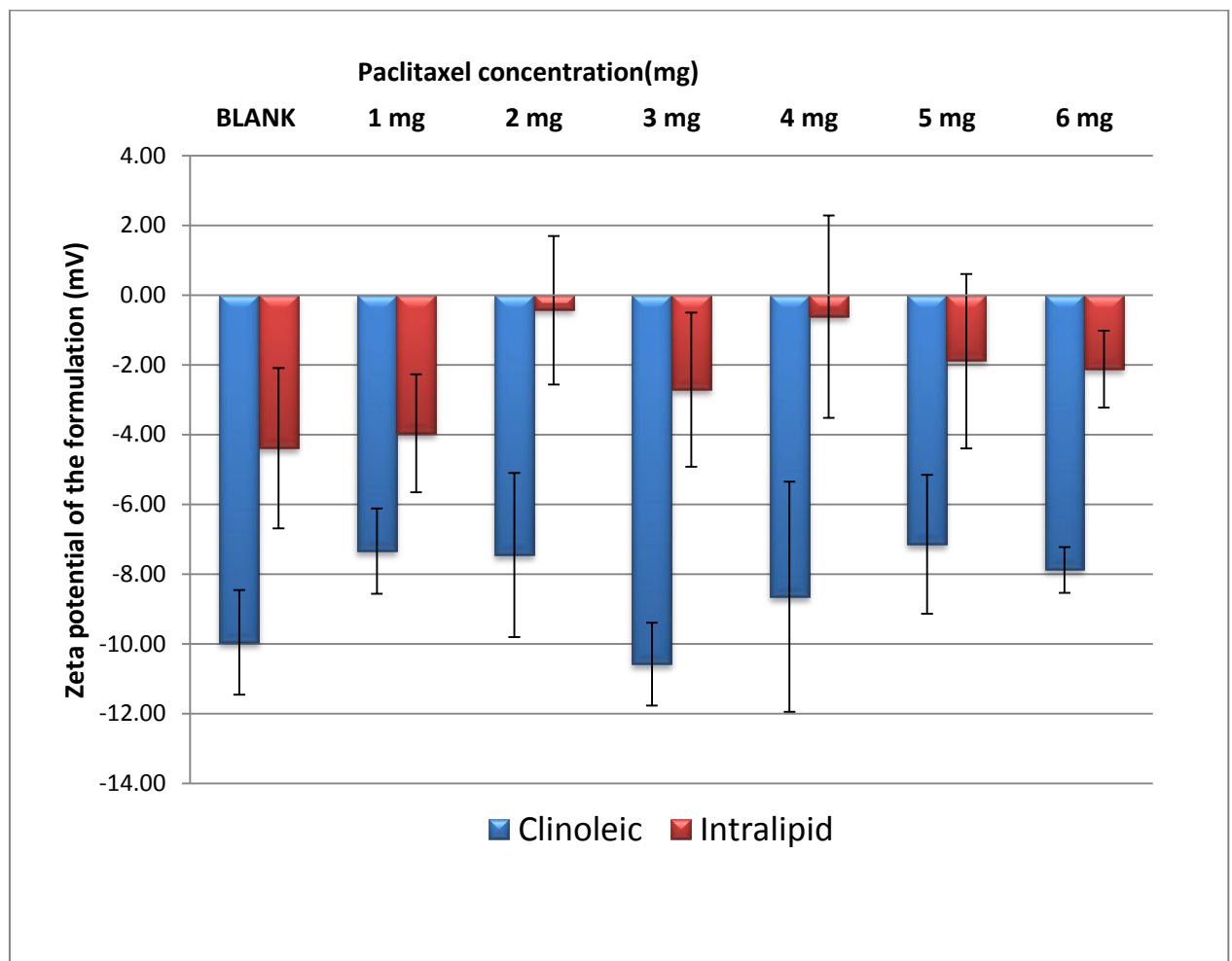


Figure 3.6: ZP values of Clinoleic and Intralipid nanoemulsions using a range of paclitaxel concentrations (n=3,  $\pm$  SD).

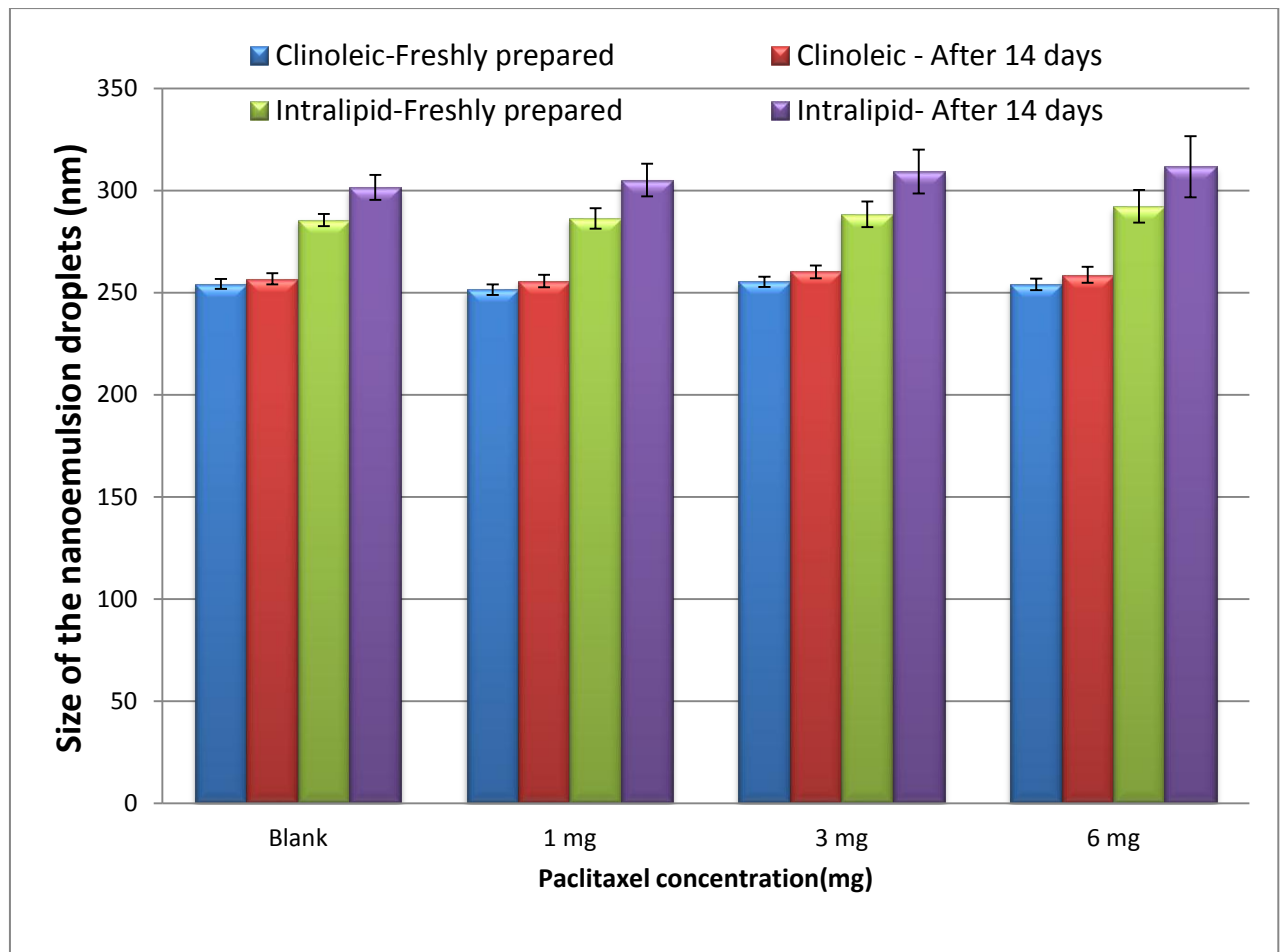
It has been previously reported that the zeta potential of a nanoemulsion formulation depends on its pH. If the pH is high (i.e. basic), the ZP value is likely to be negative and if the pH is low (acidic), the ZP value will be neutral or positive (Poluri *et al.*, 2011). For example in a recent study the ZP value of emulsified soybean oil decreased from +12mV to -20mV when the pH was increased from 2.0 to 8.0 (Iwanaga *et al.*, 2007) Thus the more negative zeta potential values of the Clinoleic emulsions might be justified by the higher pH values of this emulsion compared with the Intralipid emulsions (Figure 3.6).

For a nanoemulsion formulation to be electro-statically stable so that it is not susceptible to coalescence or breaking during storage, the ZP values should be close to or over  $\pm 30$  mV (Elsheikh *et al.*, 2012). As the values for Clinoleic are closer to  $\pm 30$  mV than the ZP values of Intralipid, it can be concluded that Clinoleic might be more electro-statically stable. Long-term stability studies using paclitaxel with Clinoleic or Intralipid emulsions are needed to verify if this assumption is correct.

### 3.5 Stability of Nanoemulsion formulations.

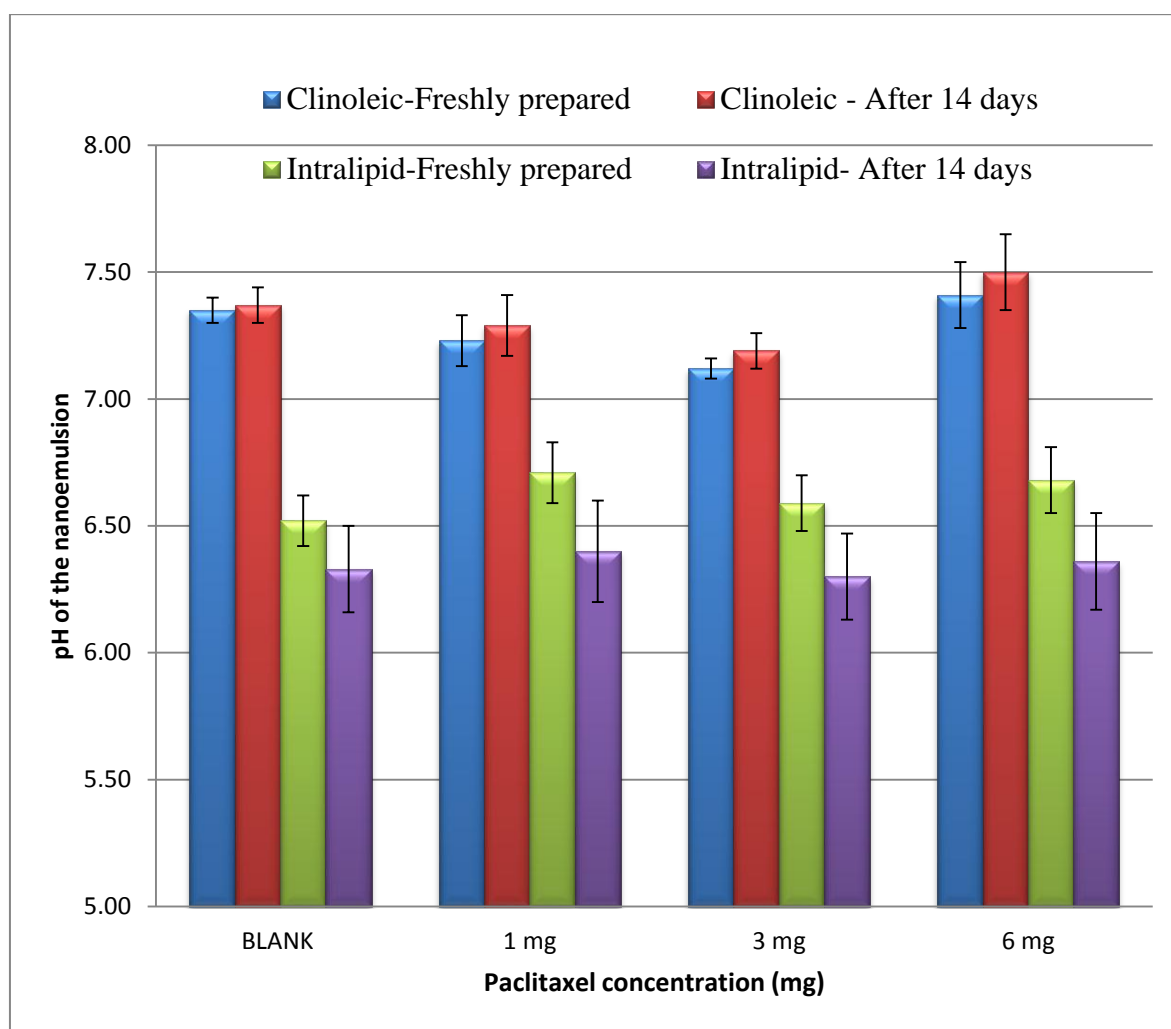
#### 3.5.1 Formulations stored at 4°C

Figure 3.7 represents the variations in size when a formulation is stored at 4°C for two weeks. For Clinoleic, the size showed a trend to increase slightly but was not significant ( $P>0.05$ ), indicating that size of droplets of this emulsion did not change upon storage for two weeks at 4°C. The minimum droplet size of the emulsion being 254.3 nm and the maximum was 258.7 nm when analysis was performed on freshly prepared samples and those stored for two weeks at 4°C.



**Figure 3.7: Size analysis of Clinoleic and Intralipid formulations stored at 4°C using a range of paclitaxel concentrations (n=3, ± SD)**

Intralipid formulations showed an increase in the droplet size over the two-week period of storage at 4°C (Figure 3.7). The minimum size measured was 285.6 nm on freshly prepared samples and the maximum was 311.7 on day 14. The statistical analysis on the Intralipid emulsions has shown that the slight increase was statistically significant ( $P>0.05$ ).



**Figure 3.8: pH analysis of Clinoleic and Intralipid nanoemulsions containing a range of paclitaxel concentrations when stored at 4°C for two weeks (n=3, ± SD)**

Figure 3.8 represents the pH values for Clinoleic and Intralipid nanoemulsions as freshly prepared and upon storage for 14 days at 4° C. Clinoleic formulations did not show any change in pH values but the Intralipid formulations showed a significant ( $p < 0.05$ ) decrease in the values after 14 days storage when compared to the freshly prepared samples, suggesting that the formulations have become acidic. For both nanoemulsions, the paclitaxel concentration had no effect or only a slight effect on the pH, indicating that it is the length of storage which affects the pH of these emulsions.

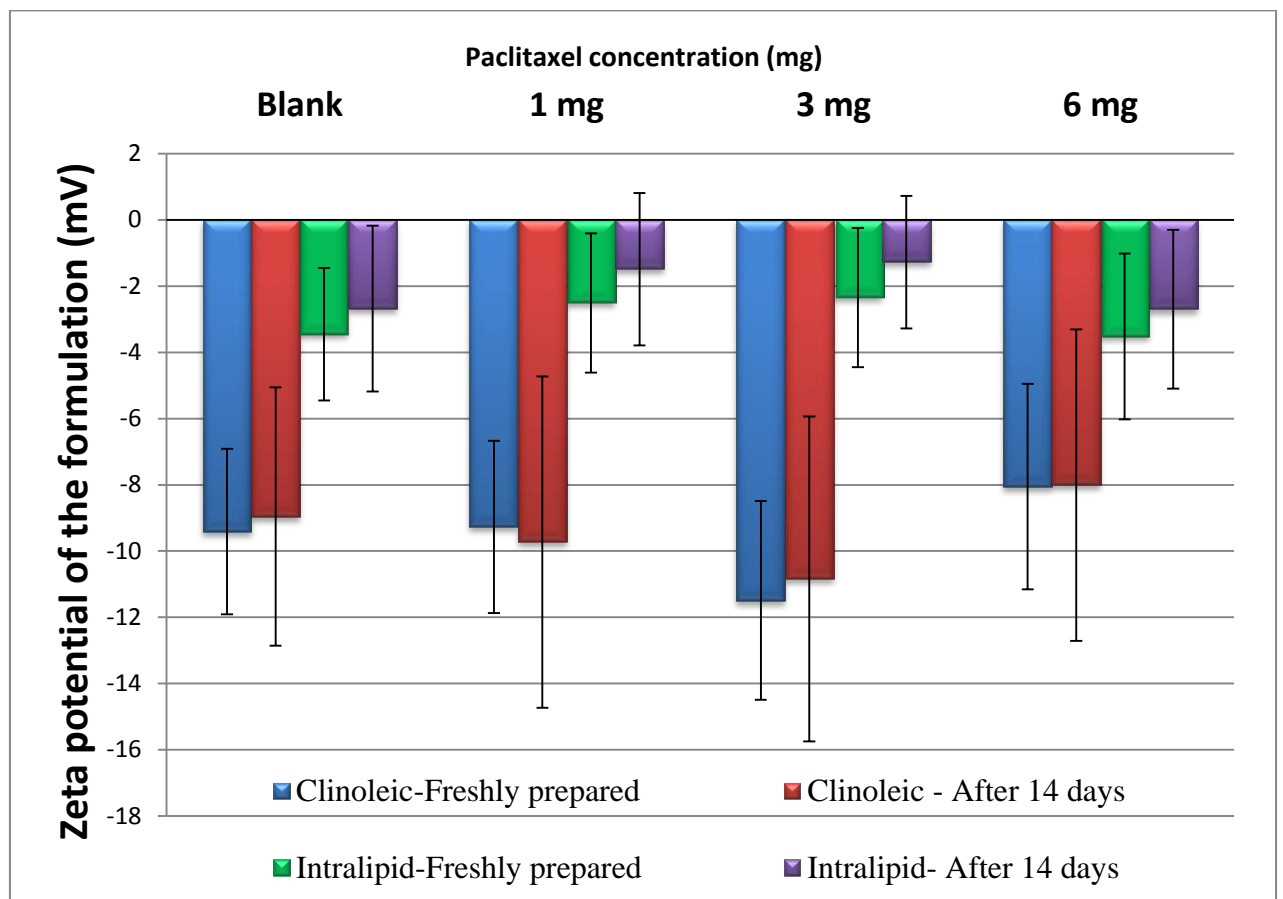


**Figure 3.9: Zeta potential analysis of Clinoleic and Intralipid nanoemulsions upon storage for two weeks at 4° C (n=3, ± SD).**

Figure 3.9 shows the changes in ZP that occur when nanoemulsion formulations are stored at 4° C for two weeks. There were no significant differences in the ZP vales for either nanoemulsion.

### **3.5.2 Formulations stored at room temperature**

The size of the Clinoleic droplets (Figure 3.10) showed a trend of slight increase when stored at room temperature, indicating that some of the paclitaxel might have collected at the surface of the droplets. However, the size of the Intralipid droplets increased significantly ( $P < 0.05$ ) suggesting that more paclitaxel has localised near the surface if the nanoemulsion droplets.

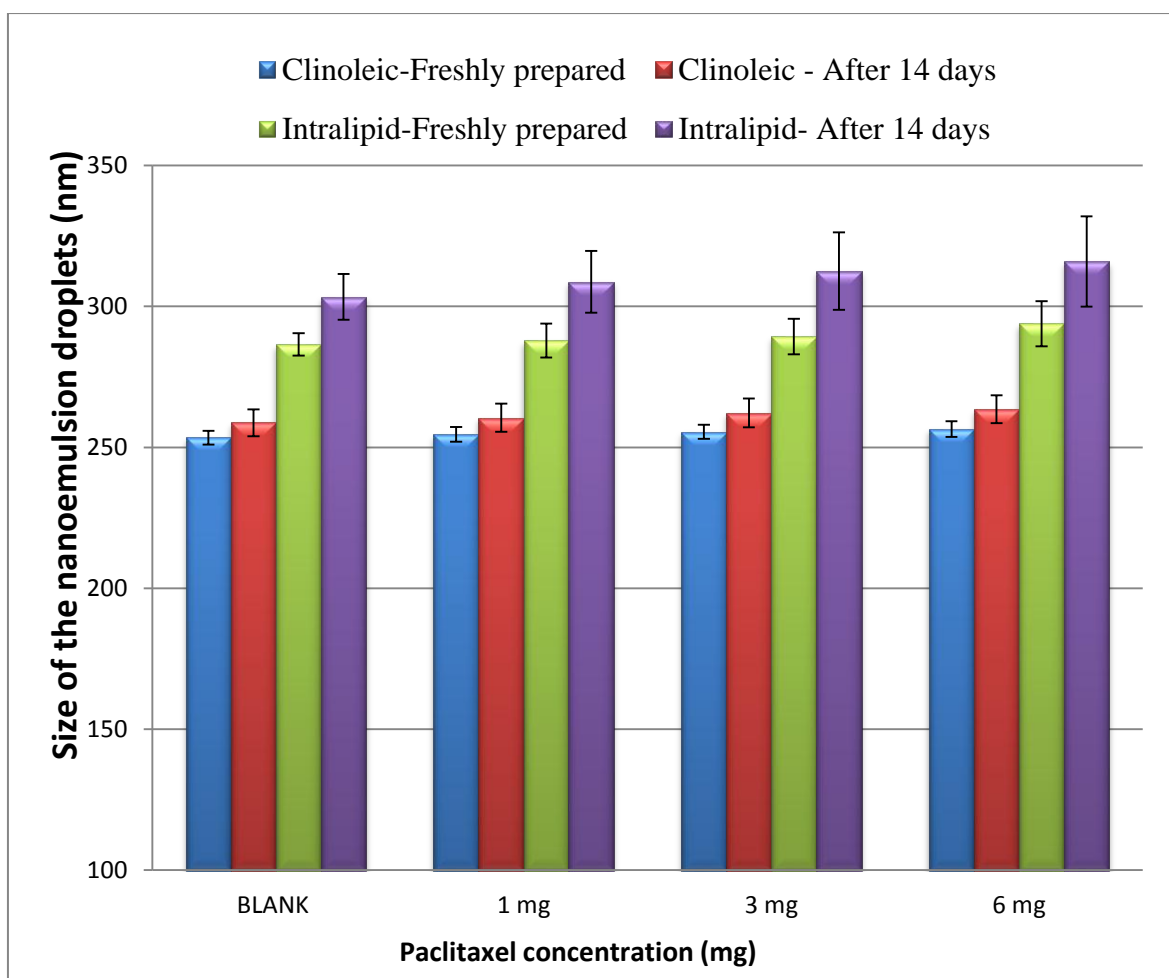


**Figure 3.10: Size analysis of Clinoleic and Intralipid formulations stored at room temperature for a 14 days (n=3,  $\pm$  SD).**

The PDI values for the Intralipid also increased from  $0.175 \pm 0.026$  to  $0.225 \pm 0.031$  when stored at RT for two weeks. This is a significant ( $P < 0.05$ ) increase in PDI which confirms that paclitaxel is causing droplet aggregation by locating at the surface of the droplets, causing them to be more hydrophobic and hence more liable to aggregation. When these values are compared with those of the formulations stored at  $4^{\circ}\text{C}$ , it is evident that the size and PDI increased more when stored at RT, suggesting that the formulations are more stable when stored at  $4^{\circ}\text{C}$ .

As shown in Figure 3.11 the pH of nanoemulsion formulations was highly dependent on storage and nanoemulsion type rather than paclitaxel concentration. This was manifested by the significant decrease ( $P < 0.05$ ) in pH of the Clinoleic and Intralipid formulations when stored at RT for 14 days (Figure 3.11)

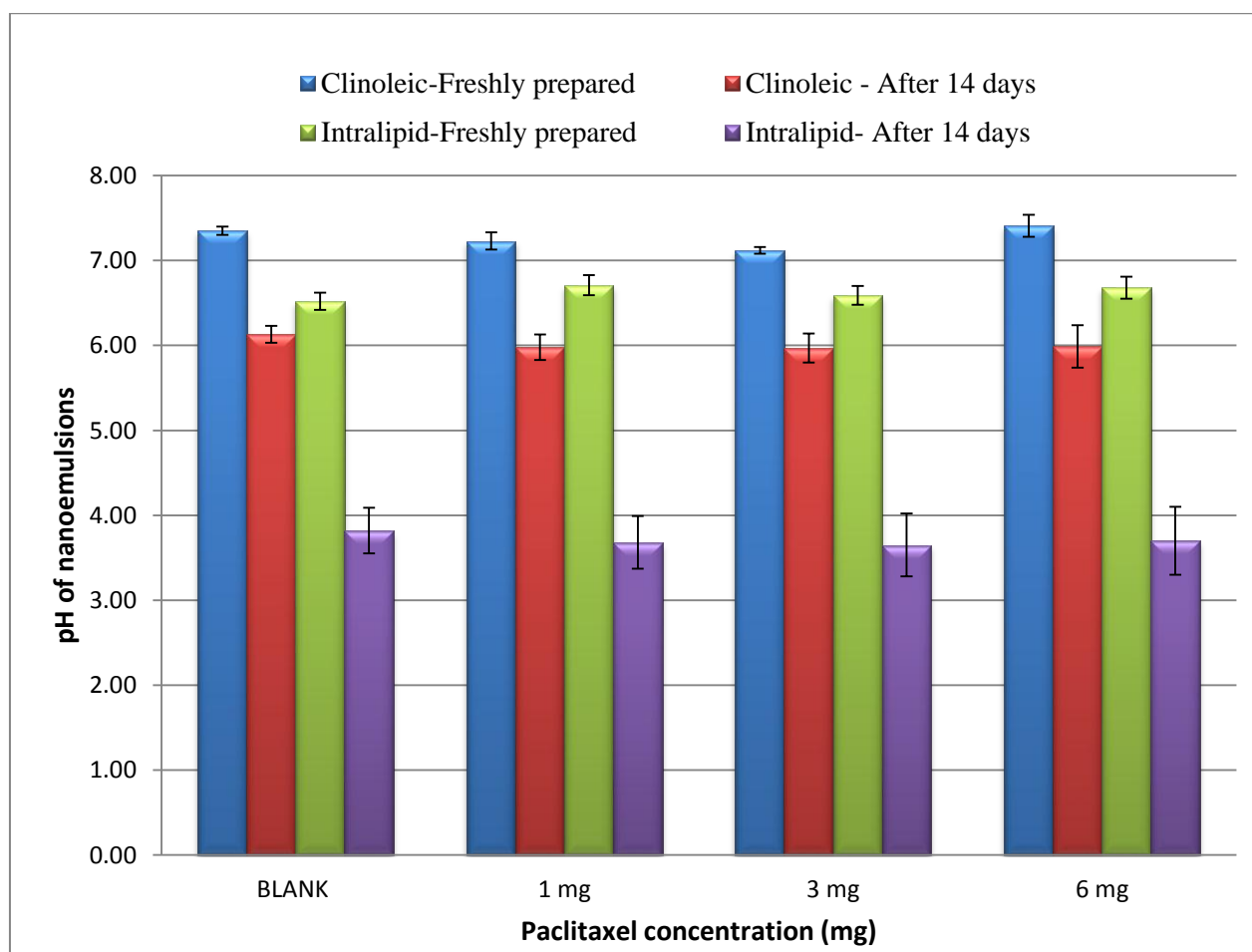


**Figure 3.11: Changes in pH for the Clinoleic and Intralipid formulations when stored for two weeks at RT ( $n=3, \pm SD$ ).**

When the above pH values are compared with the pH values of the formulations stored at 4° C (Figure 3.8), it is apparent that the pH has decreased more when the nanoemulsions were stored at RT; the pH at 4° c is in the range of 6.0-7.0. This advocates that the formulations are more stable when stored at 4° C as already confirmed via the size and PDI results. The reason for the decrease in pH might be the conversion of the olive oil

and soybean oil to Fatty acids at RT. Although this reaction might still be happening at 4° C, it will be faster at RT due to the higher temperature. Acids tend to have a lower pH (Scrimgeour, 2005); hence the pH of the whole formulation decreases after storage at RT.

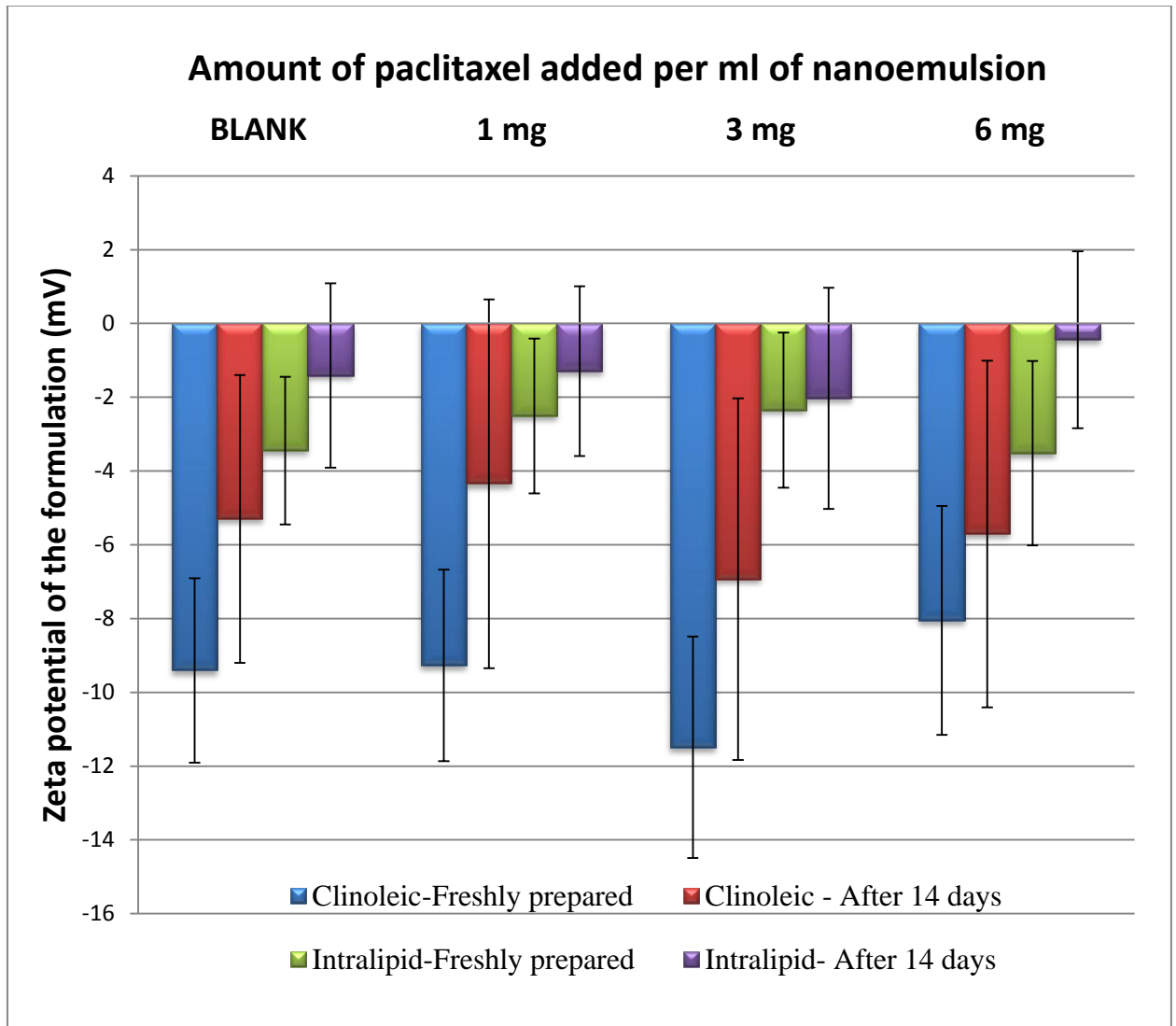


**Figure 3.12: Changes in ZP values for the Clinoleic and Intralipid formulations when stored for two weeks at RT (n=3, ± SD).**

As discussed earlier, the ZP of nanoemulsions depends on its pH. According to Figure 3.11 the pH decreases for both the nanoemulsions and as a result the ZP increases. This correlates well with the finding in Figure 3.12. There is a trend of great variability in the results indicating instabilities.

Bernardi et al (2011) stored o/w nanoemulsion at three different temperatures:  $25 \pm 2^\circ \text{C}$ ,  $40 \pm 2^\circ \text{C}$  and  $5 \pm 2^\circ \text{C}$  to test the nanoemulsions storage stability. After 90 days, they found that the droplet size had remained constant and the PDI was also below 0.2 indicating that the nanoemulsion formulations were stable at all temperatures. Only the pH reading had reduced for the sample stored at  $40 \pm 2^\circ \text{C}$ , but the pH was still in the range of 6.0-8.0. However, no drug was used in this experiment; all the formulations were drug-free. Hence, it is possible that it is the paclitaxel present in the Clinoleic and Intralipid nanoemulsions that makes the formulation unstable when stored at room temperature.

### 3.6 Loading Efficiency of nanoemulsion formulations.

A calibration curve was plotted to obtain the equation and  $R^2$  value for paclitaxel as shown in Figure 3.13. As the concentration increases, the absorbance linearly increases. Using the equation and  $R^2$  value, the entrapped paclitaxel in each nanoemulsion formulation was found.

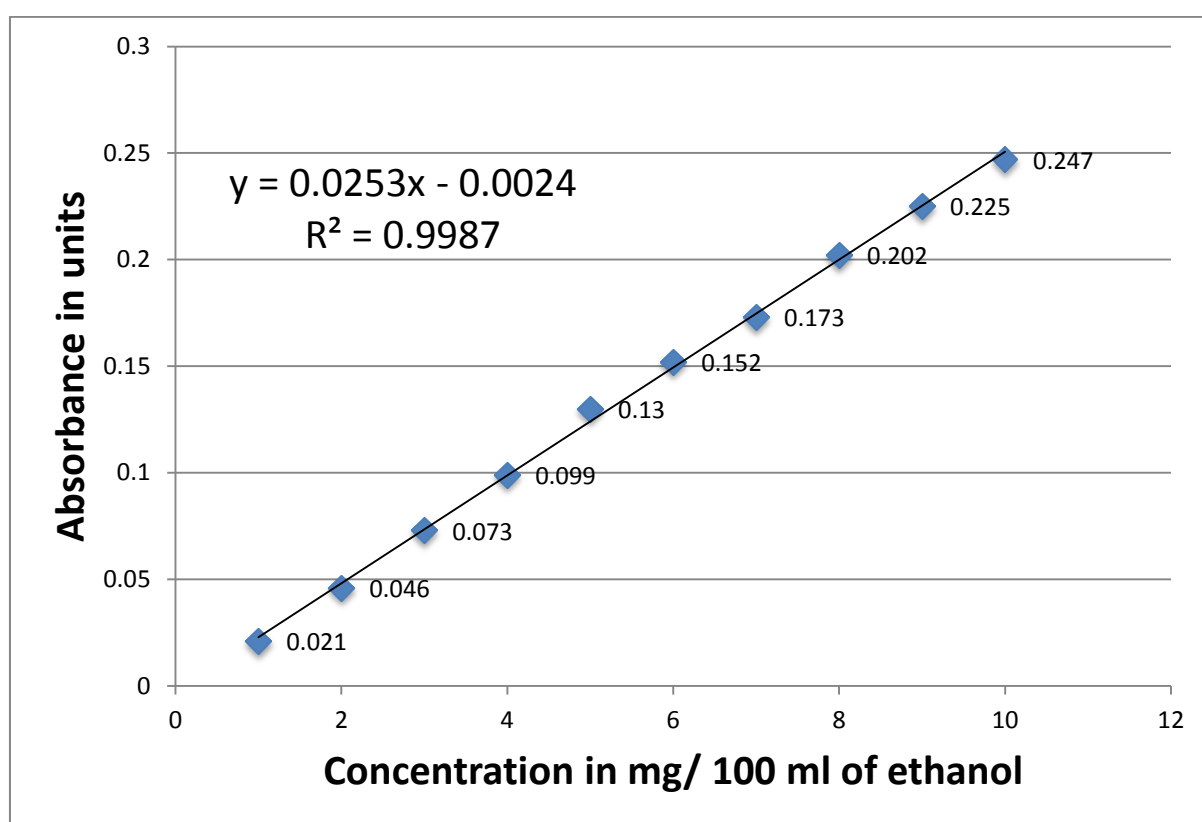
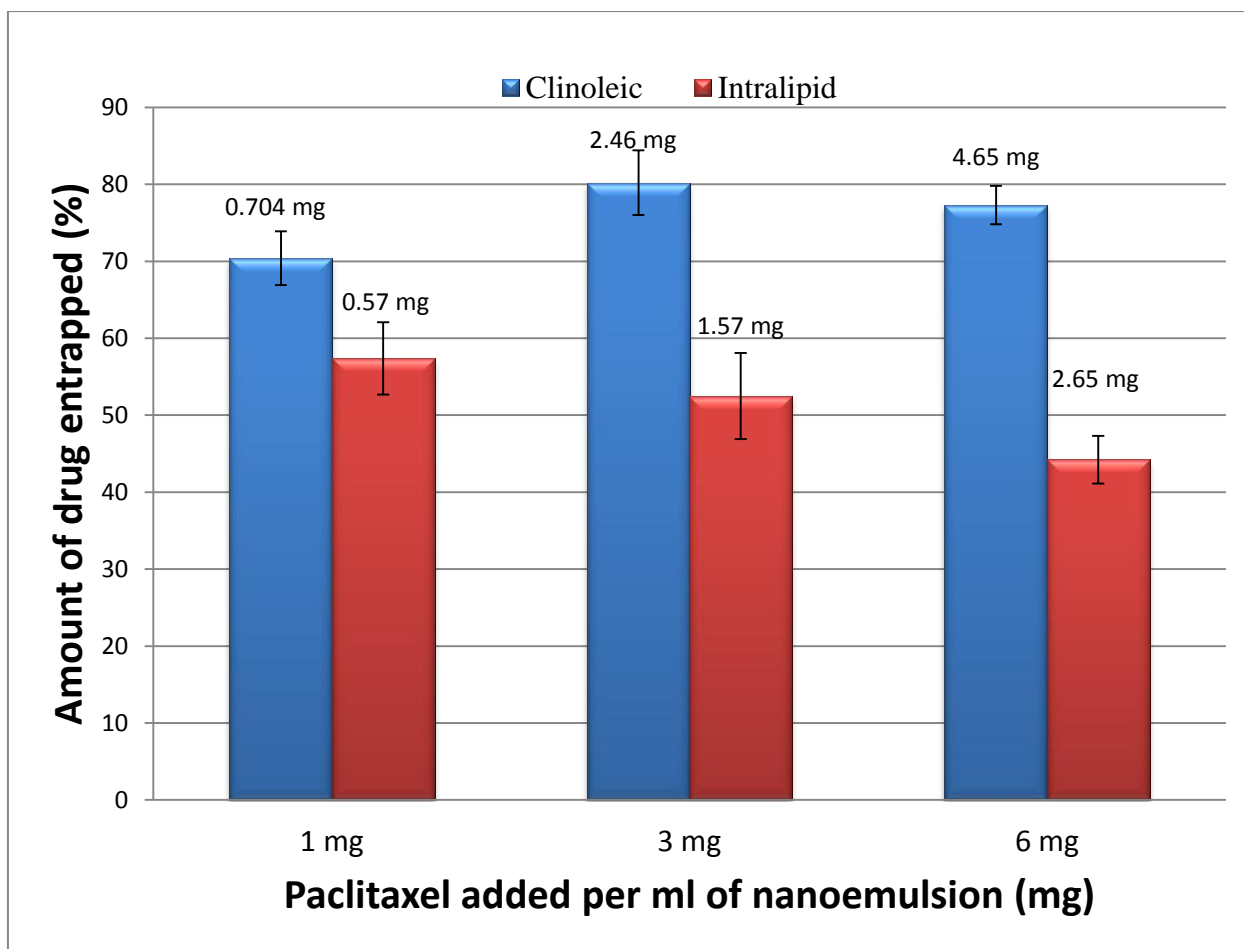


Figure 3.13 Calibration curve showing the absorbance plotted against the concentration of paclitaxel per 100 ml of ethanol.



**Figure 3.14: Loading efficiency of paclitaxel in nanoemulsion droplets using the Clinoleic and Intralipid nanoemulsions (n=3 ± SD).**

Loading efficiency of paclitaxel in the nanoemulsion was dependent on type of nanoemulsion and concentration of drug (Figure 3.14). In the Clinoleic nanoemulsions  $70.4 \pm 3.5 \%$  ( $0.704 \pm 0.035$  mg/ml),  $80.2 \pm 4.2 \%$  ( $2.46 \pm 0.126$  mg/ml) and  $77.3 \pm 2.5 \%$  ( $4.63 \pm 0.15$  mg/ml) were successfully loaded into the emulsion droplets using 1mg/ml, 3mg/ml and 6 mg/ml paclitaxel respectively. By contrast for the Intralipid emulsion, lower loading efficiencies for the drug were observed. These were  $57.38 \pm 4.7\%$  ( $0.57 \pm 0.047$  mg/ml),  $52.5 \pm 5.6 \%$  ( $1.57 \pm 0.17$  mg/ml) and  $44.2 \pm 3.1 \%$  ( $2.65 \pm 0.19$  mg/ml) for the 1mg/ml, 3 mg/ml and 6 mg/ml paclitaxel formulations respectively.

According to a recent study, paclitaxel is not highly soluble in soybean oil; showing a solubility of only 0.18 mg/ g of soybean oil (Surapareni et al, 2012; Kan *et al*, 1999). On the other hand, paclitaxel shows a solubility of 0.6 mg/ml in Oleic acid, which is the main component of Olive oil (Singla *et al*, 2002). Intralipid emulsion is composed of mainly soybean oil but Clinoleic emulsion only has 20% soybean oil, this may be a reason for the higher loading efficiency observed in Clinoleic formulations.

Clinoleic emulsion also has a few extra ingredients than Intralipid emulsion. It is possible that the extra components: Essential fats acids and Sodium oleate, allow the Clinoleic nanoemulsion to solubilise and retain more paclitaxel.

Paclitaxel is a hydrophobic drug and has a solubility of less than 0.1 µg/ ml in aqueous solutions (Konno *et al.*, 2003). By using Clinoleic and Intralipid, the solubility of paclitaxel was enhanced to 4.63 mg/ml and 2.65 mg/ml respectively (Figure 3.14).

# **Chapter 4:**

# **Tissue Culture**

A nanoemulsion is a heterogeneous dispersion of nano-sized (1-1000 nm) oil droplets in water. The advantage of using nanoemulsions in cell culture is that it increases the cellular uptake of oil-soluble supplements or drugs (Shah *et al*, 2009). Nanoemulsions increase the bioavailability of the drug to the cells. Paclitaxel is widely used anti-cancer drug. It hydrophobic drug but it dissolves readily in the oil phase of nanoemulsions (Surapaneni *et al*, 2012).

Tissue culture can be defined as the *in vitro* growth of cells, obtained from multicellular organisms, in a controlled environment. The U87-MG and SVG-P12 cell lines were used for this experiment as model cancerous and normal cells respectively. U87-MG (Human glioblastoma –astrocytoma) are grade IV glioma cells, while SVG-P12 are normal human brain cells (astrocytes).

Poly-L-lysine (PLL) and Dextran were used as positive and negative controls respectively. A positive control is well-established and should be toxic to cells in tissue culture. By contrast, a negative control is a test that confirms that a given compound has very little or no effect on the cells.

This experiment was divided into two parts: Growth curves and Cytotoxicity tests. In the first part the cells were seeded in the densities of  $10^3$ ,  $10^4$  and  $10^5$  cells per well and allowed to grow for seven days. The absorbance was measured every day. The aim of this experiment was to find the most appropriate seeding density for the cytotoxicity tests. The appropriate seeding density in this case is one that gives a relatively high absorbance value (0.7-0.9) for pure media (MEM). Only if the absorbance is sufficiently high, the cytotoxic effects of formulations can be properly detected.

The next part of the experiment was to carry out the MTT (cytotoxicity) assays. MTT (3-(4,5-Dimethylthiazol-2-yl)-2,5-diphenyltetrazolium bromide) is a yellow tetrazole

compound that is reduced to purple formazan crystals by living cells. Hence the amount of purple formazan crystals in a given well (of a 96 well plate) is an indicator of the number of living cells in that well. DMSO was used to solubilize the crystals and obtain a bluish-purple coloured solution; the absorbance of which was measured at 612 nm.

In this study the cytotoxicity of a range of paclitaxel formulations was investigated using Clinoleic nanoemulsions, Intralipid nanoemulsions and paclitaxel solution. SVG-P12 cells and U87-MG cells were used as model normal cells and cancerous cells respectively.

## 4.1 Growth Curves

In this study the percentage growth of cells using a range of seeding densities was compared for the SVG-P12 cells (Figure 4.1). The growth for the SVG-P12 using a seeding density of  $10^3$  cells/ well increased to nearly  $200 \pm 6.86\%$  but the absorbance readings were only in the range of 0.1-0.15 at day 7. By contrast, the growth using  $10^4$  cells/well seeding density increased to approximately  $261 \pm 7.9\%$  and the absorbance readings were in the range of 0.27-0.31 units at day 7. However, when the seeding density was  $10^5$  cells/well, the percentage growth for the SVG-P12 was  $256 \pm 8.72\%$  and the absorbance reading was in the range of 0.7-0.75.

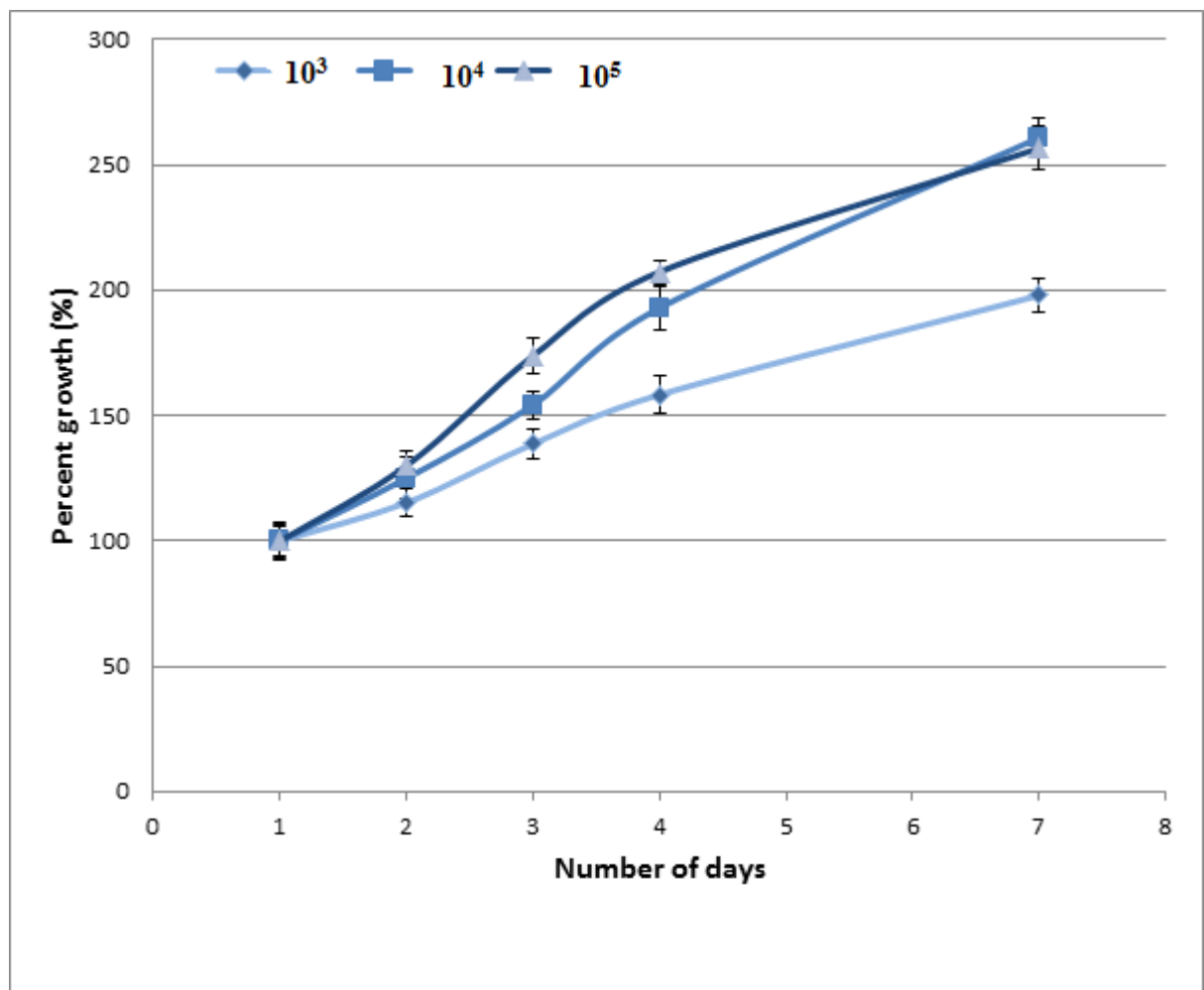


**Figure 4.1: Percentage growth of the  $10^3$ ,  $10^4$  and  $10^5$  seeding densities of the SVG-P12 cell line.**

Hence the  $10^5$  cells/well seeding density was the most appropriate as it has the highest rate of cell proliferation and had optimal absorbance readings at the final day (Figure 4.1). The absorbance values for the growth curves were significantly different for all seeding densities measured at each day ( $P < 0.05$ ).

The percentage growth for the  $10^5$  cells/well density was less than the percentage growth of the  $10^4$  cells/well density on day 7. This was due to the limited space and nutrients in the well.

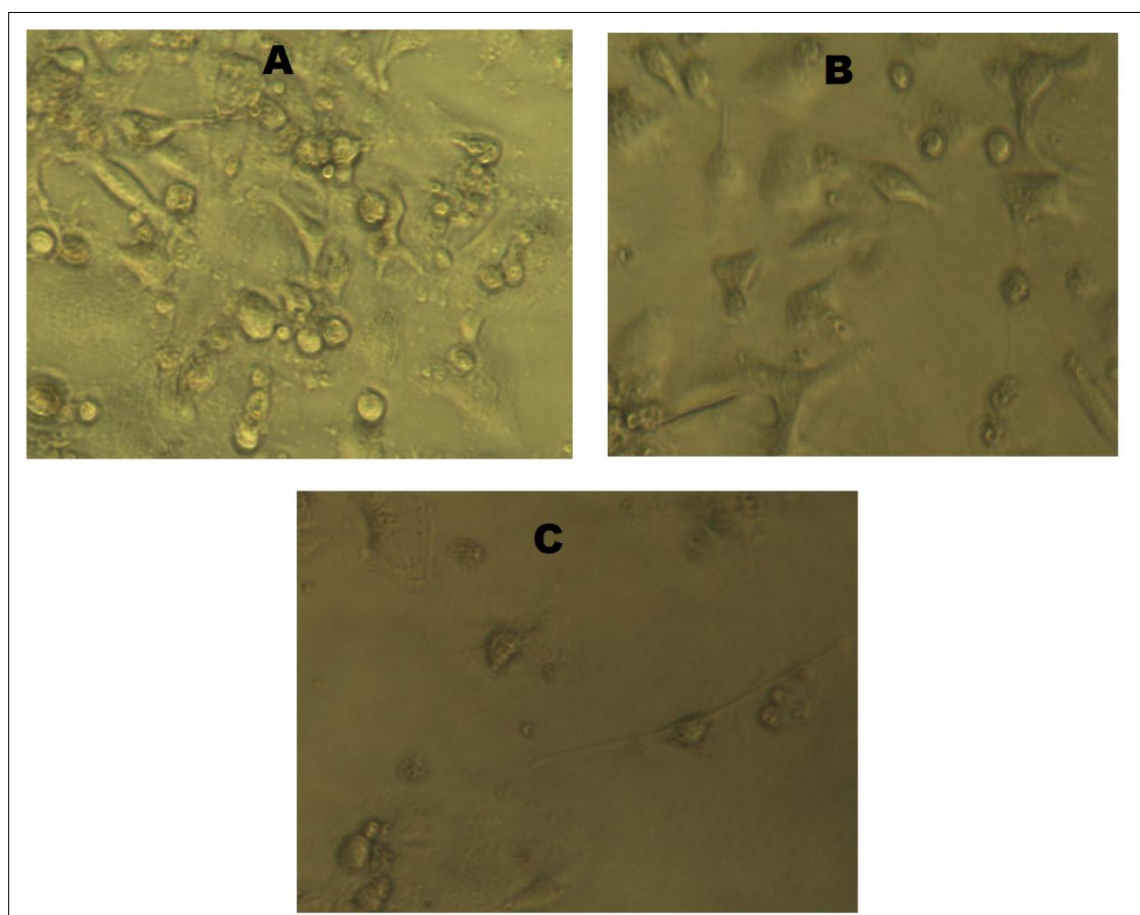


**Figure 4.2:** Microscopic photographs showing the SVG-P12 cells using three different seeding densities [ $10^5$  (A),  $10^4$  (B) and  $10^3$  (C)].

Figure 4.2 shows the inverted light microscopic images of the SVG-P12 cells at three different seeding densities. The images are in accordance with the growth curves obtained via the absorbance readings (Figure 4.1) as the number of cells per well is directly proportional to the absorbance or cell viability. The highest number of cells is observed in the  $10^5$  cells/well seeding density and the lowest in the  $10^3$  seeding density.

According to Figure 4.3, the seeding density of  $10^3$  cells/ well caused a cellular growth by nearly  $222 \pm 6.55\%$  but the absorbance readings were only in the range of 0.1-0.15 units at day 7. By contrast, the growth for the  $10^4$  cells/well density was approximately  $292 \pm 5.5 \%$  and the absorbance readings were in the range of 0.31-0.35 at day 7. However, the growth percentage for the  $10^5$  cells/well density was  $282.5 \pm 6.15 \%$  and the absorbance was in the range of 0.94-0.97.

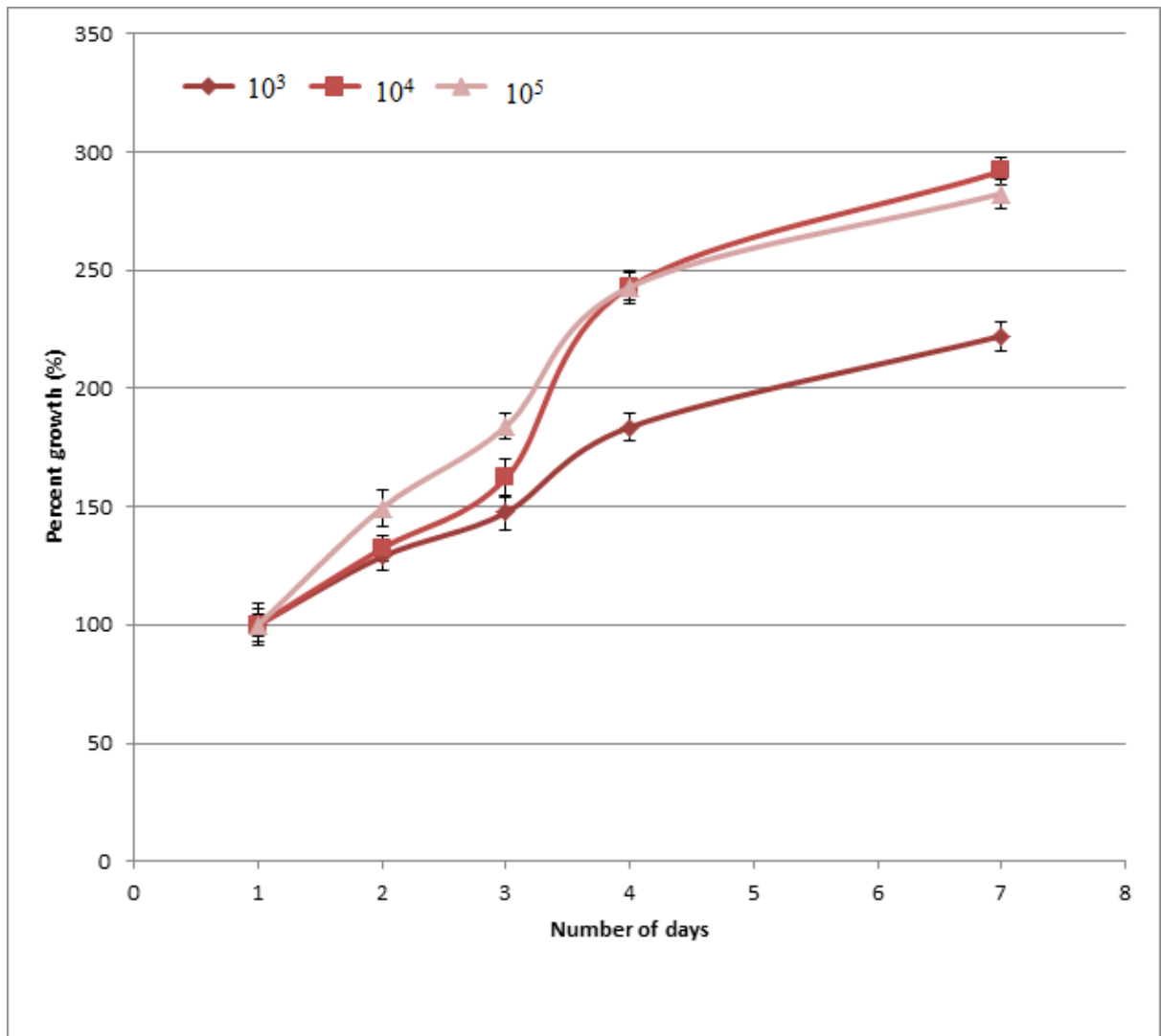


**Figure 4.3: Percentage growth using  $10^3$ ,  $10^4$  and  $10^5$  seeding densities of the U87-MG cell line.**

Thus the  $10^5$  cells/well seeding density is most appropriate due to the fast rate of growth and the high absorbance readings. The absorbance values were significantly different ( $P < 0.05$ ) when compared with the corresponding day of the other two seeding densities, (e.g., day 4).

As seen with SVG-P12 cells, the growth for the  $10^5$  cells/well density is less compared to the growth of the  $10^4$  cells/well density on day 7 as well. This is also due to the limitation of space and nutrients in the well as previously explained.

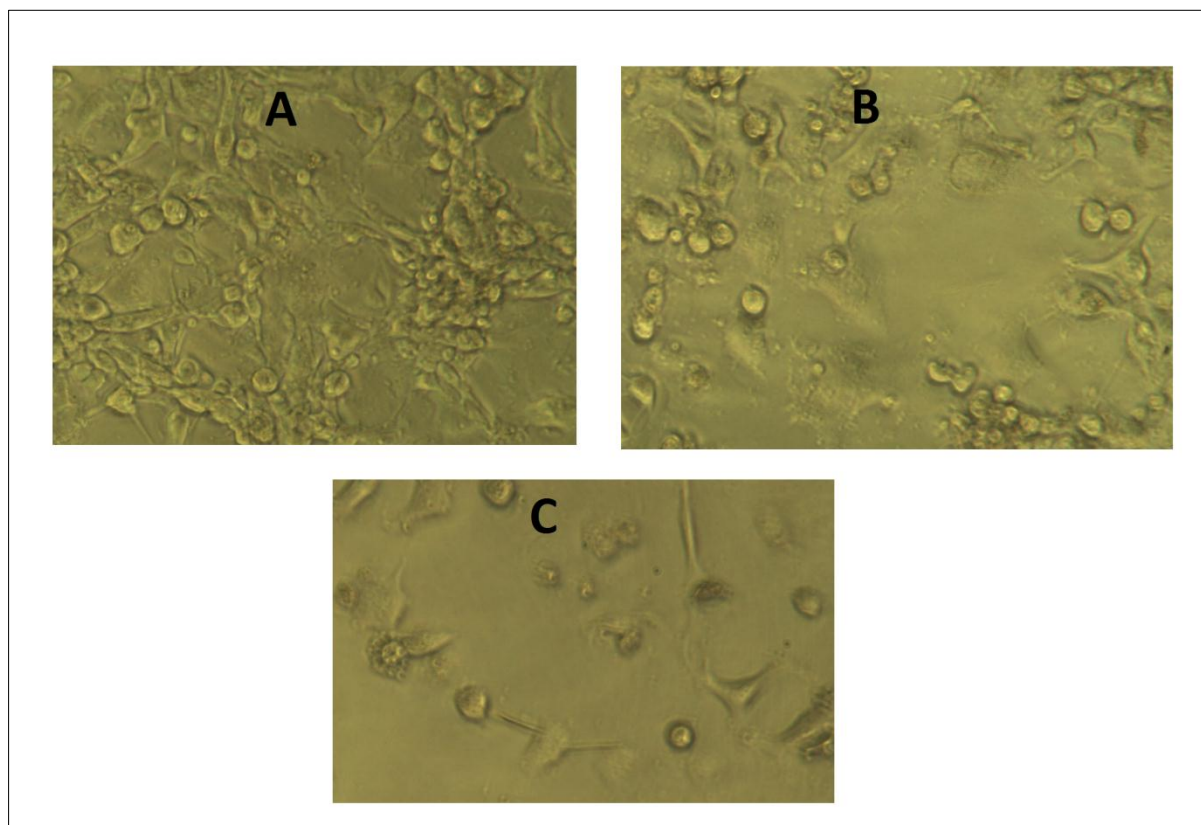


**Figure 4.4: Microscopic photographs showing the U87-MG cells using three different seeding densities [ $10^5$  (A),  $10^4$  (B) and  $10^3$  (C)].**

Figure 4.4 shows the inverted light microscopic images of the U87-MG cells at three different seeding densities. The images are in accordance with the growth curves obtained via the absorbance readings (Figure 4.3) as the number of cells per well is directly proportional to the absorbance or cell viability. The highest number of cells is observed in the  $10^5$  cells/well seeding density and the lowest in the  $10^3$  seeding density.

#### **4.2 MTT Assays for assessing the cytotoxicity of formulations.**

The negative control Dextran did not have any toxic effect on the glial cells as expected. In fact a very slight growth of the cells was observed from 100% to  $105.6 \pm 1.02\%$  when 5mg of dextran per ml of media was added (Figure 4.5). Conversely, the positive control PLL had a very toxic effect on the cells and the cell viability dropped to  $5.12 \pm 3.17\%$  when 5 mg of PLL was added per ml of media. Paclitaxel also had a similar effect on the cells as PLL; the cell viability rate dropped to  $4.95 \pm 2.1\%$  when 6 mg of Paclitaxel was added per ml of media.

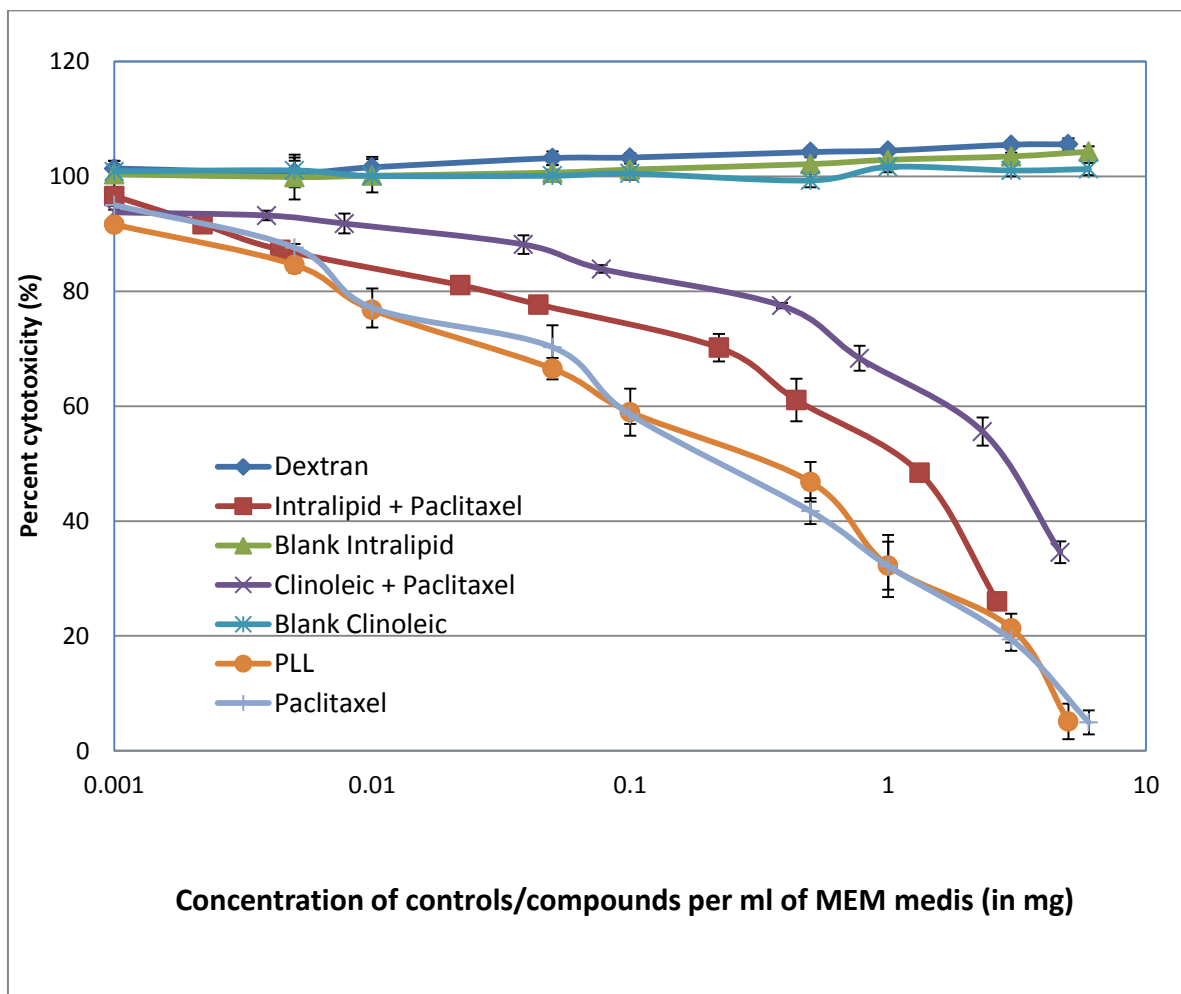


**Figure 4.5: Cytotoxic effects of the formulations on the SVG-P12 cells: Dextran, Blank Clinoleic, Blank Intralipid, Clinoleic loaded with paclitaxel, Intralipid loaded with paclitaxel, PLL and Paclitaxel.**

In the case of Blank nanoemulsions (Clinoleic and Intralipid) – they acted as negative controls as they were expected not to have toxic effects on the glial cells (Figure 4.5). These drug-free nanoemulsions however caused a slight increase in the growth of the cells. Blank Clinoleic lead to an increase in the cell viability of SVG-P12 cells by  $101.3 \pm$

0.95% which happened when the cells were supported by the drug-free Clinoleic formulation instead of MEM as nutrition. Similarly, Blank Intralipid increased the cell viability from 100% to  $104.32 \pm 1.04\%$  (Figure 4.5).

When Clinoleic loaded with paclitaxel was applied to the cells, the cell viability decreased to  $34.57 \pm 1.9\%$  for the concentration of 6 mg of paclitaxel per ml of the media. Similarly, Intralipid loaded with paclitaxel lowered the cell viability to  $26.04 \pm 1.06\%$ . Although the entrapment efficiency of Clinoleic emulsion is higher, its cell toxicity is slightly lower than Intralipid emulsion (Figure 3.14). The reason for this may be that Clinoleic is able to retain drug for a longer period ( $>72$  hours) and releases it in the external phase from the droplets slowly. The reason for this sustained release of paclitaxel might be the difference in the constituents as Paclitaxel is more soluble in Olive oil than it is in soybean oil.

There is a noticeable difference between cell viability values of the nanoemulsions containing paclitaxel and paclitaxel on its own. Paclitaxel by itself is more toxic to the cells compared to when it is loaded inside the nanoemulsions. As these are normal glial cells, lower cytotoxicity is highly desirable indicating that paclitaxel loaded in nanoemulsions was advantageous to paclitaxel alone. The nanoemulsion formed a protective barrier between the cells and paclitaxel; hence they showed lower cell toxicity than paclitaxel by itself.

There is a significant difference between the absorbance readings obtained for Paclitaxel and the nanoemulsions (Clinoleic and Intralipid) loaded with paclitaxel ( $P < 0.05$ ).

<b>Formulation</b>	<b>IC<sub>50</sub> Value (mg) ± SD</b>
<b>Paclitaxel</b>	0.26 ± 0.02
<b>PLL</b>	0.40 ± 0.024
<b>Intralipid with Paclitaxel</b>	2.7 ± 0.43
<b>Clinoleic with Paclitaxel</b>	3.7 ± 0.18

**Table 4.1: IC<sub>50</sub> Values of the formulations in mg for SVG-P12 cells**

According to Table 4.1, it is seen that paclitaxel by itself has the lowest IC<sub>50</sub> value indicating that it has the highest cytotoxicity followed by PLL, Intralipid with paclitaxel and Clinoleic with paclitaxel in that order. This means that only 0.026 mg of paclitaxel alone was required to kill 50% of the SVG-P12 cells. By contrast, 2.7 mg of paclitaxel loaded in Intralipid and 3.7 mg of paclitaxel loaded in Clinoleic was required to kill the same amount of cells. The reason for this may be attributed to the protective external phase barrier between the cells and the drug-loaded oil droplets (Surapaneni *et al*, 2012).

There is a significant difference between all the IC<sub>50</sub> values when compared with one another ( $P < 0.05$ ).

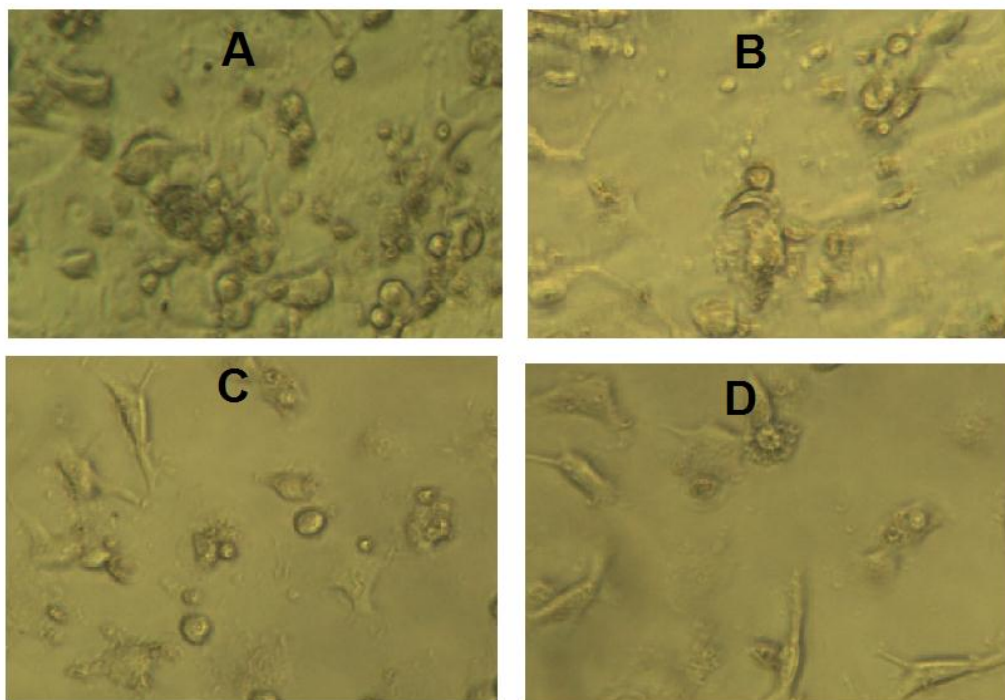


**Figure 4.6: Inverted light microscopic photographs of SVG-P12 cells treated with Clinoleic containing paclitaxel. These images show the declining number of cells as more paclitaxel is added per ml of media. [0.0 mg (A), 0.5 mg (B), 1.5 mg (C) and 3 mg (D) per ml]**

The images above agree with the findings presented in Figure 4.5, as it confirms that as the concentration of paclitaxel (entrapped in Clinoleic) increased, the number of viable cells decreased.

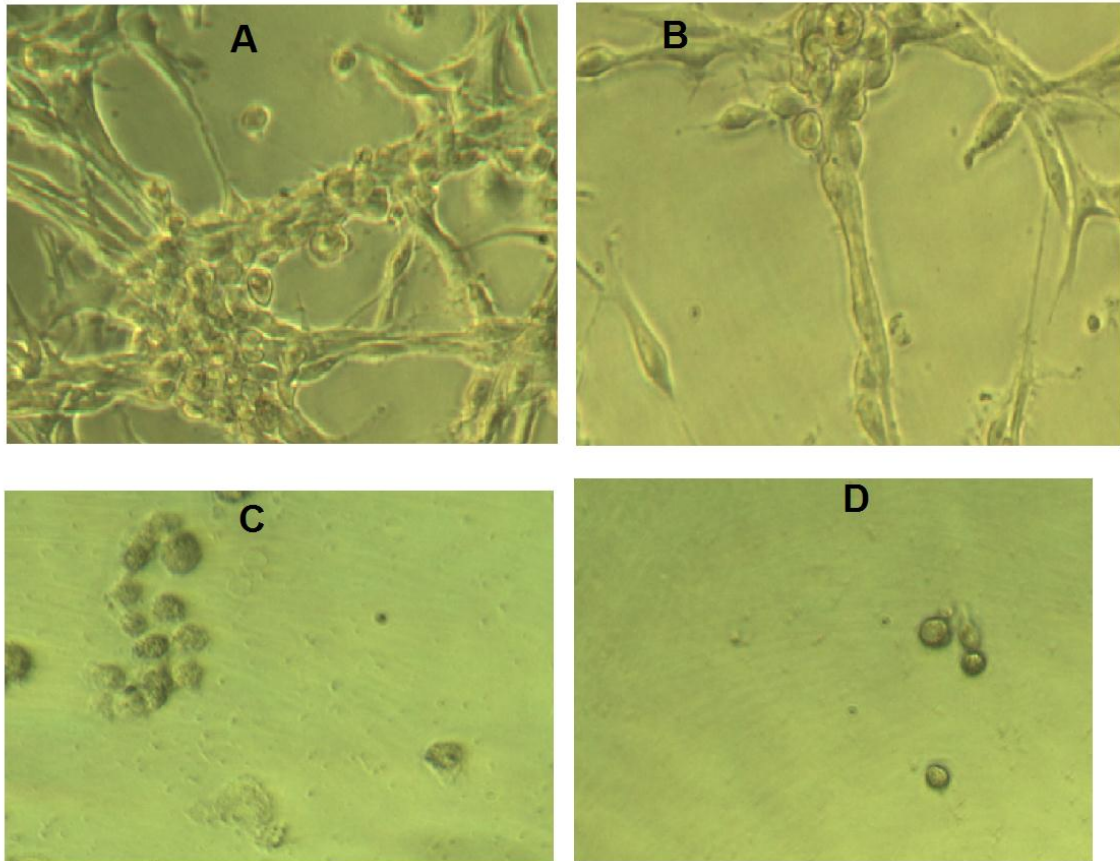


**Figure 4.7: Inverted light microscopic images of SVG-P12 cells treated with Intralipid containing paclitaxel. These images show the decreasing number of cells as higher concentrations of paclitaxel were added [0.0 mg (A), 0.5 mg (B), 1.5 mg (C) and 3 mg (D) per ml].**

The images above agree with the scatter plot (Figure 4.2.1) as it confirms the converse relationship between paclitaxel concentration (entrapped in Intralipid) and the number of viable cells.

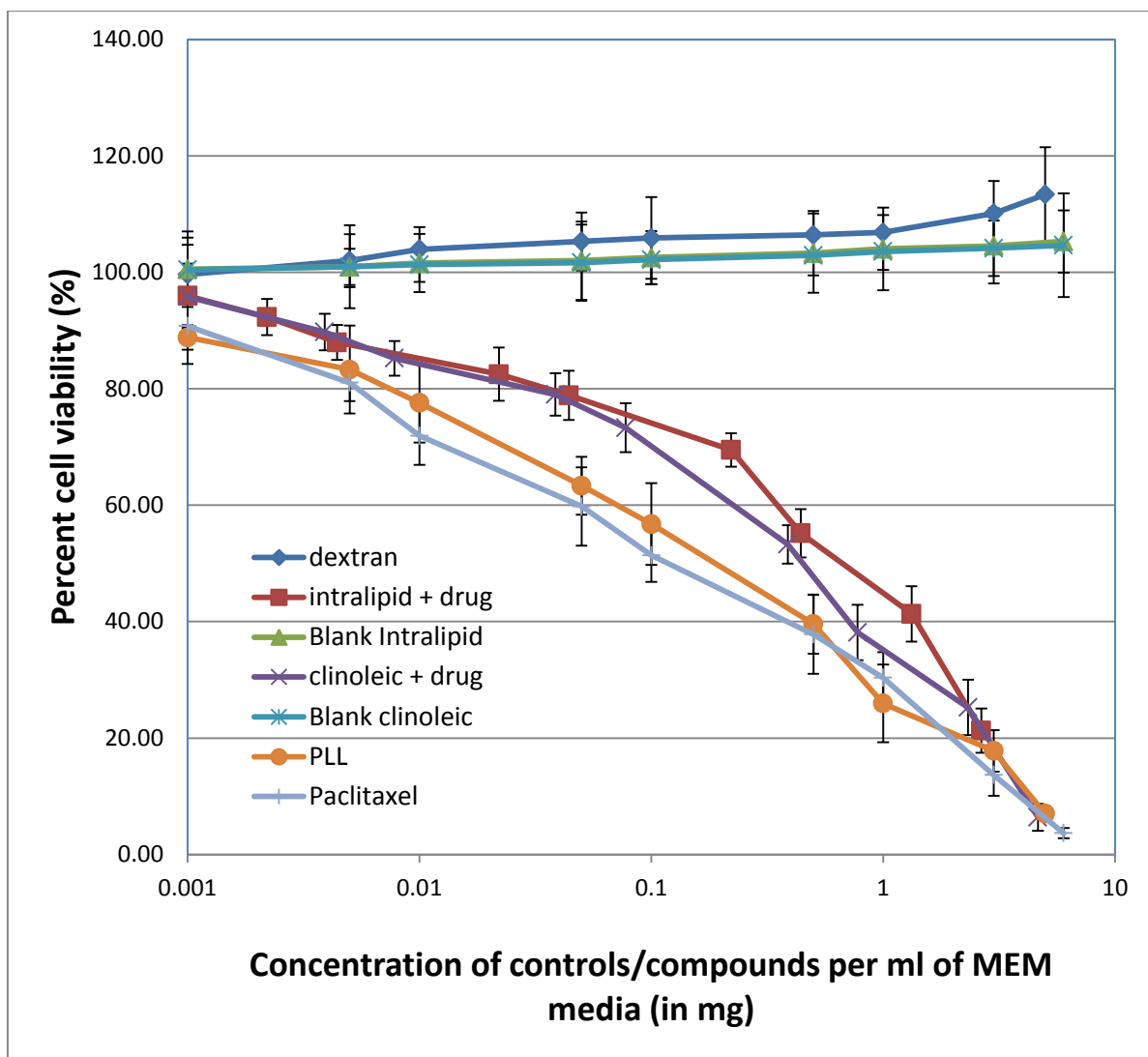


**Figure 4.8: U87-MG showing the cytotoxic effects of the formulations in percent cytotoxicity: Dextran, Blank Clinoleic, Blank Intralipid, Clinoleic loaded with paclitaxel, Intralipid loaded with paclitaxel, PLL and Paclitaxel**

As seen with SVG-P12, the negative control Dextran did not have any toxic effect on U87-MG as well; and slightly aided in the growth of the cancerous cells. The cell viability increased from 100% to  $113.34 \pm 8.11\%$  for the 5mg/ml Dextran concentration. On the contrary, the positive control PLL had a very toxic effect on the cells as expected. The cell viability dropped to  $7.01 \pm 1.17\%$  for PLL. Paclitaxel being an established anti-

cancer agent also has a similar effect on the cells as PLL; the cell viability rate dropped to  $3.67 \pm 0.87\%$ .

When the blank nanoemulsions (Clinoleic and Intralipid) were used, their effect on the viability of the cancerous cells was similar to that on SVG-P12 cells. They had no cytotoxic effects but actually assisted in the growth of the cells. Blank Clinoleic increased the viability of U87-MG cells to  $104.64 \pm 8.91\%$ . Similarly, the blank Intralipid increased the viability from 100% to  $105.29 \pm 5.35\%$

When Clinoleic loaded with paclitaxel was introduced to the U87-MG cells, the cell viability decreases to  $6.4 \pm 2.3 \%$  for the concentration of 6 mg of paclitaxel per ml of media. Similarly, Intralipid loaded with paclitaxel lowered the cell viability to  $21.29 \pm 3.82\%$ . Clinoleic killed more cancerous cells than Intralipid emulsions; this might be due to the higher entrapment efficiency of Clinoleic formulations (Figure 3.14). Another reason may be the different components that these two nanoemulsions are comprised of leading to different rates of drug-release.

There is a very small difference between the cell viability values for nanoemulsions with paclitaxel and paclitaxel by itself. This shows that both efficiently inhibit or destroy the grade IV glioma cells. As these are Grade IV glioblastoma cells, lower cell viability is the desired result.

There is a significant difference between the absorbance readings of the positive and negative controls ( $P < 0.05$ ). But when the readings for Blank Clinoleic, Blank Intralipid and Dextran are compared, there is no significant difference. But these three compounds are significantly distinct from the absorbance readings obtained for Paclitaxel and the nanoemulsions (Clinoleic and Intralipid) loaded with paclitaxel ( $P < 0.05$ ).

Both drug-loaded Clinoleic and Intralipid nanoemulsions killed a greater number of U87-MG cells than normal glial SVG-P12 cells. A possible reason for this may be that as cancerous cells divide and multiply faster, their intake of the nutrients in the surrounding media is also faster (Miller *et al*, 2007). Hence the U87-MG cells are exposed to more paclitaxel than the SVG-P12 cells, leading to higher cell death.

<b>Formulations</b>	<b>IC<sub>50</sub> value</b>
<b>Paclitaxel</b>	<b>0.092 ± 0.009</b>
<b>PLL</b>	<b>0.33 ± 0.042</b>
<b>Clinoleic with paclitaxel</b>	<b>0.66 ± 0.05</b>
<b>Intralipid with paclitaxel</b>	<b>1.8 ± 0.29</b>

**Table 4.2: IC<sub>50</sub> Values of the formulations in mg for U87-MG cells**

Paclitaxel by itself has the lowest IC<sub>50</sub> value indicating that it has the highest cytotoxicity followed by PLL, Clinoleic with paclitaxel and Intralipid with paclitaxel respectively. There is a significant difference between all the IC<sub>50</sub> values when compared with one another ( $P < 0.05$ ).

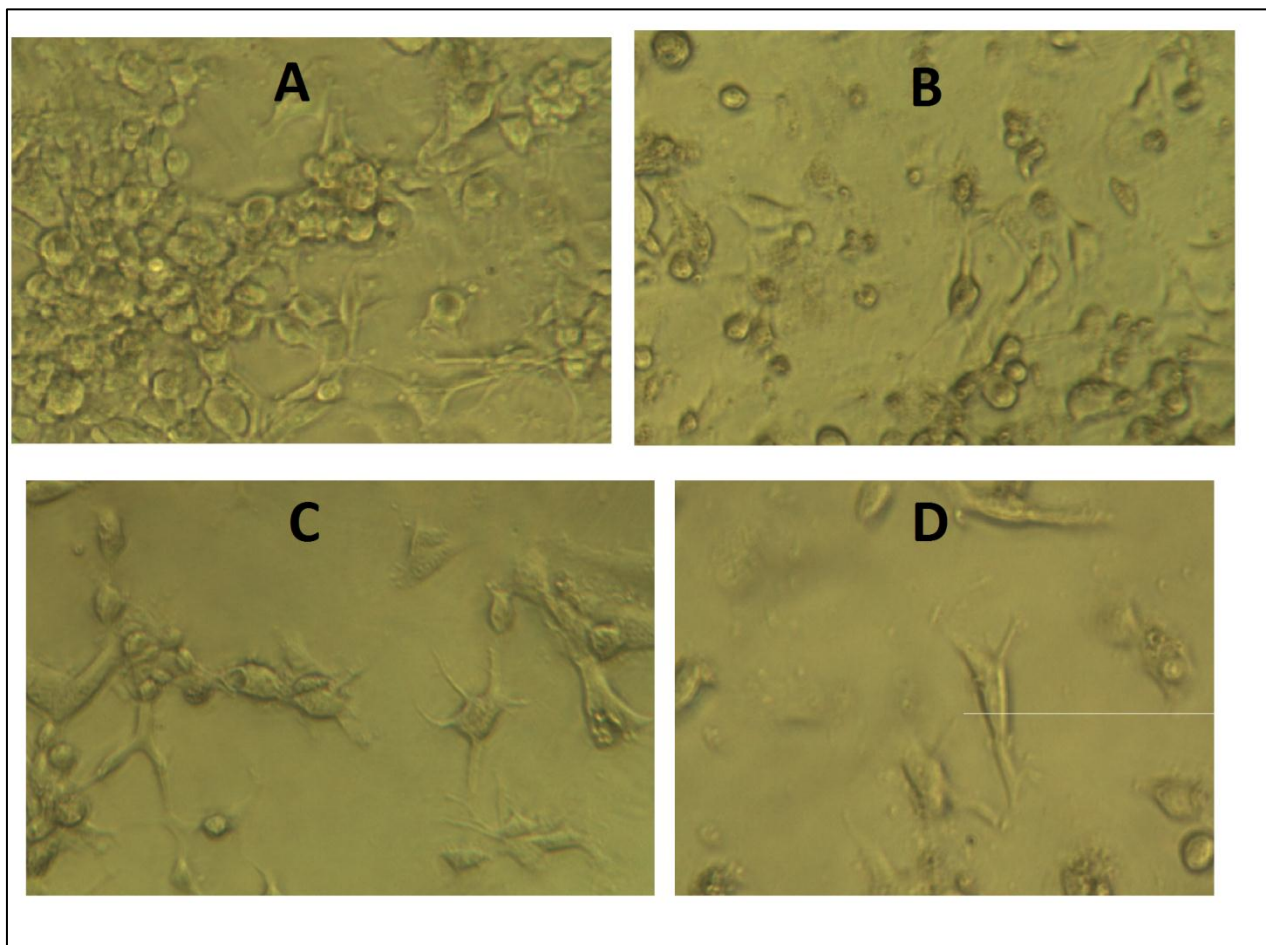


**Figure 4.9: Inverted light microscopic images of U87-MG cells treated with Clinoleic containing paclitaxel. These images show the dwindling number of cells as more paclitaxel was added. [0.0 mg (A), 0.5 mg (B), 1.5 mg (C) and 3 mg (D) per ml].**

The images above agree with Figure 4.8 demonstrating the influence of higher paclitaxel (in Clinoleic nanoemulsions) concentration on the viability of cells.

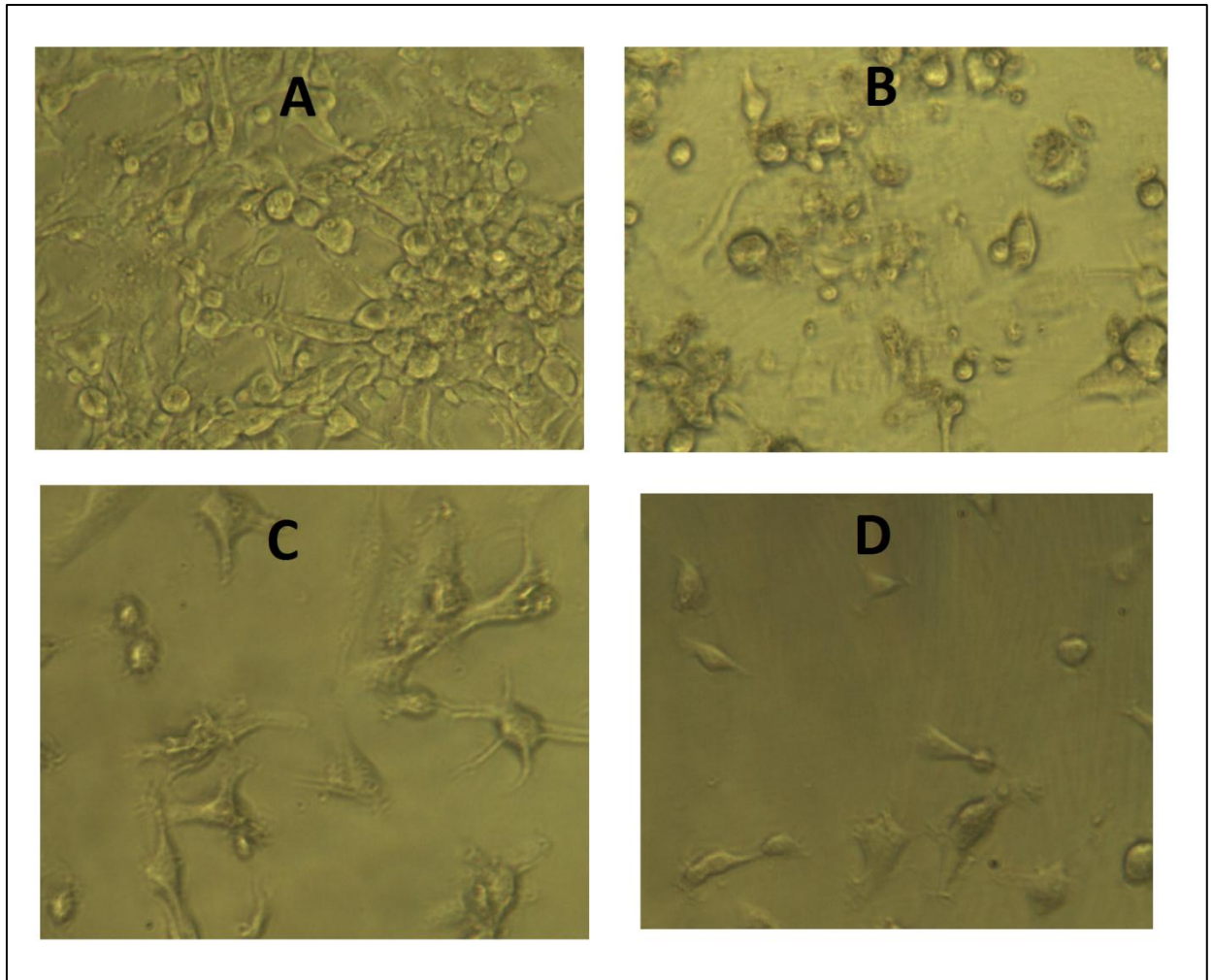


**Figure 4.10: Inverted light microscopic images of U87-MG cells treated with Intralipid containing paclitaxel. These images show the dwindling number of cells as more paclitaxel was added. [0.0 mg (A), 0.5 mg (B), 1.5 mg (C) and 3 mg (D) per ml].**

Similarly, the images above (Figure 4.10) also agree with the cytotoxicity curve (Figure 4.8) as it confirms that as the concentration of paclitaxel (encapsulated in Intralipid) increases, the number of viable cells decreases.

When compared with each other, Clinoleic is more potent in decreasing the number of U87-MG cells as compared to Intralipid; but it is less toxic to the SVG-P12 cells. The amount of paclitaxel required ( $IC_{50}$  value) for Clinoleic to kill 50% of U87-MG cells is  $0.66 \pm 0.05$  mg/ml, while it takes  $3.7 \pm 0.18$  mg/ml of the same to destroy 50% of SVG-P12 cells. Similarly, the amount of paclitaxel required ( $IC_{50}$  value) for Intralipid to kill 50% of U87-MG cells is  $1.8 \pm 0.29$  mg/ml, while it takes  $2.7 \pm 0.43$  mg/ml of the same to destroy 50% of SVG-P12 cells. Paclitaxel is highly toxic to both cell lines having an  $IC_{50}$  value of  $0.092 \pm 0.009$  mg/ml against U87-MG and  $0.26 \pm 0.02$  mg/ml against SVG-P12 cells. Both nanoemulsions are less toxic to the normal glial cells (SVG-P12) than paclitaxel alone, but Clinoleic has noticeably milder toxicity to the SVG-P12 cells.

As discussed earlier, the reasons for the differences in cell toxicity and  $IC_{50}$  values can be attributed to the different components of the two nanoemulsions, different loading efficiencies and the faster cell proliferation of the U87-MG cells. The higher loading efficiency and sustained release of paclitaxel by the Clinoleic emulsion makes it a superior emulsion than Intralipid for *in vitro* glioma therapy with paclitaxel.

# **Chapter 5:**

## **Conclusions and Future prospects**

## 5.1 General conclusions

- **Comparison of characteristics of the Clinoleic and Intralipid nanoemulsions**

The droplet size of both Clinoleic and Intralipid formulations increased as higher Paclitaxel concentrations were included. Droplet size of the Clinoleic emulsion was increased from 254.1 nm for drug-free nanoemulsions to 264.7 nm when paclitaxel (6 mg/ml) was loaded into the formulation. Similarly with the Intralipid, the measured size was 283.3 nm and upon inclusion of 6mg/ml paclitaxel the size increased to 294.6 nm. The increase of droplet size as a result of drug loading indicates that paclitaxel has possibly influenced the interfacial properties of the o/w emulsions, suggesting that drug molecules might partially localise at the o/w interface.

The PDI of all nanoemulsion formulations (Clinoleic and Intralipid) were lower than 0.2 irrespective of paclitaxel concentration indicating that all the nanoemulsion formulations were homogenous. There was a 16.6 % rise in the PDI of Clinoleic when 6mg/ml paclitaxel was added. By contrast there was an increase by 39.25% in the PDI of Intralipid when 6mg/ml of paclitaxel was added. This indicates that Clinoleic retains its homogeneity more successfully compared to the Intralipid emulsions on addition of paclitaxel.

The pH values for the Clinoleic formulations (7.1-7.5) were slightly more basic than those of the Intralipid formulations (6.5-6.9). For both nanoemulsions, the influence of paclitaxel concentration on the measured pH was minimal; with no

specific trend of increase or decrease in pH as a result of drug inclusion. A pH value in the range of 6.0-8.0 is considered ideal for intravenous administration. This clearly suggests that these nanoemulsions would be suitable for intravenous administration with accordance to the pH values.

The ZP of Clinoleic has a greater negative intensity than that of Intralipid. The values for Intralipid are closer to neutral. However, on addition of paclitaxel (2 mg/ml and 4 mg/ml) the intensity of the charge decreased substantially for Intralipid when compared to the drug-free formulation. This indicates that paclitaxel had an effect on the surface charge of the Intralipid droplets.

For a nanoemulsion formulation to be electro-statically stable during storage (so that it is not susceptible to coalescence or phase separation), the ZP values should have a high intensity; preferably over  $\pm 30$  mV (Elsheikh *et al.*, 2012). As the ZP values for Clinoleic are closer to  $\pm 30$  mV as compared to Intralipid, it can be concluded that Clinoleic might be more electro-statically stable than Intralipid.

Clinoleic is composed of refined olive oil, refined soybean oil, essential fatty acids, purified egg phosphatides, glycerol, sodium oleate and sodium hydroxide. While Intralipid contains purified soybean oil, purified egg phospholipids, glycerol anhydrous and sodium hydroxide. The difference in the composition of the nanoemulsions may be responsible for the difference in size, ZP, pH and PDI.

- **Clinoleic formulations are more stable than Intralipid formulations.**

After 14 days of storage at 4° C the droplet size of Clinoleic nanoemulsion increased from 254.3 to 258.7 nm, which is not a substantial increase. On the other hand, Intralipid droplet size increased from 285.6 to 311.7 nm after 14 days of storage at 4° C, which is a significant increase in size. There is no significant difference in the PDI values for both nanoemulsions upon storage for 14 days at 4° C. The pH of Clinoleic did not show any change when stored at 4° C for two weeks, but the Intralipid formulations showed a downwards trend as the pH values became more acidic after 14 days. For both nanoemulsions, paclitaxel concentration had very little or no effect on the pH, indicating that it is the length of the storage which affects the pH of these formulations. When stored at 4° C no significant difference in the ZP values for both nanoemulsions after 14 days was detected.

When stored at room temperature, all the formulations (of Clinoleic and Intralipid) showed a trend of increase in droplet size after 14 days, indicating that some of the paclitaxel may have leaked out of the droplets and located at the interface, causing the droplet's surface to become more hydrophobic with a subsequent aggregation. The PDI values for the Clinoleic formulations did not show much change, but the PDI values for the Intralipid formulations increased from  $0.175 \pm 0.026$  to  $0.225 \pm 0.031$  after two weeks at room temperature. There is a significant increase in PDI that confirms that paclitaxel is causing droplet aggregation by localizing at the surface of the droplets and increasing their hydrophobicity; hence they are more prone to form aggregates. The pH for both

the Clinoleic and Intralipid formulations also decreased considerably when stored at RT for two weeks; it reduced to below 6.0 in both cases reducing their suitability for intravenous administration. There is a trend of decrease in the intensity of the ZP values of both Clinoleic and Intralipid when stored at RT for 14 days which is in accordance with the decrease in the pH readings.

All the characteristics showed greater variances in their measurements when stored at RT and it is apparent that the nanoemulsions are generally more stable when stored at 4° C. Clinoleic showed more stability than Intralipid formulations when stored at both RT and 4° C. This stability can be attributed to the presence of sodium oleate in Clinoleic TPN. Sodium oleate is a commonly used emulsifier (surfactant) which has been known to improve the stability of emulsions.

- **Clinoleic has better loading efficiency for Paclitaxel as compared to Intralipid.**

In the Clinoleic formulations  $70.4 \pm 3.5 \%$  ( $0.704 \pm 0.035$  mg/ml),  $80.2 \pm 4.2 \%$  ( $2.46 \pm 0.126$  mg/ml) and  $77.3 \pm 2.5 \%$  ( $4.63 \pm 0.15$  mg/ml) of paclitaxel was successfully loaded into the droplets for the 1 mg/ml, 3 mg/ml and 6mg/ml paclitaxel concentrations respectively. Conversely, lower loading efficiencies were obtained for the Intralipid formulations:  $57.38 \pm 4.7\%$  ( $0.57 \pm 0.047$  mg/ml),  $52.5 \pm 5.6 \%$  ( $1.57 \pm 0.17$  mg/ml) and  $44.2 \pm 3.1 \%$  ( $2.65 \pm 0.19$  mg/ml) of paclitaxel was successfully loaded into the droplets for the 1 mg/ml, 3 mg/ml and 6 mg/ml Intralipid formulations respectively.

Clinoleic TPN is comprised of more ingredients when compared to Intralipid TPN; these are refined olive oil, essential fatty acids and sodium oleate. These ingredients may be responsible for the improved loading efficiency of paclitaxel in the Clinoleic emulsions. Olive oil has been proven to be a better alternative to soybean oil for emulsions in previous studies (Gobel *et al.*, 2003; Deshpande *et al.*, 2009).

- **Clinoleic formulations show greater toxicity towards Grade IV glioma cells (U87-MG)**

When Clinoleic loaded with paclitaxel was introduced to the U87-MG cells, the cell viability decreased to  $6.4 \pm 2.3$  % for the concentration of 6 mg of paclitaxel per ml of media. Similarly, Intralipid loaded with paclitaxel lowered the cell viability to  $21.29 \pm 3.82$ %. The  $IC_{50}$  values for paclitaxel loaded into Clinoleic and Intralipid were  $0.66 \pm 0.05$  and  $1.8 \pm 0.29$  respectively indicating that Clinoleic loaded with paclitaxel was more toxic towards the glioma cells. This difference in cytotoxicity may be due to the higher entrapment efficiency observed in the Clinoleic formulation (Figure 3.14)

- **Intralipid formulations show greater toxicity towards normal glial cells (SVG-P12)**

When Clinoleic loaded with paclitaxel was added to the SVG-P12 cells, their viability decreased to  $34.57 \pm 1.9$  % for the concentration of 6 mg of paclitaxel per ml of media. Similarly, Intralipid loaded with paclitaxel lowered the cell viability of SVG-P12 to  $26.04 \pm 1.06$ %. Also,  $2.7 \pm 0.43$  mg of paclitaxel loaded in Intralipid was required to kill 50% of the normal glial cells whilst  $3.7 \pm 0.18$  of paclitaxel loaded in Clinoleic was required to do the same effect. This indicates that Intralipid loaded with paclitaxel shows greater toxicity towards the SVG-P12 cells. The reason for this may be that Clinoleic is able to retain drug for a longer period (>72 hours) and releases it in the external phase from the droplets slowly (Aboofazeli *et al*, 2003).

- **Both Clinoleic formulations and Intralipid formulations are less toxic than Paclitaxel by itself**

Paclitaxel by itself has the lowest IC<sub>50</sub> value for U87-MG cells indicating that it has the highest cytotoxicity followed by PLL, Clinoleic with paclitaxel and Intralipid with paclitaxel. In the case of SVG-P12 cells, paclitaxel by itself has the lowest IC<sub>50</sub> value indicating that it has the highest cytotoxicity followed by PLL, Intralipid with paclitaxel and Clinoleic with paclitaxel. Paclitaxel kills about 95% of the SVG-P12 normal glial cells, while paclitaxel in Clinoleic and Intralipid kills only around 66% and 74% respectively. This indicates that paclitaxel does not

differentiate between normal and glial cells, killing both the normal glial and grade IV glioblastoma cells equally. On the other hand the nanoemulsion formulations (containing paclitaxel) show sustained release of the drug, killing less SVG-P12 cells in comparison to the U87-MG cells.

## 5.2 Future work

Due to the constraints of time a number of studies were not performed. For example, more research can be carried out on the stability of nanoemulsions by storing them at higher temperatures (more than 30° C). In addition, it would have been useful to observe the effects of storing the nanoemulsion formulations for a longer duration at various temperatures.

Also, it would have been interesting to study the effects of these nanoemulsions on an additional cell line for a moderate (grade II) glioma like the 1321N1 cell line. It would also be useful to test these formulations on other cancer cell lines (like breast cancer) just to measure the efficacy of the formulations.

It would have been very useful to study the potency of the nanoemulsion formulations *in vivo* and compare the results with that of paclitaxel administered via another delivery vehicle like Cremophor EL.

# References

Abbott J., Ronnback L., Hansson E., Astrocyte–endothelial interactions at the blood–brain barrier, *Nature Rev Neuro*, 2006, 7, 41-53.

Aboofazeli, R., Nanometric scaled emulsions (Nanoemulsions), *Iranian J Pharmaceut Res*, 2010, 9, 325-326.

Alvarado V., Wang X., Moradi M., Stability Proxies for Water-in-Oil Emulsions and Implications in Aqueous-based Enhanced Oil Recovery, *Energies*, 2011, 4(7), 1058-1086

Angelini P., Hawkins C., Laparriere N., Bouffet E., Bartels U., Post mortem examinations in diffuse intrinsic pontine glioma: challenges and chances, *J Neuro-Oncology*, 2011, 101, 75-81.

Bernardi D. S., Pereira T. A., Maciel N. R., Bortoloto J., Viera G. S., Oliveira G. C., Rocha-Filho P. A., Formation and stability of oil-in-water nanoemulsions containing rice bran oil in vitro and in vivo assessments, *J Nanobio*, 2011, 9-44

Bouchemal K., Briançon S., Perrier E., Fessi H., Nano-emulsion formulation using spontaneous emulsification: solvent, oil and surfactant optimisation, *Int J Pharmaceut*, 2004, 280, 241-251, ISSN 0378-5173

Carter R., Aldridge S., Page M., Parker S., Frith C. D., Frith U., Shulman M. B., 2009, The Human Brain Book, D. K. Publications, New York.

Dall'Oglio S., D'Amico A., Pioli F., Gabbani M., Pasini F., Passarin M., Talacchi A., Turazzi S., Maluta S., Dose-intensity temozolomide after concurrent chemoradiotherapy in operated high-grade gliomas, *J Neurooncol*, 2008, 90, 315–319

Deshpande GC, Simmer K, Mori T, Croft K., Parenteral lipid emulsions based on olive oil compared with soybean oil in preterm (<28 weeks' gestation) neonates: a randomised controlled trial, *J Pediatr Gastroentero Nutr*, 2009 Nov, 49(5), 619-25.

Driscoll, D. F., Lipid injectable emulsions: pharmacopeial and safety issues. *Pharmaceut Res*, 2006, 23(9), 1959–1969.

Eccleston G., 2007, Emulsions and Microemulsions, Encyclopedia of Pharmaceutical Technology (3<sup>rd</sup> edition), Informa healthcare.

Elhissi A. M. A., Faizi M., Naji W. F., Gill H. S., Taylor K. M. G., Physical stability and aerosol properties of liposomes delivered using an air-jet nebulizer and a novel micropump device with large mesh apertures, *Int J Pharmaceut*, 2007, 334, 62–70

Elsheikh M., Elnaggar Y., Gohar E., Abdallah O., Nanoemulsion liquid preconcentrates for raloxifene hydrochloride: optimization and in vivo appraisal, *Int J Nanomedicine*, 2012, 7, 3787–3802

Förster T., Schambil F., Tesmann H., Emulsification by the phase inversion temperature method: the role of self-bodying agents and the influence of oil polarity, *Int J Cosmet Sci*, 1990 Oct, 12(5), 217-27.

Garcia-Garcia E., Andrieux K., Gil S., Couvreur P., Colloidal carriers and blood–brain barrier (BBB) translocation: A way to deliver drugs to the brain?, *Int J Pharmaceut*, 2005, 298, 274–292

Göbel Y, Koletzko B, Böhles HJ, Engelsberger I, Forget D, Le Brun A, Peters J, Zimmermann A., Parenteral fat emulsions based on olive and soybean oils: a randomized clinical trial in preterm infants, *J Pediatr Gastroenterol Nutr*, 2003 Aug, 37(2), 161-7.

Gusnard D. A., Cerebellar neoplasms in children, *Semin Roentgenol*, 1990, 25, 263-278

Hanahan D., Weinberg R., The Hallmarks of Cancer, *Cell*, 2000, 100 , 57-70.

Hofman J. A. M. H., Stein H. N., Destabilization of emulsions through deformation of the droplets, *J Col Inter Sci*, 1991, 147, 508-516

Howlader N., Noone A., Krapcho M., Neyman N., Aminou R., Altekruse S. F., Kosary C. L., Ruhl J., Tatalovich Z., Cho H., Mariotto A., Eisner M. P., Lewis D. R., Chen H. S., Feuer E. J., Cronin K.A., *SEER Cancer Statistics Review 1975-2009*, 2011.

Iwanaga D., Gray D., Fisk I., Decker E., Weiss J., McClements D., Extraction and characterization of oil bodies from soy beans: a natural source of pre-emulsified soybean oil. *J Agric Food Chem*, 2007 Oct 17;55(21):8711-6.

Jafari S. M., He Y., Bhandari B., Optimization of nano-emulsions production by microfluidization. *Euro Food Res Tech*, 2007, 225 (5-6), 733-741

Jong W. D. H., Borm P. B. J., Drug delivery and nanoparticles: Applications and hazards, *Int J Nanomedicine*, 2008 June; 3(2): 133–149.

Kan P., Chen Z., Lee C., Chu I., Development of nonionic surfactant/phospholipid o/w emulsion as a paclitaxel delivery system, *J Controlled Release*, 1999, 58 (3), 271–278.

Konno T., Watanabe J., Ishihara K., Enhanced solubility of paclitaxel using water-soluble and biocompatible 2-methacryloyloxyethyl phosphorylcholine polymers, *J Biomedical Materials Res Part A*, 1 May 2003, 65A (2), 209–214.

Larjavaara S., Mäntylä R., Salminen T., Haapasalo H., Raitanen J., Jääskeläinen J., Auvinen A., Incidence of gliomas by anatomic location, *Neuro Oncol*, 2007, 9, 319–325.

Lawrence M. J., Rees R. D., Microemulsion based media as novel drug delivery systems, *Advanced Drug Delivery Reviews*, 2000, 45, 89-12.

Mastropaolo D., Camerman A., Luo Y., Brayer G., Camerman N., Crystal and Molecular structure of Paclitaxel (taxol), *Proc Natl Acad Sci U S A*. 1995 July 18; 92(15): 6920–6924.

McClements D. J., Colloidal bases of emulsion colour, *Cur Opinion Col Int Sci*, 2002, 7, 451- 455.

Miller C. R., Perry A., Glioblastoma: Morphologic and Molecular Genetic Diversity, *Arch Pathol Lab Med*, March 2007, 131.

Mohanraj V. J., Chen Y., Nanoparticles- A review, *Tropical J Pharm res*, 2005, 5, 561 – 573.

Mohammadi A., Esmaeili F., Dinarvand R., Atyabi F., Walker R. B., Development and Validation of a Stability-Indicating Method for the Quantitation of Paclitaxel in Pharmaceutical Dosage Forms, *J Chrom Sci*, 2009, 47, 599-604

Musteata F. M., Paulisyzn J., Determination of Free Concentration of Paclitaxel in Liposome Formulations, *J Pharm Pharmaceut Sci*, 2006, 9, 231-237

Nasr M., Nawaz S., Elhissi A., Amphotericin B lipid nanoemulsion aerosols for targeting peripheral respiratory airways via nebulization, *Int J Pharmaceut*, 2012, 436, 611– 616

Nieuwenhuys R., Voogd J., van Huijzen C., 2008, *The Human Central Nervous System*, Springer, Berlin.

Ohgaki H., Kleihues P., Epidemiology and etiology of gliomas, *Acta Neuropathologica*, 2005, 109 (1), 93-108

Panayiotis P. Constantinides, Mahesh V. Chaubal, Robert Shorr,(2008), Advances in lipid nanodispersions for parenteral drug delivery and targeting, *Adv Drug Del Rev*,2008, 60, 757-767

Poluri K., Sistla R., Veerareddy P., Narasu L., Raje A., Hebsiba S., Formulation, Characterization and Pharmacokinetic Studies of Carvedilol Nanoemulsions, *Cur Trend Biotech Pharm*, April 2011, 5 (2) 1110-1122

Rahman R., Smith S., Rahman C., Grundy R., Anti-angiogenic therapy and mechanisms of tumour resistance in malignant glioma, *J Oncology*, 2010, 1-16

Schvartzman J., Sotillo R., Benezra R., Mitotic chromosomal instability and cancer: mouse modelling of the human disease, *Nature Rev Can*, 2010, 10, 102-113.

Scrimgeour C., *Bailey's Industrial Oil and Fat Products*, Sixth Edition, Six Volume Set. 2005, John Wiley & Sons, Inc.

Shah P., Bhalodia D., Shelat P., Nanoelumsion: A Pharmaceutical Review, *Sys Rev Pharm*, 2010, 24-32.

Sheng Hong Tseng, Michael S. Bobola, Mitchel S. Berger, John R. Silber, Characterization of paclitaxel (Taxol<sup>®</sup>) sensitivity in human glioma- and medulloblastoma- derived cell lines, *Neuro-Oncology*, 1999, 101-108.

Siew-Ju S., Gilbert M., Chemotherapy in adults with Glioma, *ANNALS aca med*, 2007, 36, 364-9.

Silva A. G., Nanotechnology approaches to crossing the blood-brain barrier and drug delivery to the CNS, *BMC Neurosci*, 2008, 9 (3), 4-6.

Singla A. K., Garg A., Aggarwal A., Paclitaxel and its formulations, *Int J Pharmaceut*, 2002, 235, 179-192.

Smoll N., Schaller K., Gautschi O. P., The Cure Fraction of Glioblastoma Multiforme, *Neuroepidemiology*, 2012, 39.

Surapaneni M., Das S. K., Das N. G., Designing Paclitaxel Drug Delivery Systems Aimed at Improved Patient Outcomes: Current Status and Challenges, *ISRN Pharm*, 2012, Article ID 623139, 1-15

Terzis A-JA., Thorsen F., Heese O., Visted T., Bjerkvig R., Dahl O., Arnold H., Gundersen G., Proliferation, migration and invasion of human glioma cells exposed to Paclitaxel (Taxol) in vitro, *Brit J Cancer*, 1997, 75 (12), 1744-1752.

Theissen O., Gompper G., Lattice-Boltzmann study of spontaneous emulsification, *Eur. Phys. J. B*, 1999, 11, 91-100.

Wang S., Wang H., Liang W., Huang Y., An injectable hybrid nanoparticle-in-oil-in-water submicron emulsion for improved delivery of poorly soluble drugs, *Nano Res Let*, 2012, 7, 219

Xu X., Yu Z., Zhu Y., Wang B., Effect of sodium oleate adsorption on the colloidal stability and zeta potential of detonation synthesized diamond particles in aqueous solutions, *Dia Rel Mat*, 2005, 14, 206– 212

Zhao M., Liang C., Li A., Chang J., Wang H., Yan R., Zhang J., Tai J., Magnetic Paclitaxel nanoparticles inhibit glioma growth and improve the survival of rats bearing glioma xenografts, *Anticancer Res*, 2010, 30 (6), 2217-2223.